UNIVERSITÀ DEGLI STUDI DI PADOVA

DEPARTMENT OF CIVIL, ENVIRONMENTAL AND ARCHITECTURAL ENGINEERING

MASTER THESIS IN WATER AND GEOLOGICAL RISK ENGINEERING

DEVELOPMENT AND APPLICATION OF SUSTAINABLE AQUIFER RECHARGE MEASURES IN DATA-SCARCE REGIONS IN SOMALIA

SUPERVISOR

Marco Marani

CO-SUPERVISOR

Paolo Mastrocola

MASTER CANDIDATE

Urooj Qayyum

STUDENT ID

2073524

ACADEMIC YEAR
2023/2024

ACKNOWLEDGEMENTS

I would like to express my deepest gratitude to my parents, who have been my greatest support system throughout this master program in Water and Geological Risk Engineering. Their encouragement has been invaluable to me.

I am also profoundly grateful to Professor Marco Marani for recognizing my potential and welcoming me into the WGRE family. His decision to award me the Padua International Excellence Scholarship allowed me to focus on my studies and thesis work with full dedication and enthusiasm. I am thankful to him for connecting me with Hydro Nova s.r.l., where I received immense support, time, and guidance from Paolo Mastrocola. I would like to acknowledge the support and guidance I have received from Giacomo Cogo of Hydro Nova, and take this opportunity to thank him for being my mentor during this journey. I would like to acknowledge the support and guidance I have received from Giacomo Cogo, from Hydro Nova and would take this as an opportunity to thank him for being my mentor during this journey. I would also like to extend my thanks to the Ministry of Planning and Ministry of Water Resources of Somaliland, the owners of the data and information collected by Hydro Nova, which I was later able to use in my research. This work would not have been possible without the collective effort of all these individuals.

Finally, I would like to extend my sincere thanks to Dr. Valentina Zanaga for her unwavering support throughout my two years at WGRE, and to my friends, who made my time away from home easier and memorable.

ABSTRACT

Somaliland, similarly to many Countries in Africa and globally, is characterized by hydrological data and water scarcity, and faces immense challenges in accessing clean water for its rural communities. The lack of hydrological and hydrogeological ground information, combined with land and vegetation degradation, exacerbated by climatic challenges, set significant limitations in the ability to identify sustainable water management strategies and access aquifers resources. This underscores the urgent need for the identification and adoption of effective and sustainable water management strategies.

In this thesis I focused on developing and applying sustainable Managed Aquifer Recharge (MAR) strategies in data-scarce regions, specifically in the Darar-weyne Basin in Somaliland. The goal was to enhance the provision of clean water to rural populations through MAR techniques. This was achieved by using global hydrological datasets such as CHIRPS, GPM and ERA5-Land and hydrological modeling using Soil Moisture Accounting (SMA) method within the widely-adopted hydrologic modelling system developed by the US Army Corps of Engineers, HEC-HMS, one of the standards in this field. The study explores three nature-based solutions (NBS); sand dams, semi-circular soil bunds, and increased vegetation cover, particularly grasslands to analyze their impacts on aquifer recharge. For each NBS three scenarios were modeled in HEC-HMS using SMA method, with primary input variables being surface storage (SS, mm), maximum infiltration rate (MIR, mm/hr) and soil storage (SoilS, mm). These scenarios were compared to a baseline scenario, representing the absence of NBS interventions. A percentage-based comparison was also performed to evaluate the effectiveness of each scenario relative to the baseline scenario. The key output layers considered in this study resulting from the SMA model include the average annual cumulative values (mm/year) for aquifer recharge, infiltration, direct runoff, and base flow.

While all strategies showed distinct impacts on the hydrological cycle, sand dams and semi-circular soil bunds offer substantial benefits, particularly in eliminating direct runoff (100% elimination) and sustaining base flow (3-15%), with semi-circular soil bunds showing slightly higher efficiency in recharging aquifers (11-15%) than sand dam (3-6%). Increased vegetation cover, however, stands out for its superior performance in aquifer recharge (16-17%) and base flow enhancement (17-18%), making it an effective strategy for long-term water resource sustainability.

TABLE OF CONTENTS

1 INTRODUCTION 12

1.1 STUDY OUTLINE 14
1.1.1 SOURCE OF THE STUDY 14
1.1.2 AIM OF THE STUDY 15
1.1.3 DISCIPLINARY FIELD OF REFERENCE 15
1.1.4 OBJECTIVES AND METHODS 15
1.1.5 EXPECTED RESULTS AND FUTURE DEVELOPMENTS 16
1.2 OVERVIEW OF SOMALILAND'S CLIMATE 16

2 DATA AND METHODS 17

2.1 STUDY AREA 17
2.1.1 CLIMATIC ZONES OF SOMALILAND 19
2.1.2 RAINFALL DISTRIBUTION IN SOMALILAND 20
2.1.3 CLIMATE VARIABILITY AND LIVELIHOOD SITUATION IN SOMALILAND 21
2.2 HYDROGEOLOGY 24
2.3 RAIN GAUGE DATA 25
2.4 GLOBAL PRECIPITATION DATASETS 26
2.4.1 THE CLIMATE HAZARDS GROUP INFRARED PRECIPITATION (CHIRPS) 27
2.4.2 GLOBAL PRECIPITATION MEASUREMENT (GPM) 28
2.4.3 ERA5-LAND 29
2.5 COMPARISON OF RAINFALL DATASETS 29
2.5.1 PIXEL VS. POINT COMPARISON 32
2.6 POTENTIAL EVAPOTRANSPIRATION DATA 35
2.7 A SIMPLE HYDROLOGICAL MODEL 36
2.7.1 SOIL MOISTURE ACCOUNTING (SMA) 36
2.7.2 SCS-CURVE NUMBER 41
2.7.3 CANOPY METHOD 41
2.7.4 SURFACE METHOD 41
2.7.5 CLARK UNIT HYDROGRAPH- TRANSFORM METHOD 41
2.7.5.1 TIME OF CONCENTRATION 42
2.7.6 LINEAR RESERVOIR- BASE FLOW 42
2.8 NATURE-BASED SOLUTIONS 48
2.8.1 SAND DAMS 49
2.8.1.1 Sensitivity Analysis for Maximum Infiltration Rate 50
2.8.1.2 Experimental Design 51
2.8.2 SEMI-CIRCULAR SOIL BUNDS 52
2.8.2.1 Experimental Design 52
2.8.3 INCREASED VEGETATION COVER 56

3 RESULTS 60

3.1 SAND DAM IMPLEMENTATION 60
3.1.1 ANALYSIS OF MAXIMUM INFILTRATION RATE (MIR) PARAMETER 60
3.1.2 ANALYSIS OF SURFACE STORAGE (SS) PARAMETER 62
3.1.3 ANALYSIS OF SOIL STORAGE (SoilS) PARAMETER 63
3.1.4 ANALYSIS OF COMBINED PARAMETER CHANGES ON HYDROLOGICAL OUTPUTS 65
3.2 SEMI-CIRCULAR SOIL BUND IMPLEMENTATION 66
3.2.1 ANALYSIS OF MAXIMUM INFILTRATION RATE (MIR) PARAMETER 66
3.2.2 ANALYSIS OF SURFACE STORAGE (SS) PARAMETER 68
3.2.3 ANALYSIS OF SOIL STORAGE (SoilS) PARAMETER 70
3.2.4 ANALYSIS OF COMBINED PARAMETER CHANGES ON HYDROLOGICAL OUTPUTS 72
3.3 AN INCREASED VEGETATION 74

3.3.1 ANALYSIS OF MAXIMUM INFILTRATION RATE (MIR) PARAMETER 74
3.3.2 ANALYSIS OF SURFACE STORAGE (SS) PARAMETER 75
3.3.3 ANALYSIS OF SOIL STORAGE (SoilS) PARAMETER 77
3.3.4 ANALYSIS OF COMBINED PARAMETER CHANGES ON HYDROLOGICAL OUTPUTS 79

4 DISCUSSION ON ANALYSIS 81

4.1 PERCENTAGE CHANGE IN HYDROLOGICAL PARAMETERS DUE TO SAND DAM 81
4.2 PERCENTAGE CHANGE IN HYDROLOGICAL PARAMETERS DUE TO SEMI-CIRCULAR SOIL BUNDS 82
4.3 PERCENTAGE CHANGE IN HYDROLOGICAL PARAMETERS DUE TO AN INCREASED VEGETATION COVER . 83

5 CONCLUSION 85

6 REFERENCES 87

APPENDIX A: MEAN MONTHLY PET IN SOMALIA (1963-1990) 93

LIST OF FIGURES

Figure 1 Map of 37 major global aquifers [7] 13
Figure 2 Darar-weyne Basin – Location map 18
Figure 3 Aerial View of the village of Darar-weyne [19] 18
Figure 4 Somaliland climate zones [17] 19
Figure 5 Somaliland mean annual rainfall spatial distribution [17] 20
Figure 6 Annual spatial distribution of drought in Somaliland from 1981 to 2020 [23]. 22
Figure 7 The Berkad [24] 23
Figure 8 Geological frame – PCB: Precambrian basement – YE: Yesomma Fm – AU: Auradu Fm – AL: alluvial deposits – BAS: basalts – red dashed lines: supposed faults ((Source: Construction Investment Report - Darar-weyne Site [19]) 25
Figure 9 (a) Manual Rainfall stations in Somaliland [26] (b) Rain gauges near Darar-weyne Basin 26
Figure 10 Darar-weyne Basin and weather stations over which rainfall data from CHIRPS, GPM and ERA5-Land are acquired 27
Figure 11 Global Precipitation datasets (CHIRPS, GPM, ERA5-LAND) average rainfall at the location of Hargeisa Station (2000-2023) 30
Figure 12 Global Precipitation datasets (CHIRPS, GPM, ERA5-LAND) average rainfall at the location of Dararweyne Station (2000-2023) 31
Figure 13 Cumulative yearly rainfall of Hargeisa station and Satellite derived Rainfall (2005-2023) 33
Figure 14 Cumulative yearly rainfall of Dararweyne station and Satellite derived Rainfall (2011-2023) 33
Figure 15 Average cumulative monthly rainfall data comparison between the Hargeisa weather station and the GPM rainfall 35
Figure 16 Mean monthly PET, Hargeisa Station 35
Figure 17 Conceptual Schematic of the Soil Moisture Accounting Method (Source: Bennett, 2000 [38]) 37
Figure 18 The conceptual model of Clark method (Source: Yannopoulos, S et al, 2013 [43]) 42
Figure 19 Hydrograph generated by initial SMA method simulation 45
Figure 20 Hydrograph generated by SCS-CN method simulation 45
Figure 21 Hydrograph generated by SMA method simulation after the adjustment of parameters with SCS-CN model 46
Figure 22 Conceptual model of Darar-weyne basin with subbasins created by GIS extension in HEC HMS 47
Figure 23 Schematic diagram of a sand dam showing important flow components (Source: Bouzouidja ,2021 [47]).. 50
Figure 24 Sand Dam considered in Subbasin-4 50
Figure 25 Semi-circular soil bund 52
Figure 26 Semi-circular soil bunds considered in Subbasin-2 53
Figure 27 Semi-circular soil bund dimensions by FAO for 2% slope 54
Figure 28 Semi-circular bunds field layout by FAO for slope 2% 54
Figure 29 Land Cover and NDVI Map of the Darar-weyne basin 57
Figure 30 MODIS Land Cover Type- Legend 58
Figure 31 Increased vegetation cover considered in Subbasin-1 59
Figure 32 Hydrological fluxes, baseline scenario without NBS interventions 60
Figure 33 Hydrological fluxes resulting from Maximum Infiltration Rate (MIR) Analysis, Sand Dam 61
Figure 34 Hydrological fluxes resulting from Surface Storage (SS) Analysis, Sand Dam 62
Figure 35 Hydrological fluxes resulting from Soil Storage (SoilS) parameter, Sand Dam 64
Figure 36 Hydrological fluxes resulting from combined parameter Maximum Infiltration Rate (MIR), Surface Storage (SS), Soil Storage (SoilS) changes, Sand Dam 65
Figure 37 Hydrological fluxes resulting from Maximum Infiltration Rate (MIR) Analysis, Semi-circular soil bunds 67
Figure 38 Hydrological fluxes resulting from Surface Storage (SS) Analysis, Semi-circular soil bunds 68
Figure 39 Hydrological fluxes resulting from Soil Storage (SoilS) Analysis, Semi-circular soil bunds 71
Figure 40 Hydrological fluxes resulting from combined parameter Maximum Infiltration Rate (MIR), Surface Storage (SS), Soil Storage (SoilS) changes, Semi-circular soil bunds 72

FIGURE 41 HYDROLOGICAL FLUXES RESULTING FROM MAXIMUM INFILTRATION RATE (MIR) ANALYSIS, INCREASED VEGETATION COVER 74
FIGURE 42 HYDROLOGICAL FLUXES RESULTING FROM SURFACE STORAGE (SS) ANALYSIS, INCREASED VEGETATION COVER 76
FIGURE 43 HYDROLOGICAL FLUXES RESULTING FROM SOIL STORAGE (SOILS) ANALYSIS, INCREASED VEGETATION COVER 77
FIGURE 44 HYDROLOGICAL FLUXES RESULTING FROM COMBINED PARAMETER MAXIMUM INFILTRATION RATE (MIR), SURFACE STORAGE (SS), SOIL STORAGE (SOILS) CHANGES, INCREASED VEGETATION COVER 79
FIGURE 45 PERCENTAGE CHANGE IN HYDROLOGICAL FLUXES ACROSS SCENARIOS WITH SAND DAMS (SS: SURFACE STORAGE, MIR: MAXIMUM INFILTRATION RATE, SOILS: SOIL STORAGE) 81
FIGURE 46 PERCENTAGE CHANGE IN HYDROLOGICAL FLUXES ACROSS SCENARIOS WITH SEMI-CIRCULAR (SS: SURFACE STORAGE, MIR: MAXIMUM INFILTRATION RATE, SOILS: SOIL STORAGE) 82
FIGURE 47 PERCENTAGE CHANGE IN HYDROLOGICAL FLUXES ACROSS SCENARIOS WITH INCREASED VEGETATION COVER (SS: SURFACE STORAGE, MIR: MAXIMUM INFILTRATION RATE, SOILS: SOIL STORAGE) 83

LIST OF TABLES

TABLE 1 COMPARISON BETWEEN THE CUMULATIVE ANNUAL RAINFALL BETWEEN THE HARGEISA STATION AND THE SATELLITE DERIVED RAINFALL AT THE STATIONS 34
TABLE 2 COMPARISON BETWEEN THE CUMULATIVE ANNUAL RAINFALL BETWEEN THE DARARWEYNE STATION AND THE SATELLITE DERIVED RAINFALL AT THE STATIONS 34
TABLE 3 SELECTED BASIN AND METEOROLOGICAL METHODS 43
TABLE 4 SELECTED PARAMETERS FOR SMA IN HEC-HMS 46
TABLE 5 CHARACTERISTICS OF THE DARAR-WEYNE SUBBASINS 47
TABLE 6 TIME OF CONCENTRATION VALUES 48
TABLE 7 PARAMETERS FOR THE SAND DAM NBS 52
TABLE 8 SEMI-CIRCULAR SOIL BUND DESIGN PARAMETERS AT DIFFERENT % SLOPES 53
TABLE 9 SEMI-CIRCULAR SOIL BUND CLASSES BASED ON BUND HEIGHTS 55
TABLE 10 MAX INFILTRATION RATE (MM/HR) VALUES FOR BUNDS FROM LITERATURE 55
TABLE 11 SURFACE STORAGE (MM) PARAMETER FOR SEMI-CIRCULAR SOIL BUNDS 56
TABLE 12 SOIL STORAGE (MM) PARAMETER FOR SEMI-CIRCULAR SOIL BUNDS 56
TABLE 13 PARAMETERS FOR THE INCREASED VEGETATION COVER NBS 59
TABLE 14 SUMMARY OF PERCENTAGE CHANGES IN HYDROLOGICAL FLUXES COMPARED TO THE BASELINE SCENARIO FOR SAND DAMS, SEMI-CIRCULAR SOIL BUNDS, AND INCREASED VEGETATION COVER 84

1 INTRODUCTION

A supply of clean, adequate, and safe water supply is a most fundamental human need and human right. Yet, according to United Nations (UN) estimates in 2003, more than 1.1 billion people are estimated to lack access to safe drinking water [1]. Hence, the efficient use and the adoption of strategies and infrastructure to increase the amount of available water resources, is of key importance in improving livelihoods, amid the growing population in drylands [2]. Dry lands cover about 5.2 billion hectares, a third of the land area of the globe. Roughly one fifth of the world population lives in these areas. The main feature of "dryness" is the negative water balance between the annual rainfall (supply) and the evaporative demand [3].

Somaliland is a water-scarce country as it regularly experiences water shortages during the dry season and recurrent droughts [4]. Dry soil is less capable of absorbing water, and arid and semi-arid lands stretch across 80 per cent of the Somali landmass. In the central semiarid parts (i.e. dry areas that still receive some rain), the rainfall is as low as 50–100 mm/year [5].

Depletion of groundwater, which provides fresh water for >1500 million people around the world is one of the leading causes of water scarcity in many areas around the globe [6], including Somaliland State. The growing population and increasing water demand have added more stress on traditional water resources. Climate change has further worsened this water crisis as it creates a large uncertainty in predicting the availability and natural replenishment of local water resources. Over the past century, groundwater has been overexploited to meet growing agricultural demand and industrial use both of which constitute 69% of total groundwater use. Around 21 out of 37 major global aquifers have already been depleted. The depletion is disproportionally severe in semi-arid or arid regions [6]. Figure 1 shows a map of 37 major global aquifers acquired from GRACE data from NASA [7]. GRACE is a collaboration of the US and German space agencies (NASA and DLR). The GRACE twin satellites, launched 17 March 2002, have been making detailed measurements about Earth's water reservoirs over land, ice and oceans, as well as earthquakes and crustal deformations [8]. Map shows the depletion and replenishment in millimeters of water per year [7].

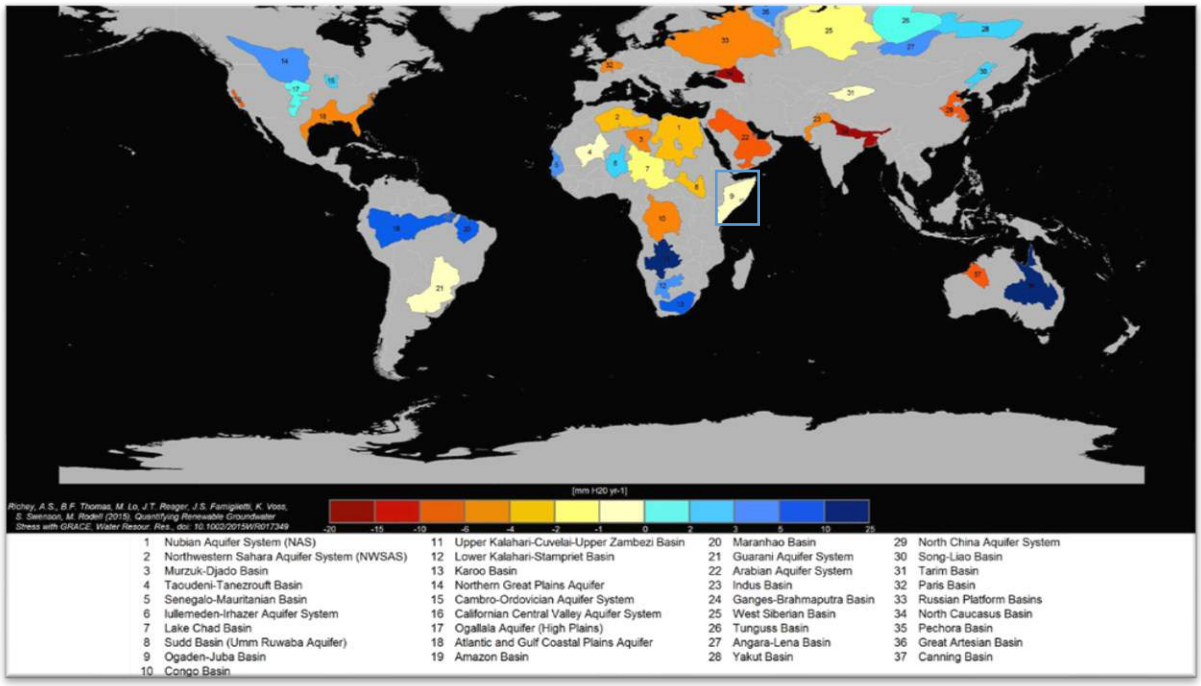

Figure 1 Map of 37 major global aquifers [7]

The relevant aquifer for Somaliland is the Ogaden-Juba Basin which is marked with number 9 on the map. The light-yellow color on the map indicates a slight depletion of groundwater.

Managed Aquifer Recharge (MAR), the intentional act of recharging water into an aquifer for later use, is becoming an increasingly important tool for balancing water supply and demand over time. Three objectives commonly defined for MAR are to (1) maximize the amount of water infiltrated, (2) maximize the amount of water recovered, and (3) maximize the improvement in quality of recovered water [9]. Among different types of groundwater management strategies MAR is a popular one because of its low implementation cost, low evaporation loss compared to surface reservoir, and ability to infiltrate large volume of water from different sources, including river or stream waters, urban and agricultural runoff, and treated municipal wastewater. MAR methods are designed to intentionally infiltrate water from different sources into an aquifer and extract the treated water for later use [6]. The extent to which MAR can achieve its potential for water supply will depend on an understanding of the capabilities and limitations of various techniques that may be used to implement it within a catchment. These techniques can be aquifer storage and recovery, aquifer storage transfer and recovery, bank filtration, dune filtration, infiltration ponds, percolation tanks, rainwater harvesting, soil aquifer treatment, underground dams and sand dams [10]. However, the implementation of these techniques is often hindered by gaps in hydrogeological data, particularly in data-scarce regions like Somaliland. The present study aims to bridge this gap

by obtaining hydrological data, such as rainfall, from global precipitation datasets and determining key parameters such as infiltration rate and storage capacity of a soil from existing literature. By addressing these data limitations, the research enhances the feasibility and effectiveness of MAR strategies.

Somaliland has an arid to semi-arid climate [11]. They are generally defined as regions where rate of evaporation is greater than precipitation [12]. Arid areas are extremely susceptible to climate variability [13]. Being dry already, a more irregular availability of water is bound to generate greater impacts due to which they have limited natural water resources, and are vulnerable to extreme occurrences such as droughts and heatwaves which also results in rapid environmental and land degradation [13]. These factors threaten the livelihoods of local communities, many of whom practice pastoralism, a way of life that depends on dryland resources [11], chief among which is precipitation. The amount of precipitation received by a territory plays a crucial role in water resource planning, agriculture activities, and disaster mitigation. Accurate precipitation data is required for evaluating long-term water resources availability and for the calibration and validation of hydrological models to model extreme events (e.g., floods and droughts). The most reliable and accurate way of measuring precipitation is from ground-based rain gauges. However, rain-gauge networks are typically sparse, particularly in remote areas and developing countries, and have been active for a limited number of years [14]. As a result, the acquisition of reliable and consistent precipitation series is a challenging task throughout the world. The advent of global precipitation datasets including gauge-based, satellite-related, and reanalysis datasets, brings an unprecedented opportunity for precipitation estimation and hydrological application [15].

1.1 STUDY OUTLINE

1.1.1 SOURCE OF THE STUDY

The present study is the result of a collaboration between the University of Padova and Hydro Nova s.r.l. The motivation of the work originates from the recent and ongoing project pursued by Hydro Nova, the Water for Rural Resilience Project 'Barwaaqo,' funded by the World Bank in collaboration with the Somalia and Somaliland Ministries of Planning.

The 'Barwaaqo' project endeavors to provide support to the Federal States Government and to Somaliland in selecting the location, conducting field survey, design and monitoring supervision for 105 water harvesting structures. In addition, the project focuses on the identification of sustainable land management approaches around the newly created water

withdrawal points, which includes adaptation to climate change vulnerabilities and focused climate mitigation measures. The project aims to provide water to an estimated 500,000 people, or 15% of the rural population who currently only have access to limited service or unimproved water.

1.1.2 AIM OF THE STUDY

This thesis aims to contribute to UN sustainable development goal no. 6, 'Clean Water and Sanitation', by enhancing access to clean water for vulnerable population of Somalia.

1.1.3 DISCIPLINARY FIELD OF REFERENCE

This thesis lies within the realm of hydrology, water engineering, and sustainable development, focusing on nature-based Managed Aquifer Recharge techniques in regions with limited data availability, with a focus on Somaliland State.

1.1.4 OBJECTIVES AND METHODS

Somaliland, similarly to many Countries in Africa and globally, is characterized by hydrological data scarcity while facing immense challenges in accessing clean water, particularly in its rural communities. The lack of hydrological and hydrogeological information, combined with land and vegetation degradation, exacerbated by climatic challenges, set significant limitations in the ability to identify sustainable water management strategies and access aquifers resources. This underscores the urgent need for sustainable water management strategies. The present Thesis seeks to address these challenges by investigating the potential of MAR approaches, such as semi-circular soil bunds and sand dams, to improve infiltration rates, and to introduce and expand vegetated areas, in order to provide clean water to rural populations.

A major limitation in sustainable water strategies in data-scarce regions like Somaliland, is the lack of data on the hydrologic cycle, which prevents the identification of areas and sites suitable for increasing rainfall infiltration to recharge the aquifer and of information on which the most suitable measure can be selected and sized in order to fill this observational gap. The present work uses global precipitation datasets, such as CHIRPS, GPM, and ERA5-Land in conjunction with hydrological modeling, using the Soil Moisture Accounting method within HEC-HMS, to identify suitable MAR techniques and to analyze the impact of nature-based solutions in recharging the aquifer to support local water needs. The study explores three

nature-based solutions - sand dams, semi-circular soil bunds, and increased vegetation cover, particularly grasslands - and analyzes their impacts on aquifer recharge.

1.1.5 EXPECTED RESULTS AND FUTURE DEVELOPMENTS

The expected results of this experimental thesis include identifying optimal MAR techniques for implementation in Somaliland, to define sustainable water management approaches in data-scarce regions, and contributing to the resilience of rural communities, against water scarcity. The practices and methods developed within the thesis are also expected to contribute to the wider global goal of sustainable aquifer management in data-scarce regions.

1.2 OVERVIEW OF SOMALILAND'S CLIMATE

Somaliland is situated 78° north of the equator. Climatically, it is semiarid. The average daily temperatures range from 25°C to 35°C [16]. The highest temperatures are experienced in the months of June through September, becoming cooler in January and February when temperatures decrease substantially to as low as 15 °C [17]. The humidity in the country varies from 63% in the dry season to 82% in the wet season [16]. Potential Evaporation Transpiration (PET) varies between 1000 to 3000 mm/year with mean annual values for the region being greater than 2000 mm/year. PET exceeds rainfall across the region and is highest in dry seasons with values between 280 mm/month inland and 440 mm/month in the coastal areas [17]. The annual rainfall in Somaliland ranges 200 mm in coastal area to 600 mm in mountains area [4]. The rest of Somaliland receives an annual rainfall of 200 to 300mm [18]. The mean annual rainfall map of Somaliland is provided in section 2, Figure 5 of this report.

2 DATA AND METHODS

2.1 STUDY AREA

The Darar-weyne basin, located about 500 meters to the Dararweyne village and about 25 kilometers northeast of the capital city Hargeisa and in the Somaliland State (Latitude: 9.7203°, Longitude: 44.2293°), was selected as the study area (Figure 2). The Darar-weyne basin, covers an area of 109.35 km².

The Dararweyne village (Figure 3) is home to approximately 1,500 households that rely mainly on farming, and approximately 300 nomadic families that rely on water availability at the site during the dry season. Livestock, including camels, goats, cattle and donkeys play a significant role in the local economy. The main water sources of the community are shallow wells located about 500 m distance in the wadi next to the village. The community is anyway served by water trucking. Currently, the community pays for water delivered by water trucking all the year. In particular, the cost of raw water can be as high as 3 $/m^3 delivered by trucks [19].

The Republic of Somaliland is located in the Horn of Africa. It has the Gulf of Aden to the North and shares borders with Djibouti to the West, Ethiopia to the South, and Somalia to the East (Figure 2). The total area of the Republic of Somaliland is 137,600 km^2 with a coastline of 850 km along the Red Sea [16]. It is home to a population of four million [20]. Approximately 55% of the population lives in rural areas, and 45% lives in urban centers [11].

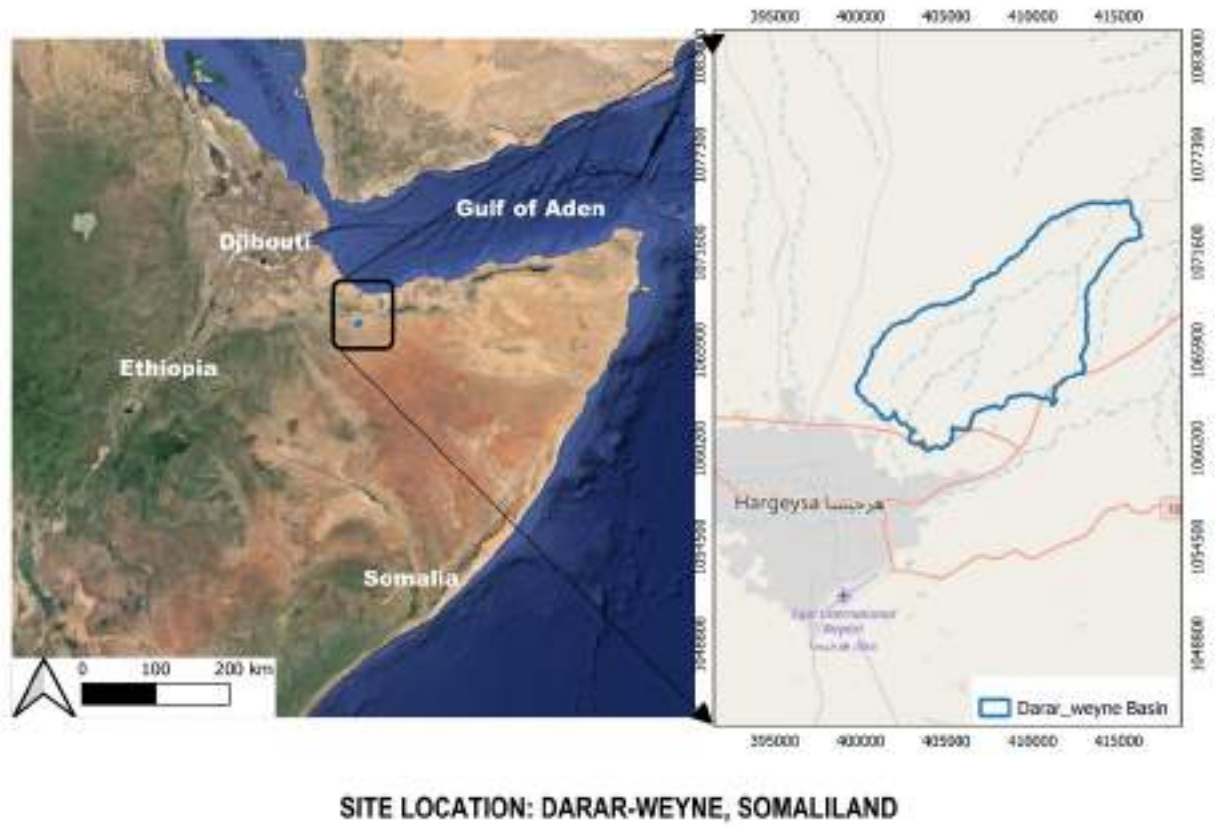

Figure 2 Darar-weyne Basin – Location map

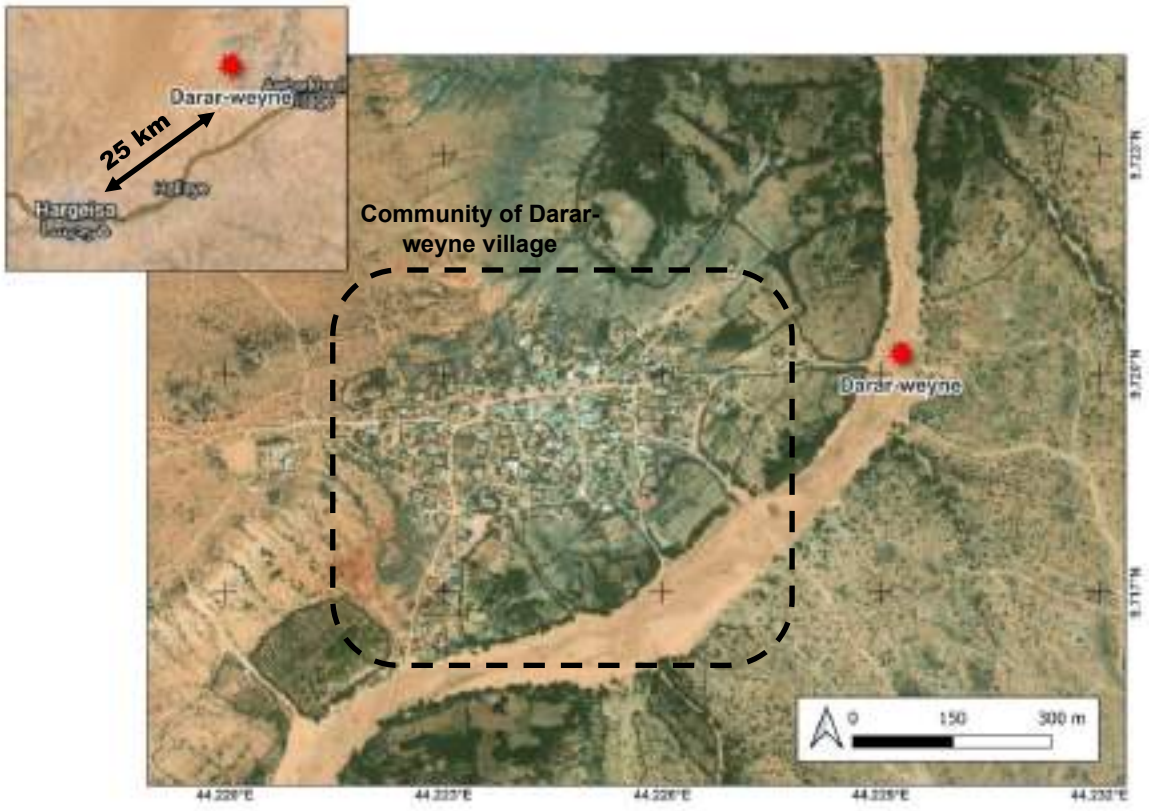

Figure 3 Aerial View of the village of Darar-weyne [19]

2.1.1 CLIMATIC ZONES OF SOMALILAND

Somaliland has three major climate zones; (a) desert zone mainly along the coastal belt, (b) very arid zone in the central and western areas and (c) semi-arid zone in the lower parts of Awdal and Waqooyi Galbeed as shown in Figure 4. Study area of the Darar-weyne basin is in the semi-arid climate zone.

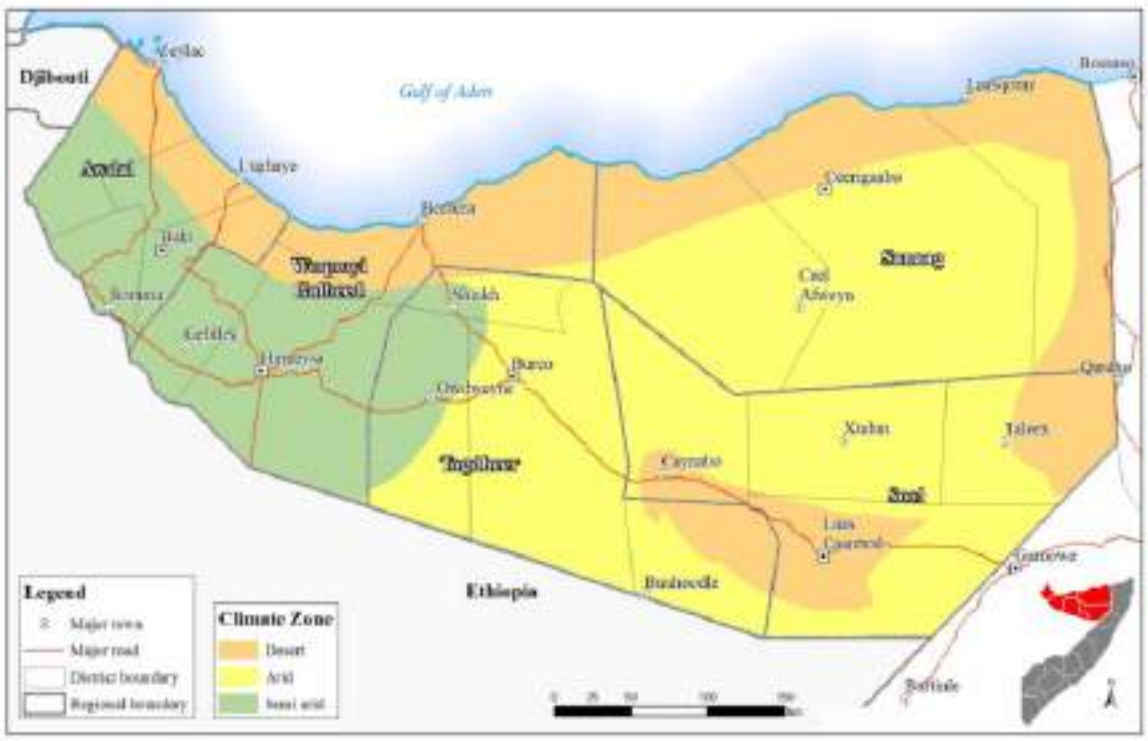

Figure 4 Somaliland climate zones [17]

The three zones are further elaborated below:

• **Desert zone:** This zone receives less than 100 mm of annual rainfall and the rain seasons lasts for one month only. The coastal belt of Somaliland and a small portion in southern Sool region falls under this kind of climate. Major towns in this zone include Zeylac, Lughaye, Berbera, Lasqooray and Laas Caanood. The desert zone is unsuitable for cropping and pastoralism which is the common land use.

• **Arid zone:** This zone receives less than 400 mm of annual rainfall and the rain season lasts for a maximum of three months. Rainfall usually comes in heavy showers and a large proportion is lost through runoff. Although cropping is possible, irrigation is absolutely essential for success. High temperatures are experienced throughout the year. This zone covers the central and eastern parts of Somaliland and includes town such as Ceerigabo, Ceel Afweyne, Burco and Xudun.

• **Semi-arid zone:** This zone receives 400 to 600 mm of annual rainfall with the rainfall seasons slightly exceeding three months. Rainfed cropping is possible but irrigation is indispensable for reliable and good crop harvests. Some drought-resistant crops such as sorghum and millet may give reasonable yields without irrigation, but there is still a risk of unreliable rainfall and subsequent crop failure. The zone includes inland areas of Awdal and Waqooyi Galbeed regions in the western parts of Somaliland which plays a major role in production of most important food crops for the whole of Somaliland [17].

2.1.2 RAINFALL DISTRIBUTION IN SOMALILAND

Mean annual rainfall situation across Somaliland is evident from Figure 5. The lower parts of Awdal and Waqooyi Galbeed regions receive the best rainfall with values between 500 to 600 mm per year. The Central and Eastern parts of Somaliland including Togdheer, Sool and Sanaag regions come next with rainfall values of 100 to 400 mm per year. The rest of the country, particularly the coastal belt and a small pocket of the area south of Sool region are characterized by very low rainfall with values less than 100 mm per year [17].

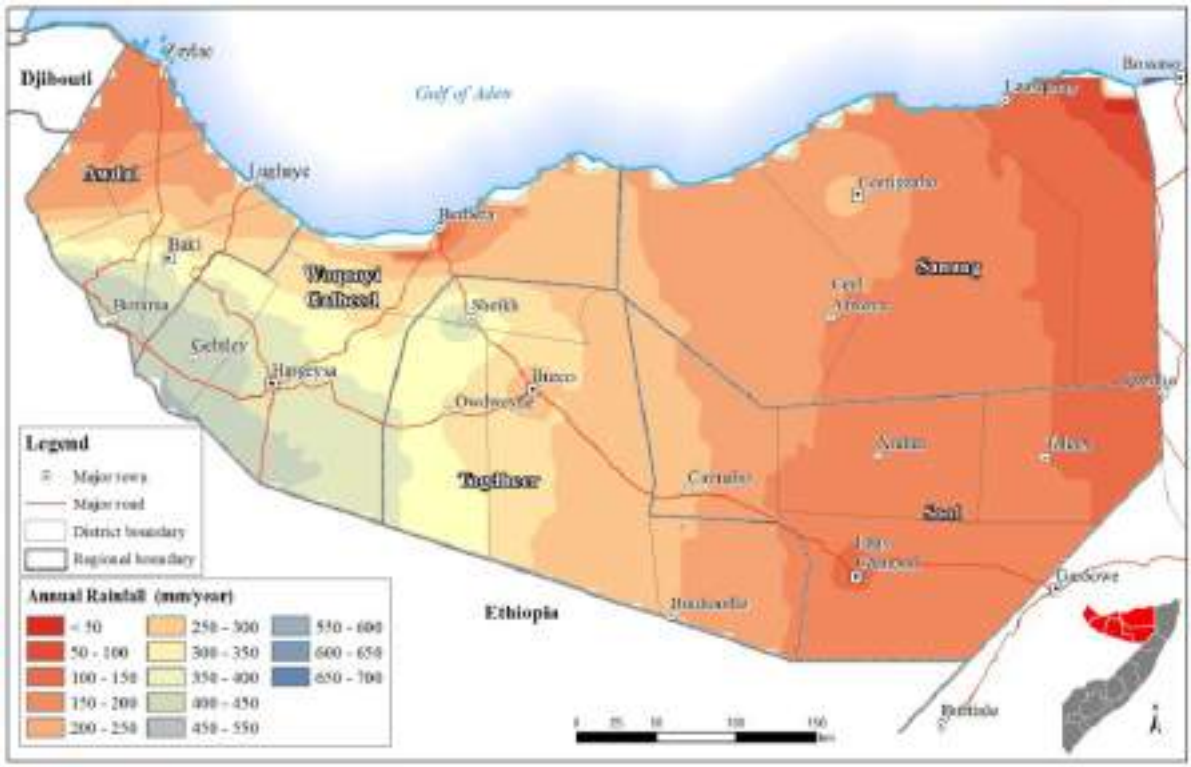

Figure 5 Somaliland mean annual rainfall spatial distribution [17]

This modest rainfall is distributed across two rain seasons that are interspaced by two dry seasons. The four seasons experienced in Somaliland are summarized below:

• **Gu:** This is the long rainy season, lasting from late March to mid June with relatively wet and hot conditions. During this season, there is plenty of water in most areas and is a breeding period for the livestock [17]. On average this season provides about 60% of the total yearly rainfall [4].

• **Deyr:** This is the short rainy season lasting form October to November. The rainfall received is less than that of the Gu rainy season [17] as it accounts 20-30% of total rainfall [21].

• **Jiilaal:** This is a dry season occurring from December to mid March. During this season the region experiences cool and dry air.

• **Hagaa:** This is a dry season occurring from late June to September. Though generally a dry season, there are areas that receive scattered showers including Baki, Borama, part of Oodweyne and Hargeisa. Other parts remain very windy and dry [17].

2.1.3 CLIMATE VARIABILITY AND LIVELIHOOD SITUATION IN SOMALILAND

Several studies examining the impacts of climate variability and changes in livelihoods in Somaliland have demonstrated that climate variation has harmed the livelihoods of the people of Somaliland [11] who are mainly dependent on the livestock subsector, which mainly relies on pastures and naturally-occurring vegetation [2]. Surface water sources rarely meet the demand for livestock water, especially during the dry season [22] as Somaliland is characterized by large variability in rainfall patterns as seen in Figure 5, and uncontrolled use of water resources [2]. It is observed that climate variability in Somalia region, including Somaliland is under desertification conditions. The United Nations Convention on Combat Desertification in 2020 defines severe drought as a situation in which rainfall decreases for two or more consecutive years in a certain region [11]. Figure 6 is acquired from a study conducted in 2022 that examined the spatial and temporal patterns of drought in Somaliland from 1981 to 2020 using Standardized Evapotranspiration Index (SPEI). The SPEI base is a global, long-term dataset based on monthly precipitation and potential evapotranspiration from the Climate Research Unit of the University of East Anglia. The spatial resolution of the dataset is 0.50 x 0.50 degrees, and the temporal resolution is monthly. A drought event is identified when the SPEI values are continuously negative and reach a value of -1.0 or less [23]. The study measured drought severity and found a significant increase in drought frequency and intensity [11] in Somaliland.

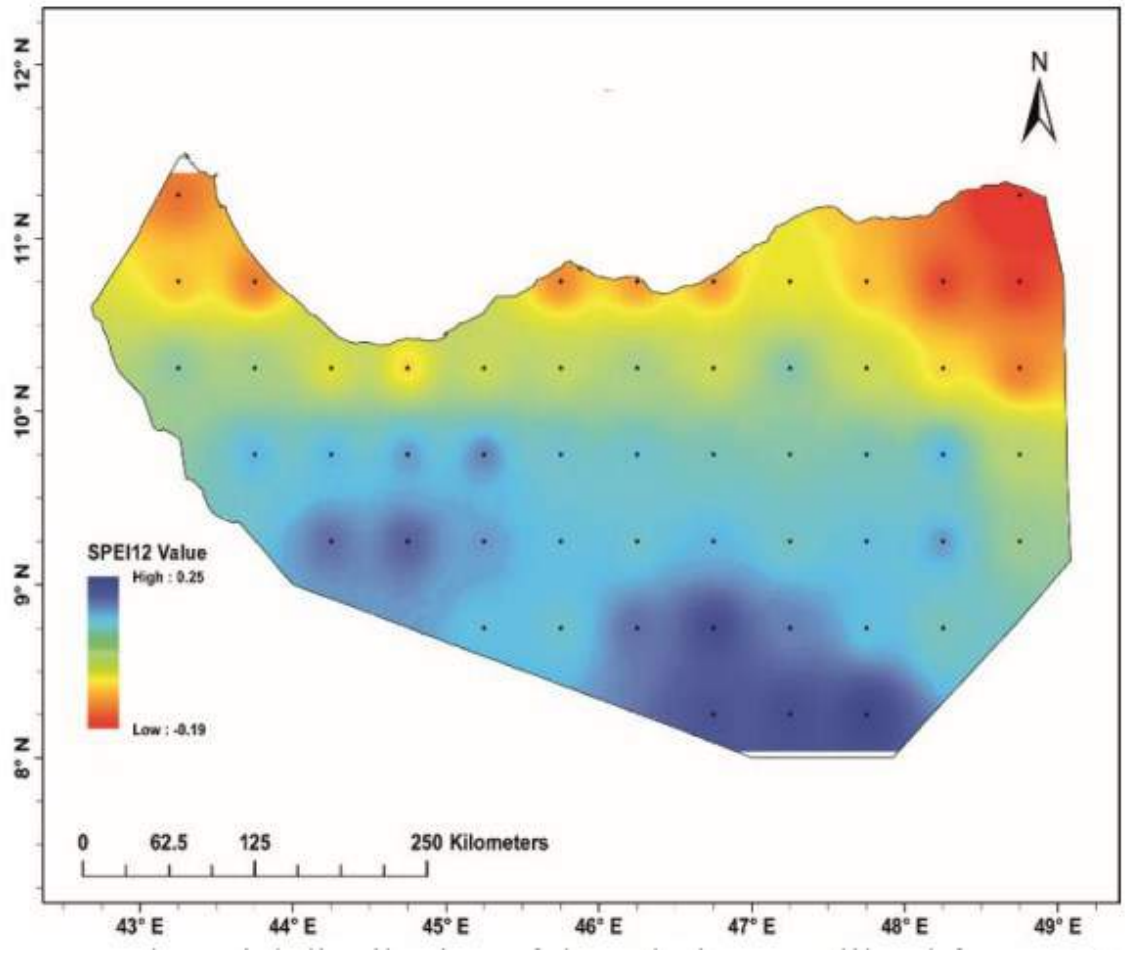

Figure 6 Annual spatial distribution of drought in Somaliland from 1981 to 2020 [23].

The annual spatial distribution of drought represented by SPEI values indicate that the northern part of the country, particularly the northwestern and northeastern regions, experienced severe drought. These are the country's coastal areas, where the rainfall is very low [23] as low as less than 100 mm of annual rainfall [17] and the temperature is high. Generally, drought conditions decreased from the country's north (coast) to the south (inland), as indicated in Figure 5 [23].

Somaliland suffered 11 severe droughts from 1964 to 2017. The most devastating events occurred in 1973–1974, 1984, 1991, 2010/2011, and 2016/2017, affecting the Sanaag, Togdheer, and Sool Regions for prolonged periods. These droughts caused damage and losses that exceeded USD 874 million. Drought is also the main cause of livestock deaths, up to 60% in Somaliland, severely affecting pastoralists livelihoods. According to the United Nations and UNICEF, drought emergencies in Somaliland and Somalia have dire consequences for millions of people. They displaced 771,400 people searching for water, food, and pasture and put more than 1.4 million children at risk of acute malnutrition. The drought impacted 6.1

million Somalis in total where more than 1.15 million people left their homes between January 2016 and May 2018, often when they were already weak and hungry from the drought [23].

In present, ground water is the only major water resource for people in Somaliland [17] as there are no major rivers or other major permanent surface water resources in the country [22]. However, ground water availability is not sufficient due to increasing climatic impacts [17] on livelihoods and also due to recurring droughts. Rural communities have to rely on other water sources, mainly springs and shallow wells in the mountainous areas and the coastal plain, and berkads, and balleys (dams) at the plateau [22]. A berkad is a catchment for the surface run-off resulting from intense rainfall episodes. It is typically constructed in areas of gently sloping terrain and in its most evolved form, it is lined with masonry and/or concrete and often comprise a small catch-pool to trap sediment. During rainy periods, the berkad may fill in a matter of hours, and may last for several months throughout a dry period. Figure 7 shows a berkad structure [24]. Evaporation accounts for significant water loss from berkads due to high temperatures experienced. To reduce loss, people cover berkads with locally available material, e.g. tree branches and shrubs.

Figure 7 The Berkad [24]

Balleys are the other surface water sources used in Somaliland. They range in size from small harvesting balleys to big earth dams with capacities up to 150 000 m^3. Six high-capacity earth dams were built in rural Somaliland in the 1980s. Although a problem with balleys is the siltation and long-term damage of the dam. However, berkads and earth dams contributed significantly to water availability in the regions before 1991. The local communities of the Somaliland have adopted different means of coping with water shortages, some agro-pastoralist households harvest and store rainwater in underground ditches with capacities of about 6m^3. Groundwater movement and availability varies from place to place, depending on the geology and hydrogeology of a particular area. In mountainous regions the water table is only a few meters below the surface, making shallow wells a common source of water. The depth of shallow wells in this area ranges from 5 m to about 20m. On the plateaus the water table is quite deep, and only boreholes can be used for subsurface water supply during dry periods. Boreholes can reach depths of 400 m below the surface [22].

This highlights the scarcity of water for the population of Somaliland. As a result, the Somaliland government acknowledges that the management and utilization of the country's water resources are crucial to promoting public health, economic independence, good governance, and social peace [25]. The low effective rainfall experienced in different part of the regions calls for under-ground water development such as MAR strategies as a viable solution to water shortages [22].

2.2 HYDROGEOLOGY

The Darar-weyne basin in the village of Dararweyne is located on a rocky hill, made by Precambrian basement (PCB), at an elevation of 1,080 m asl, some 22 km NE of the capital Hargeisa. In the area north of the basement outcrop important aquifers (Geed Deedle, Laas Durreh, Jaleelo-Xomboweyne), up to 200 m thick, are hosted in the tectonics valleys filled by sandy-silty deposits. In the streams are present minor aquifers (Dararweyne, Awbarakhadle), few meters thick, with a seasonal behavior but, for the most, never dry; the shallow aquifers too contribute to supply the town of Hargeisa by water trucking. Both deep and shallow aquifers have a good water quality.

The hill is cut by a wadi that is bordered by rocky outcrops and alluvial terraces where farming activity develops (refer to Figure 3). The area is at the western edge of a wide PCB strip that marks the higher section of the Haud plateau. Southward of the PCB outcrop a long and important fault drops at depth of 200-500 m the basement and the Yesomma Sandstones Fm

(YE, Cretaceous), covered by sandy alluvial/aeolian deposits, extends. More southward the hills of the Auradu limestones Fm (AU, Eocene) cover the Yesomma Fm. Northward the basement is carved by deep tectonic valleys filled by thick alluvial deposits (AL), that host powerful aquifers. More northward a wide basalt flow covers (BAS, Mio-Pliocene) directly the PCB and extends at depth below the Dhamal fan-like structure. The observation from the hand-dug wells at the downstream part of the Darar-weyne, with depths of 4.5-5.0 m, indicates that the first 3-3.5 m are excavated in sandy deposits, while the last section, according to information provided by the community representatives, penetrates the weathered basement. The rest of the basin is observed to have 3-3.5 m of sandy alluvial/aeolian deposits, followed by sandstone. Figure 8 summarizes the geology of the area surrounding the Darar-weyne basin [19].

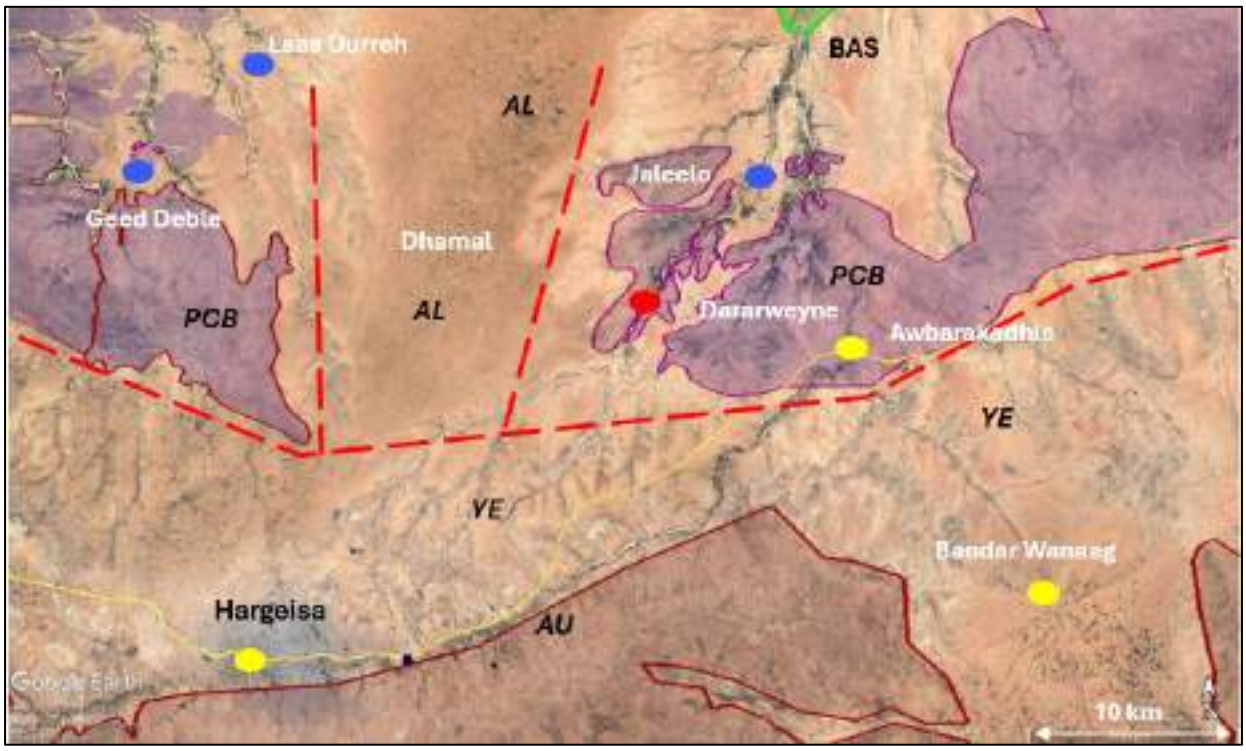

Figure 8 Geological frame – PCB: Precambrian basement – YE: Yesomma Fm – AU: Auradu Fm – AL: alluvial deposits – BAS: basalts – red dashed lines: supposed faults ((Source: Construction Investment Report - Darar-weyne Site [19])

2.3 RAIN GAUGE DATA

The amount of precipitation in a region is a crucial first step in developing a hydrological study. Observed rainfall data from two nearby gauges in the Darar-weyne basin, namely Hargeisa and Dararweyne, are accessible through the FAO-SWALIM [26] website for the years 2005-2024 and 2011-2024, respectively. The Botor rainfall station, which is also in close proximity to the basin, is a recent station with data available starting in 2016. Given the short

operation time it was not considered here. Hargeisa (Latitude: 9.55975°, Longitude: 44.0668°) and Dararweyne (Latitude: 9.7283°, Longitude: 44.23264°) are manual rainfall stations (MRS). In MRS, rain gauge is used to gather and measure the amount of liquid precipitation over an area in a daily, dekadal (10-day total rainfall), monthly and annual time period. It is used for determining the depth of precipitation (usually in mm) that occurs over a unit area and thus measuring rainfall amount. The measurements or readings are done manually [26].

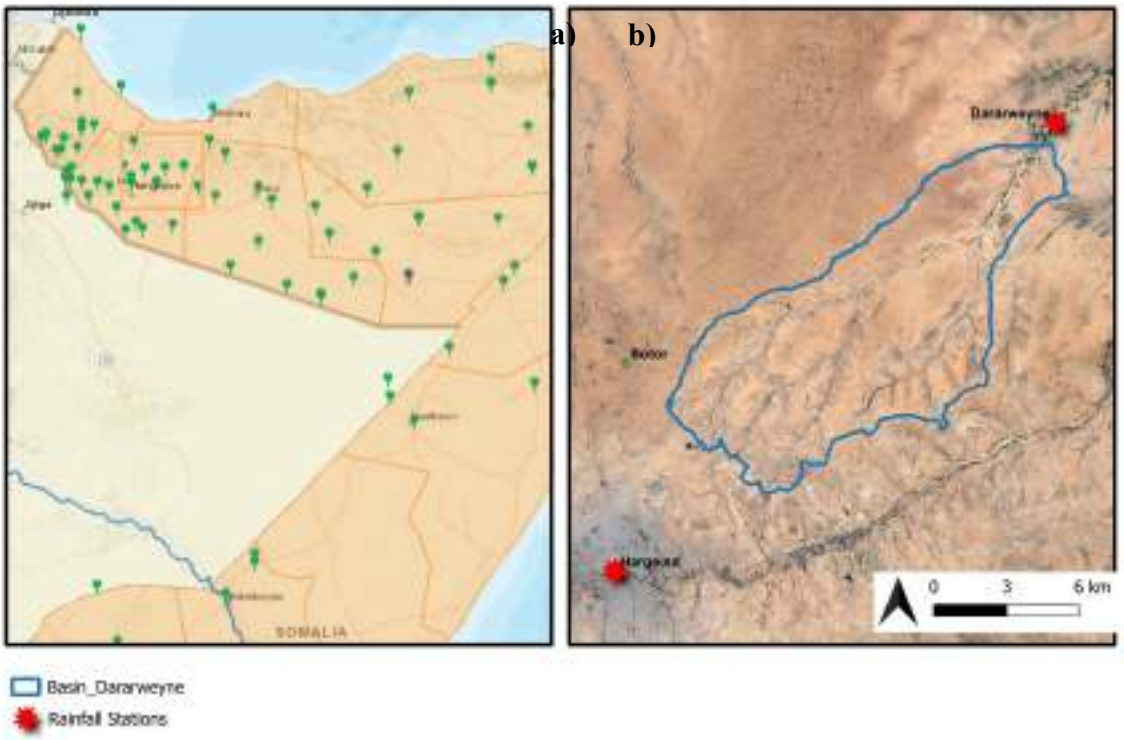

Figure 9 (a) Manual Rainfall stations in Somaliland [26] (b) Rain gauges near Darar-weyne Basin

2.4 GLOBAL PRECIPITATION DATASETS

Somaliland is a data-scarce region with limited gauge-based rainfall data. Reliable precipitation data are, however, critical to assess water availability in the region and quantify the benefits of adopting MAR strategies in the area. In particular, long-term observations of the hydrologic cycle are needed with temporal resolutions of 1 day or better. That said, acquiring consistent precipitation series for successful water resource management is a challenging task throughout the world. A number of global rainfall datasets exist, which combine in different ways remote sensing information, ground observations, and atmospheric model outputs and they differ in design objective, data sources, spatial resolution, and temporal resolution [15].

The present thesis considers the following datasets: (1) CHIRPS (CHIRPS DATASET) (2) GPM (GPM DATASET) 3) ERA5-LAND (ERA5-LAND DATASET)

The above datasets were accessed using the Google Earth Engine (GEE) platform, which allows a single access point and the possibility of processing the data prior to downloading them and to minimize the amount of information transferred to the local computing system. GEE is accessible with the following link: Google Earth Engine. In the present thesis, the rainfall data acquired from the considered datasets were averaged over the ground-based stations; Hargeisa and Dararweyne (Figure 10), resulting in the average hourly or daily rainfall datasets. The JavaScript codes for downloading rainfall data can be accessed through this GitHub Link.

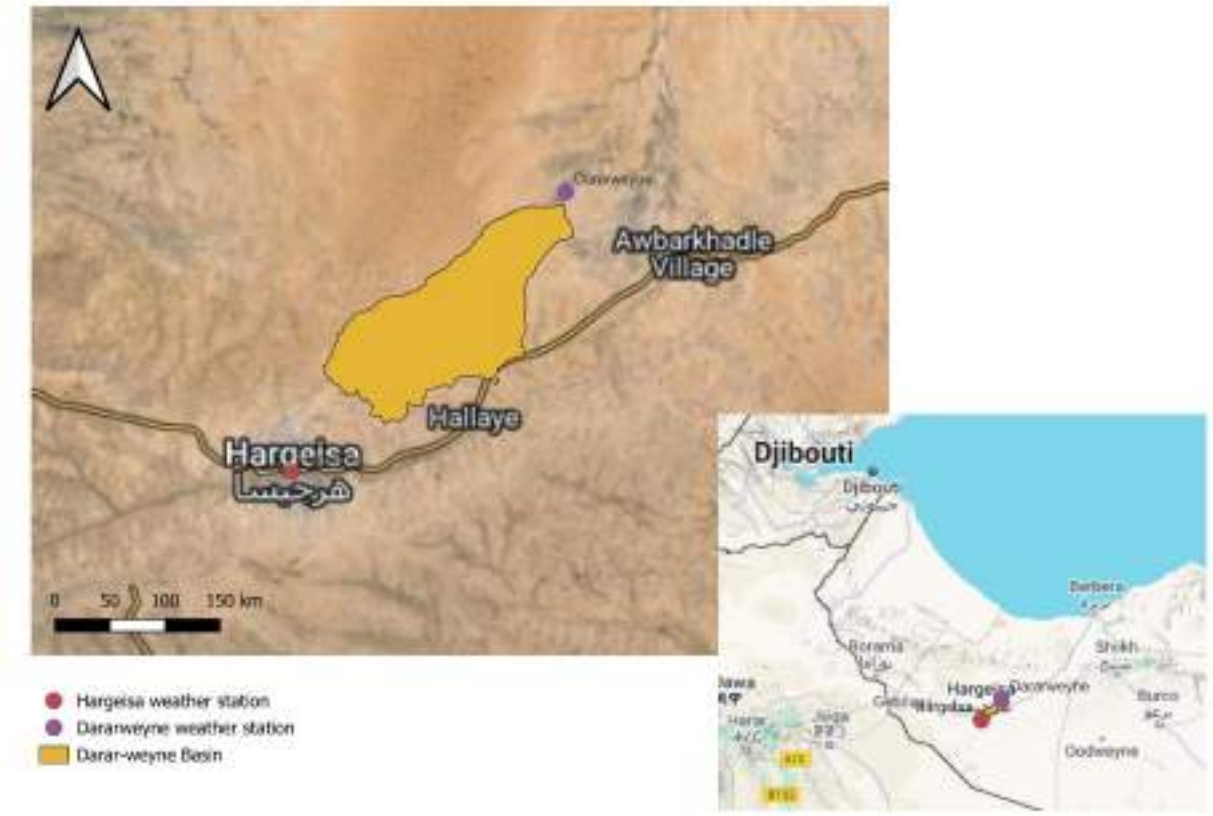

Figure 10 Darar-weyne Basin and weather stations over which rainfall data from CHIRPS, GPM and ERA5-Land are acquired

2.4.1 THE CLIMATE HAZARDS GROUP INFRARED PRECIPITATION (CHIRPS)

The Climate Hazards Group InfraRed Precipitation with Station data (CHIRPS) is developed by U.S. Geological Survey (USGS) and the Climate Hazards Group at University of California Santa Barbara for regions with scarce observation networks and complex

topography [27] to create gridded rainfall time series for trend analysis and seasonal drought monitoring [28]. CHIRPS is an IR-based [27] 35+ year quasi-global rainfall data set [28]. It has a relatively higher spatial resolution (0.05°), long records (dating back to 1981) at daily, pentadal, and monthly temporal resolutions, which are all freely downloadable [27]. This dataset merges three types of information: global climatology, satellite estimates, and in situ observations [29]. The data sources used in the development of CHIRPS dataset are TMPA 3B42, pentadal precipitation climatology, National Climatic Data Center, atmospheric model precipitation fields from National Oceanic and Atmospheric Administration climate forecast system, Thermal InfraRed satellite observation from Climate Prediction Center and SPG observations. The dataset is developed based on Inverse Distance Weightage interpolation technique and recorded precipitation based on IR Cold Cloud Duration observations [30].

In the present thesis, CHIRPS data was utilized to acquire average daily rainfall over the entire study basin and for both the locations of the rain gauges covering the time period 2000-2023.

2.4.2 GLOBAL PRECIPITATION MEASUREMENT (GPM)

The Global Precipitation Measurement (GPM) mission is a joint satellite mission led by NASA and JAXA with contributions from U.S. and international partners to unify and advance precipitation measurements from space for scientific research and societal applications. GPM mission efforts include instrument calibration, algorithm development, data production, ground validation, and science and societal applications. Central to these efforts is the GPM Core Observatory, a satellite launched in February 2014 with advanced spaceborne active and passive sensors for accurate retrievals of rainfall and snowfall. GPM products are used in a diverse range of applications, including studying the monsoons, assisting with water resource management. Vital to many of these applications is the Integrated Multi-Satellite Retrievals for GPM (IMERG), a gridded GPM precipitation product developed by the U.S. Science Team that combines observations from multiple spaceborne sensors to provide the best precipitation estimates. In IMERG V06, precipitation estimates are provided at 0.1° grids every half hour globally [31]. It provides 20-year long datasets from 2000 to present [32]. IMERG has three runs—Early, Late, and Final—to accommodate different user requirements for latency and accuracy. The Early run, available at a 4-h latency, is suitable for real-time applications such as in the prediction of flash floods. The Late run, with a 12-h latency, can be used for purposes such as water resource management. The Final run is at a 3.5-month latency and is intended for research applications [31].

In present thesis, GPM IMERG V06 data was utilized to obtain average hourly rainfall for the period from 2000 to May 2024. The dataset covers both locations of the rain gauges and the entire study basin.

2.4.3 ERA5-LAND

ERA5-Land is a reanalysis dataset, forced by meteorological fields from ERA5 [33] providing a consistent view of the evolution of land variables over several decades at an enhanced spatial resolution (9 km) compared to ERA5 (31 km). ERA5-Land contains a detailed global record from 1950 to three months from real-time, with a temporal resolution of 1 hour. ERA5-Land has been produced by running the land component of the ECMWF ERA5 climate reanalysis. A reanalysis combines model data with observations from across the world into a globally complete and consistent dataset using the laws of physics. Reanalysis produces data that goes several decades back in time, providing an accurate description of the climate of the past [34]. The ERA5-Land dataset currently available to be downloaded from the Copernicus Climate Data Store (CDS): CDS link has been regridded to a regular lat-lon grid of 0.1x0.1 degrees, although the specific party responsible for the re-gridding process is not mentioned. ECMWF member states with access to the ECMWF Meteorological Archival and Retrieval System (MARS) can retrieve the data in the native grid of 9 km [33].

In present thesis, average hourly rainfall data from the ERA5-Land dataset was acquired for period 2000 to 2023. The dataset covers both locations of the rain gauges and the entire study basin.

2.5 COMPARISON OF RAINFALL DATASETS

After downloading global precipitation datasets through GEE for the hydrological modeling, these datasets were compared to ground-based rain-gauge observations to quantify the uncertainty associated with them.

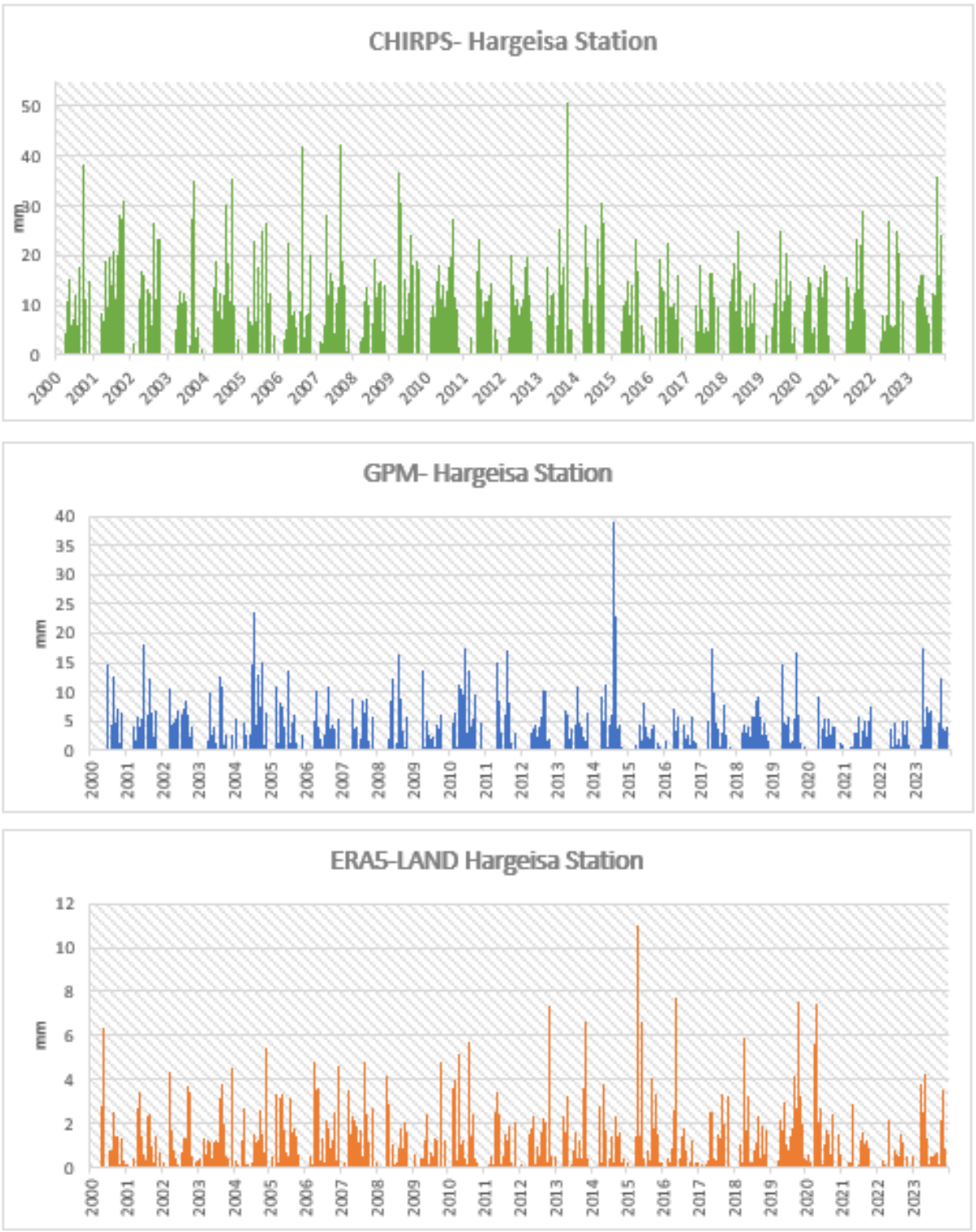

Figure 11 Global Precipitation datasets (CHIRPS, GPM, ERA5-LAND) average rainfall at the location of Hargeisa Station (2000-2023)

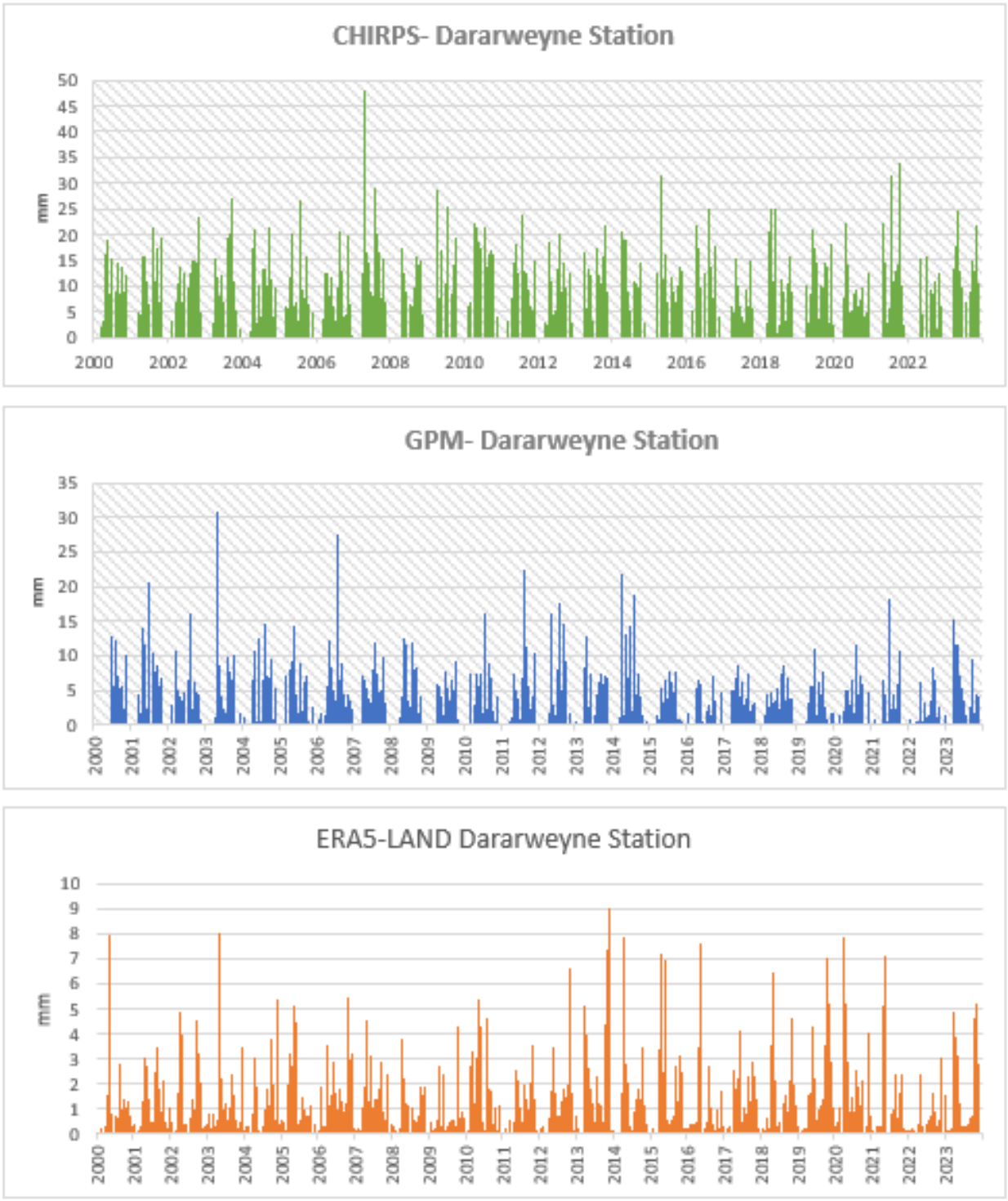

Figure 12 Global Precipitation datasets (CHIRPS, GPM, ERA5-LAND) average rainfall at the location of Dararweyne Station (2000-2023)

2.5.1 PIXEL VS. POINT COMPARISON

For comparison, individual rainfall stations were compared with the satellite data from the location corresponding to their position and over time. For all the datasets CHIRPS, GPM and ERA5-Land, the Hargeisa and Dararweyne stations were compared for the periods 2005-2023 and 2011-2023, respectively.

Figures 13 and 14 depict the yearly rainfall values from the global precipitation datasets and ground-based stations; Hargeisa and Dararweyne, respectively. Table 1 shows that at Hargeisa Station, the CHIRPS dataset shows a ratio averaging 0.9, with a percentage difference of -10%, indicating a slight underestimation of rainfall compared to the station's recorded values. Although this dataset generally underestimates the rainfall, the difference is moderate, suggesting CHIRPS can be a reasonably reliable source for estimating rainfall at this location. The GPM dataset, with an average ratio of 1.2 and a percentage difference of 20%, tends to overestimate rainfall at Hargeisa Station. The overestimation is more pronounced in certain years (e.g., 2014, 2025 and 2017), indicating that while GPM is generally consistent, it may occasionally provide exaggerated rainfall values. ERA5-Land exhibits the greatest underestimation among the three datasets, with an average ratio of 0.6 and a percentage difference of -42%. This significant underestimation suggests that ERA5-Land may not be the most reliable dataset for capturing rainfall accurately at Hargeisa Station, particularly in years where the deviation from the station data is considerable.

Table 2 shows that at Dararweyne Station, the CHIRPS dataset shows an average ratio of 2.4 and a percentage difference of 143%, indicating a substantial overestimation of rainfall. The overestimation is particularly high in some years, such as 2012 and 2013, where the percentage difference exceeds 300%. Similarly, the GPM dataset has an average ratio of 3.0 and a percentage difference of 197%, showing an even greater overestimation than CHIRPS. The GPM data often exceeds the station measurements by a large margin, highlighting its tendency to overestimate rainfall at this location. ERA5-Land, with an average ratio of 2.0 and a percentage difference of 100%, also shows a considerable overestimation, though it is generally closer to the station data than CHIRPS and GPM.

The comparison reveals that all three datasets (CHIRPS, GPM, and ERA5-Land) consistently overestimate rainfall at Dararweyne Station which could lead to significant inaccuracies in the results of hydrological modeling and thus Dararweyne station was excluded for further analysis. For hydrological modeling in HEC-HMS, the availability of hourly rainfall data is

necessary and although CHIRPS provides valuable daily data that can be informative for understanding general rainfall trends, its lack of hourly resolution makes it less suitable for the specific needs of this present study which led to the exclusion of the CHIRPS dataset from the modeling process. Given the distance between Hargeisa weather station and the centroid of the catchment upstream of Darar-weyne (about 15 km) and the satisfactory match between GPM rainfall data and ground observed data as depicted in Table 1, the GPM dataset can be employed since it is assumed to be more representative of the rainfall in the entire catchment than ERA5-Land.

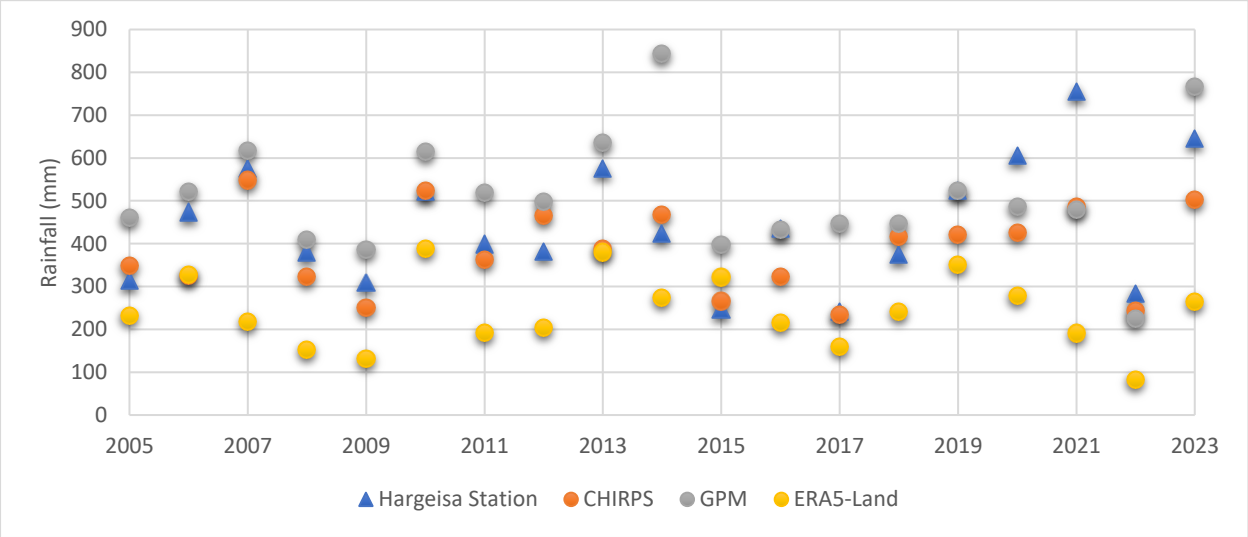

Figure 13 Cumulative yearly rainfall of Hargeisa station and Satellite derived Rainfall (2005-2023)

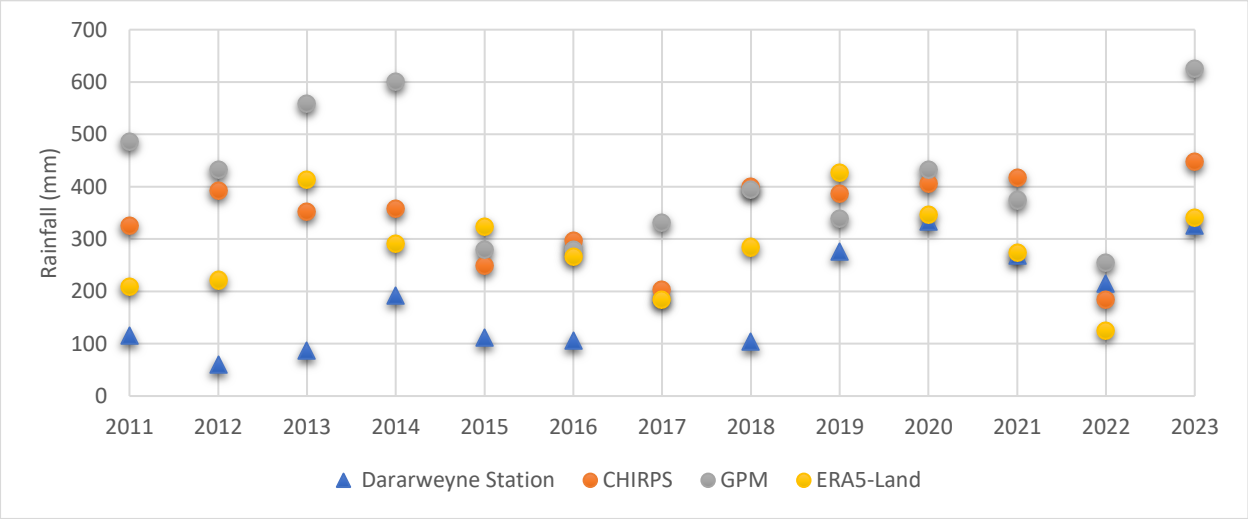

Figure 14 Cumulative yearly rainfall of Dararweyne station and Satellite derived Rainfall (2011-2023)

Table 1 Comparison between the cumulative annual rainfall between the Hargeisa station and the Satellite derived Rainfall at the stations

Station	Year	CHIRPS		GPM		ERA5-LAND	
		Ratio	% diff	Ratio	% diff	Ratio	% diff
HARGEISA STATION	**2005**	1.1	11	1.5	46	0.7	-26
	2006	0.7	-31	1.1	10	0.7	-30
	2007	1.0	-4	1.1	7	0.4	-61
	2008	0.9	-14	1.1	7	0.4	-59
	2009	0.8	-18	1.2	24	0.4	-57
	2010	1.0	0.4	1.2	17	0.7	-25
	2011	0.9	-8	1.3	30	0.5	-51
	2012	1.2	21	1.3	30	0.5	-46
	2013	0.7	-32	1.1	10	0.7	-34
	2014	1.1	10	2.0	99	0.6	-35
	2015	1.1	8	1.6	62	1.3	31
	2016	0.7	-25	1.0	-0.3	0.5	-50
	2017	1.0	-3	1.9	85	0.7	-33
	2018	1.1	11	1.2	19	0.6	-35
	2019	0.8	-19	1.0	0.3	0.7	-33
	2020	0.7	-29	0.8	-19	0.5	-54
	2021	0.6	-35	0.6	-36	0.3	-74
	2022	0.9	-13	0.8	-20	0.3	-70
	2023	0.8	-22	1.2	19	0.4	-59
	Average	**0.9**	**-10%**	**1.2**	**20%**	**0.6**	**-42%**

Table 2 Comparison between the cumulative annual rainfall between the Dararweyne station and the Satellite derived Rainfall at the stations

Station	Year	CHIRPS		GPM		ERA5-LAND	
		Ratio	% diff	Ratio	% diff	Ratio	% diff
DARARWEYNE STATION	**2011**	3	182	4	321	1.8	81
	2012	6	549	7	615	3.6	265
	2013	4	302	6	538	4.7	372
	2014	2	87	3	214	1.5	52
	2015	2	123	3	151	2.9	190
	2016	3	181	3	165	2.5	152
	2017	1	5	2	71	0.9	-5
	2018	4	286	4	282	2.8	175
	2019	1	40	1	23	1.5	55
	2020	1	22	1	30	1.0	4
	2021	2	56	1	40	1.0	2
	2022	1	-15	1	19	0.6	-42
	2023	1	37	2	92	1.0	5
	Average	**2.4**	**143%**	**3.0**	**197%**	**2.0**	**100%**

Figure 15 summarizes the average cumulative monthly rainfall data from Hargeisa weather station and GPM.

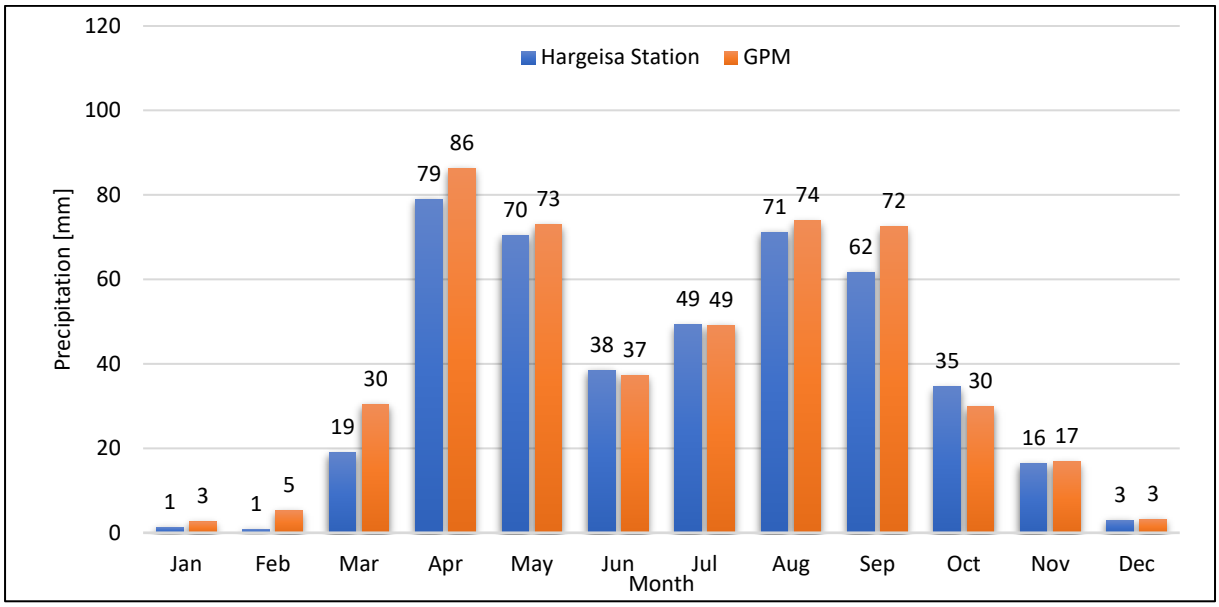

Figure 15 Average cumulative monthly rainfall data comparison between the Hargeisa weather station and the GPM rainfall

2.6 POTENTIAL EVAPOTRANSPIRATION DATA

Evapotranspiration data is obtained from the Global FAO Database. The data contains calculated mean monthly Potential Evapotranspiration (PET) values from 49 stations across the country for the period 1963-1990. Appendix A shows mean monthly PET values for the 49 stations that have been used [35]. Figure 16 graphically shows the PET values used in the hydrological model.

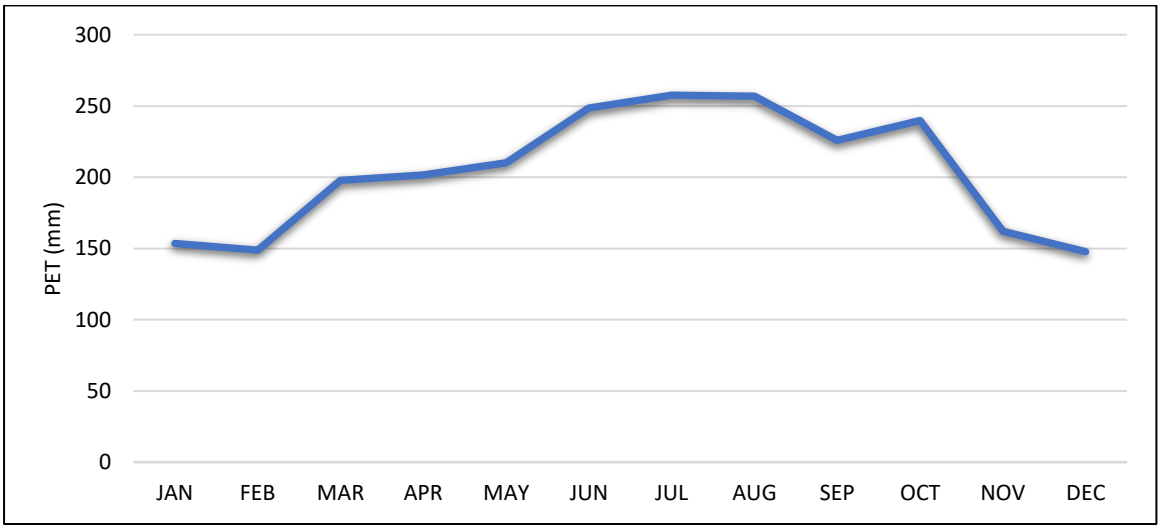

Figure 16 Mean monthly PET, Hargeisa Station

2.7 A SIMPLE HYDROLOGICAL MODEL

Hydrologic models which comprise integration of key hydrologic processes are appropriate tools for the studies of assessment of water resources. However, hydrological modeling which is a simplified representation of the real situation, is a challenging task particularly for regions with limited data and hydrologic models should be well calibrated and its performance be evaluated to provide reliable result for any study [36]. The HEC-HMS (Hydrologic Engineering Center and Hydrologic Modeling System) model was developed by the US Army Corps of Engineer and is widely used for many hydrological simulations. The HEC-HMS model has been applied to analyze urban flooding, flood frequency, flood warning system planning, reservoir spillway capacity, stream restoration, etc. [37].

2.7.1 SOIL MOISTURE ACCOUNTING (SMA)

SMA simulates the movement of water through vegetation and surface interception, the soil profile, and two groundwater layers. The SMA loss method also computes an outflow of surface runoff and groundwater flow, and losses due to ET and deep percolation, from the area to which it is applied.

Within the framework of HMS, SMA is a loss rate method associated with a subbasin. Precipitation is computed separately and then applied over the subbasin, i.e. as an input to the SMA algorithm. The SMA loss method then simulates the movement of water over time through the various storage components that represent the physical aspects of the watershed. Output from the SMA algorithm is precipitation excess (surface runoff), groundwater flow, and deep percolation. Deep percolation is water removed from the system [38]. The SMA method can be conceptualized as shown in Figure 17.

SMA should be used in combination with a Canopy Method (described in 2.7.3) that will extract water from the soil in response to potential evapotranspiration computed in the Meteorologic Model. The soil layer will dry out between precipitation events as the canopy extracts soil water. There will be no soil water extraction unless a Canopy Method is selected. It may also be used in combination with a Surface Method (described in 2.7.4) that will hold water on the land surface. The water in surface storage infiltrates to the soil layer. The infiltration rate is determined by the capacity of the soil layer to accept water. The SMA Loss Method is designed to be used in combination with the Linear Reservoir Baseflow Method (described in 2.7.6). When used in this way, water can move laterally out of upper groundwater and lower groundwater to enter baseflow. Water percolating out of lower

groundwater can be split between entering baseflow and leaving the land surface as aquifer recharge.

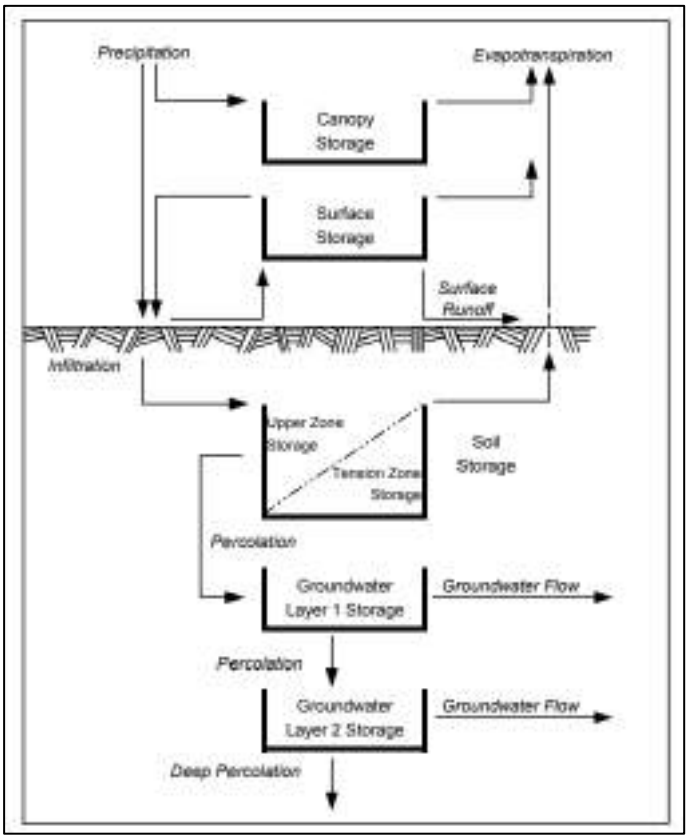

Figure 17 Conceptual Schematic of the Soil Moisture Accounting Method (Source: Bennett, 2000 [38])

Figure 17 depicts that precipitation fills the canopy storage. Precipitation that exceeds the canopy storage will overflow onto the land surface. The new precipitation is added to any water already in surface storage. Infiltration water is added to the water already in soil storage. The upper zone and tension zone both exist within the soil storage. Water will percolate from the soil to upper groundwater whenever the soil storage is between the tension zone depth and the soil storage depth. Similarly, water percolates from upper groundwater to lower groundwater. In SMA, the current infiltration rate is a function of the maximum infiltration rate, the current surface storage, and the current soil storage.

The **Maximum Infiltration Rate** sets the upper bound on infiltration from the surface storage into the soil [39]. Infiltration is water that enters the soil profile from the ground surface. Water available for infiltration during a time step comes from precipitation that passes through canopy interception, plus water already in surface storage. The volume of infiltration during a time interval is a function of the volume of water available for infiltration, the state (fraction of capacity) of the soil profile, and the maximum infiltration rate specified by the model user.

For each interval in the analysis, the SMA model computes the potential infiltration volume, PotSoilInfl, as:

$$PotSoilInfil = MaxSoilInfil - \frac{CurSoilStore}{MaxSoilStore} MaxSoilInfil \quad (1)$$

where MaxSoilInfl = the maximum infiltration rate; CurSoilStore = the volume in the soil storage at the beginning of the time step; and MaxSoilStore = the maximum volume of the soil storage. The actual infiltration rate, is the minimum of PotSoilInfil and the volume of water available for infiltration. If the water available for infiltration exceeds this calculated infiltration rate, the excess then contributes to surface interception storage [40].

Soil Storage represents the total storage available in the soil layer [39]. The soil profile storage represents water stored in the top layer of the soil. Inflow is infiltration from the surface. Outflows include percolation to a groundwater layer and ET. The soil profile zone is divided into two regions, the upper zone and the tension zone [40].

Upper Zone Soil Storage The upper zone is defined as the portion of the soil profile that will lose water to ET and/or percolation. It represents water held in the pores of the soil [40].

Tension Zone Soil Storage specifies the amount of water storage in the soil that does not drain under the effects of gravity, also known as field capacity. By definition, tension storage must be less that soil storage [39]. The tension zone represents water attached to soil particles. ET occurs from the upper zone first and tension zone last [40].

The **Soil Percolation** sets the upper bound on percolation from the soil storage into the upper groundwater [39]. Percolation is the movement of water downward from the soil profile, through the groundwater layers, and into a deep aquifer. In the SMA model, the rate of percolation between the soil storage and a groundwater layer or between two groundwater layers depends on the volume in the source and receiving layers. The rate is greatest when the source layer is nearly full and the receiving layer is nearly empty. Conversely, when the receiving layer is nearly full and the source layer is nearly empty, the percolation rate is less. In the HEC-HMS SMA model, the percolation rate from the soil profile into groundwater layer 1 is computed as:

$$PotSoilPerc = MaxSoilPerc\left(\frac{CurSoilStore}{MaxSoilStore}\right)\left(1 - \frac{CurGwStore}{MaxGwStore}\right) \quad (2)$$

where PotSoilPerc = the potential soil percolation rate; MaxSoilPerc = a user-specified maximum percolation rate; CurSoilStore = the calculated soil storage at the beginning of the time step; MaxSoilStore = a user-specified maximum storage for the soil profile; CurGwStore = the calculated groundwater storage for the upper groundwater layer at the beginning of the time step; and MaxGwStore = a user-specified maximum groundwater storage for groundwater layer 1 [40].

The potential percolation rate computed with Equation 2 is multiplied by the time step to compute an actual percolation volume. The available water for percolation is equal the initial soil storage plus infiltration. The minimum of the potential volume and the available volume percolates to groundwater layer 1 [40].

Groundwater 1 Storage represents the total storage in the upper groundwater layer [39].

The **Groundwater 1 Percolation Rate** sets the upper bound on percolation from the upper groundwater into the lower groundwater. An equation similar to equation 2 is used to compute the potential percolation from groundwater layer 1 to layer 2, PotGwPerc:

$$PotGwPerc = MaxPercGw\left(\frac{CurGwStore}{MaxGwStore}\right)\left(1 - \frac{CurGwStore}{MaxGwStore}\right) \quad (3)$$

where MaxPercGw = a user-specified maximum percolation rate; CurGwStore = the calculated groundwater storage for the groundwater layer 2; and MaxGwStore = a user-specified maximum groundwater storage for layer 2 The potential percolation rate from groundwater layer rate computed with Equation 3 is multiplied by the time step to compute an actual groundwater layer percolation volume [40].

The **Groundwater 1 Coefficient** is used as the time lag on a linear reservoir for transforming water in storage to become lateral outflow. The lateral outflow is available to become baseflow [39].

Groundwater 2 Storage represents the total storage in the lower groundwater layer.

The **Groundwater 2 Percolation Rate** sets the upper bound on deep percolation out of the system. [39].

The **Groundwater 2 Coefficient** is used as the time lag on a linear reservoir for transforming water in storage to become lateral outflow. It is usually a larger value that the groundwater 1 coefficient. The lateral outflow is likewise available to become baseflow [39].

For percolation directly from the soil profile to the deep aquifer in the absence of groundwater layers, for percolation from layer 1 when layer 2 is not used, or percolation from layer 2, the rate depends only on the storage volume in the source layer. In those cases, percolation rates are computed as:

$$PotSoilPerc = MaxSoilPerc \frac{CurSoilStore}{MaxSoilStore} \quad (4)$$

and

$$PotGwPerc = MaxPercGw \frac{CurGwStore}{MaxGwStore} \quad (5)$$

respectively, and actual percolation volumes are computed as described in soil percolation section.

Surface Runoff and Groundwater Flow. Surface runoff is the water that exceeds the infiltration rate and overflows the surface storage. This volume of water is direct runoff. Groundwater flow is the sum of the volumes of groundwater flow from each groundwater layer at the end of the time interval. The rate of flow is computed as:

$$GwFlow_{t+1} = \frac{ActSoilPerc + CurGw_iStore - PotGw_iPerc - \frac{1}{2}GwFlow_t.TimeStep}{RoutGw_iStore + \frac{1}{2}TimeStep} \quad (6)$$

where $GwFlow_t$ and $GwFlow_{t+1}$= groundwater flow rate at beginning of the time interval t and t+1, respectively; ActSoilPerc = actual percolation from the soil profile to the groundwater layer; $PotGw_iPerc$ = potential percolation from groundwater layer i; $RoutGw_iStore$ = groundwater flow routing coefficient from groundwater storage i; TimeStep = the simulation time step; and other terms are as defined previously. The volume of groundwater flow that the watershed releases, GwVolume, is the integral of the rate over the model time interval. This is computed as:

$$GwVolume = \frac{1}{2}(GwFlow_{t+1} + GwFlow_t).TimeStep \quad (7)$$

This volume may be treated as inflow to a linear reservoir model to simulate baseflow [40].

2.7.2 SCS-CURVE NUMBER

The Soil Conservation Service (SCS) curve number method implements the curve number methodology for incremental losses. The SCS curve number loss method should only be used for event simulation. Originally, the methodology was intended to calculate total infiltration during a storm. The program computes incremental precipitation during a storm by recalculating the infiltration volume at the end of each time interval [41].

2.7.3 CANOPY METHOD

This method is a simple representation of a plant canopy. All precipitation is intercepted until the storage capacity is filled. Once the storage is filled, all further precipitation falls to the surface or directly to the soil if no representation of the surface is included. The initial condition of the canopy should be specified as the percentage of the canopy storage that is full of water at the beginning of the simulation. Canopy storage represents the maximum amount of water that can be held on leaves before through-fall the surface begins. The amount of storage is specified as an effective depth of water [41].

2.7.4 SURFACE METHOD

Surface method represent the ground surface where water may accumulate in surface depression storage areas [41]. Surface depression storage is the volume of water held in shallow surface depressions. Inflows to this storage come from precipitation not captured by canopy interception and in excess of the infiltration rate. Outflows from this storage can be due to infiltration and to ET. Any contents in surface depression storage at the beginning of the time step are available for infiltration. If the water available for infiltration exceeds the infiltration rate, surface interception storage is filled. Once the volume of surface interception is exceeded, this excess water contributes to surface runoff [40].

2.7.5 CLARK UNIT HYDROGRAPH- TRANSFORM METHOD

The Clark unit hydrograph is a synthetic unit hydrograph method. This means that the user is not required to develop a unit hydrograph through the analysis of past observed hydrographs. Instead, a time versus area curve (time-area curve) is used to develop the translation

hydrograph resulting from a burst of precipitation. The resulting translation hydrograph is routed through a linear reservoir to account for storage attenuation effects across the subbasin [42]. It derives a watershed UH by explicitly representation to runoff: (i) Translation of the excess from its origin throughout the drainage system to the watershed outlet (ii) Attenuation of the magnitude of the discharge as the excess is stored throughout the watershed [41]. Clark unit hydrograph requires the specification of a time of concentration (T_c).

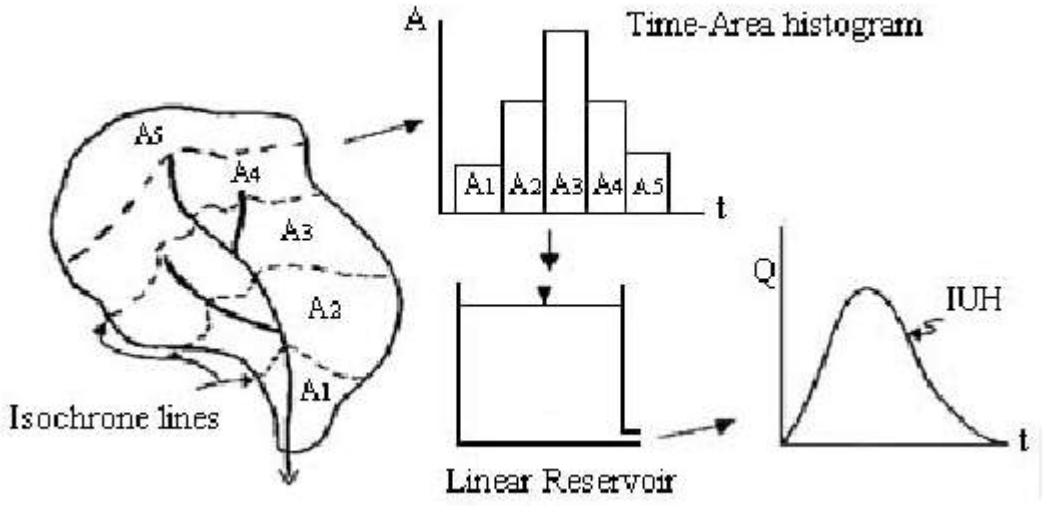

Figure 18 The conceptual model of Clark method (Source: Yannopoulos, S et al, 2013 [43])

2.7.5.1 TIME OF CONCENTRATION

The time of concentration is defined as the time duration for a drop of water falling in the most remote point of a drainage basin to travel to the outflow point [41]. The time of concentration is important to the hydrological analysis of watersheds. Being aware of the basin's behavior regarding time of concentration helps preventing and minimizing effects of natural disasters and punctual pollution of water resources. Among all response time parameters of the watershed, time of concentration is the most used one. Such parameter reflects how fast the watershed responds to rainfall events [44].

2.7.6 LINEAR RESERVOIR- BASE FLOW

The linear-reservoir base flow model is used in conjunction with the continuous soil moisture accounting model. This base flow model simulates the storage and movement of subsurface flow as storage and movement of water through reservoirs. The reservoir is linear the outflow at each time step of the simulation is a linear function of the average storage during the time

step. Mathematically, this is identical to the manner in which Clark's UH model represents watershed runoff. The outflow from groundwater layer 1 of the SMA is inflow to one linear reservoir, and the outflow from groundwater layer 2 of the SMA is inflow to another. The outflow from the two linear reservoir is combined to compute the total base flow for the watershed [41].

For the present thesis, Soil Moisture Accounting (SMA) method was selected for continuous hydrological modeling in HEC-HMS in combination with the methods described in Table 3. Three distinct scenarios were modeled, with primary input variables including surface storage (SS, mm), maximum infiltration rate (MIR, mm/hr), and soil storage (SoilS, mm). These scenarios were systematically compared to a baseline condition, representing the absence of Nature-based solution interventions.

The HEC-HMS model primarily relies on two input components: the basin model and the meteorological model. The majority of the parameters and methods chosen for modeling are detailed in Table 3.

Table 3 Selected basin and meteorological methods

LOSS METHOD: SOIL MOISTURE ACCOUNTING (SMA)			**LOSS METHOD: SCS-Curve Number (used to define basin model parameters for SMA)**	
Parameter method	*Basin Model*	*Meteorological model*	*Basin Model*	*Meteorological model*
Transform	Clark Unit Hydrograph	-	Clark Unit Hydrograph	-
Base flow	Linear Reservoir	-	-	-
Canopy	Simple Canopy	-	-	-
Surface	Simple surface	-	-	-
Rainfall		Specified Hyetograph (GPM Rainfall)		Specified Hyetograph (GPM Rainfall)

Initially, the simulation was run using the SMA loss method with 24 years of GPM rainfall data from June 2000 to May 2024. The SMA simulation depicted a peak discharge of 165.9 m^3/s on August 24, 2006 (Figure 19) utilizing parameters established by Hydro Nova for their work in the Darar-weyne basin under the Barwaqoo project. The parameters are mentioned in Table 4.

A model is considered plausible when its streamflow estimate has been successfully compared to observed streamflow [41] and the Nash Sutcliffe efficiency (NSE) is used to illustrates how well observed data and estimated data fits. Its value ranges from $-\infty$ to 1 with NSE=1 is the optimal value while NSE value ≤ 0 shows unacceptable performance level [45]. However, in the context of the present study, the lack of comparison with observed streamflow due to the unavailability of observed data precludes the use of NSE as a performance indicator.

Since the SCS-CN method is event-based and widely adopted due to its few parameters, and given the lack of physical data available, the calibration of the SMA parameters was conducted by considering the results from the SCS-CN model. Therefore, in the SCS-CN model, the observed peak rainfall event from August 22-27 was selected, with a CN of 77. The CN number is consistent with Hydro Nova's SCS-CN model fitted based on the available regional information. The SCS-CN method resulted in a peak discharge of 148.8 m^3/s (Figure 20). The SMA parameters were then adjusted until the resulting hydrographs of the two models for the same extreme event produced the same result. Following these adjustments, the peak discharge of 149.8 m^3/s ((Figure 21) in the SMA model matched the SCS-CN simulation.

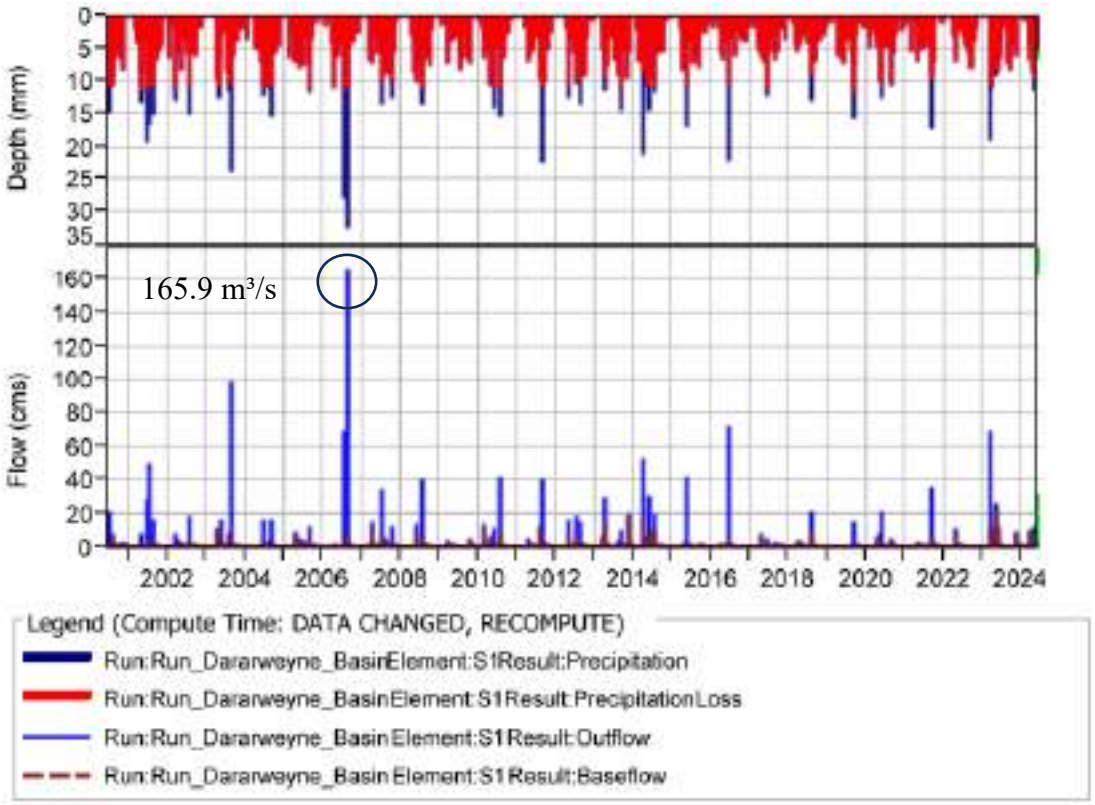

Figure 19 Hydrograph generated by initial SMA method simulation

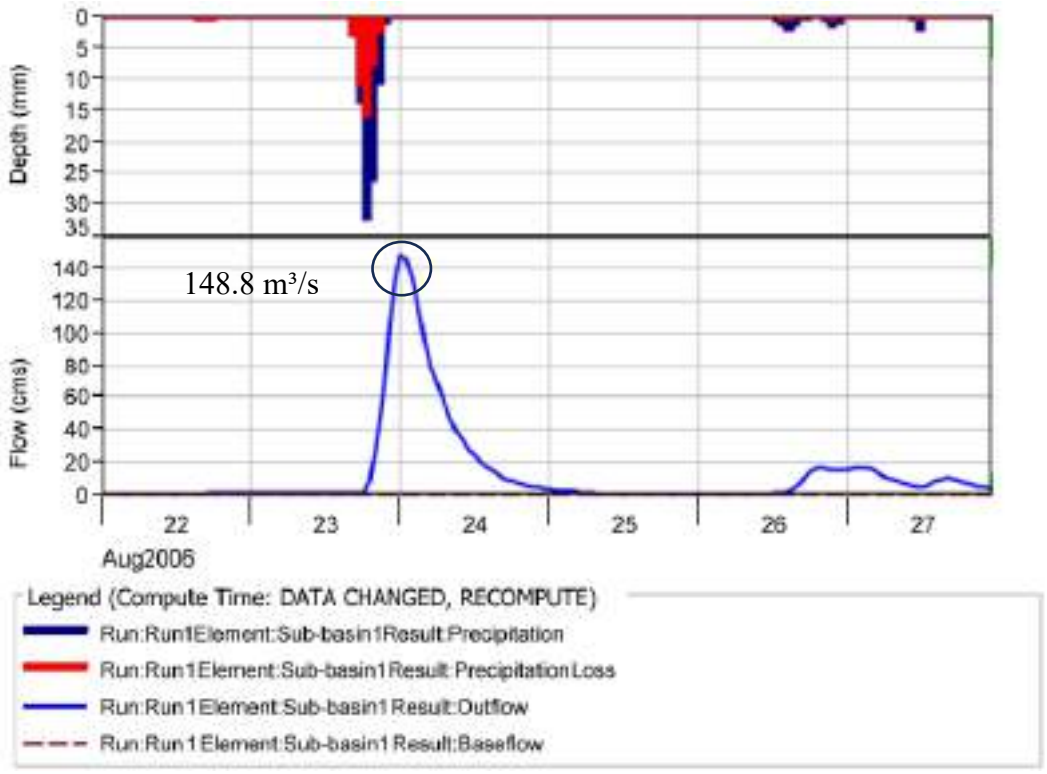

Figure 20 Hydrograph generated by SCS-CN method simulation

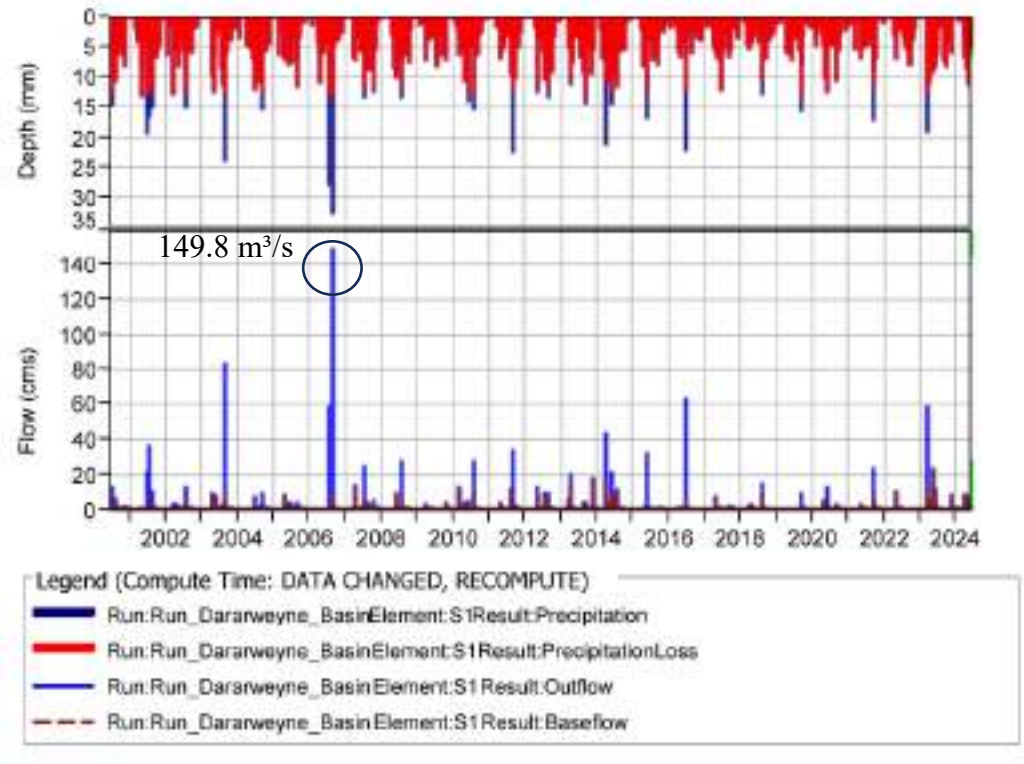

Figure 21 Hydrograph generated by SMA method simulation after the adjustment of parameters with SCS-CN model

Therefore, the parameters for the continuous SMA modeling of the baseline scenario (without the presence of any NBS) before and after the adjustments are detailed in Table 4.

Table 4 Selected parameters for SMA in HEC-HMS

Parameters	**Before adjustment (initial run)**	**After adjustment with SCS-CN method**
Max Surface storage (mm)	2	2
Max Infiltration Rate (mm/hr)	9	11
Soil Storage (mm)	100	100
Tension Storage (mm)	20	20
Soil Percolation (mm/hr)	10	10
GW 1 Storage (mm)	250	200
GW 1 Percolation (mm/hr)	10	10
GW 1 Coefficient (hr)	50	50
GW 2 Storage (mm)	500	500

GW 2 Percolation (mm/hr)	10	10
GW 2 Coefficient (hr)	100	100

The Darar-weyne basin was divided into homogeneous areas (sub-basins) for the application of specific nature-based solutions using the GIS extension of HEC-HMS. The properties and characteristics of each subbasin are outlined in Table 5.

Figure 22 Conceptual model of Darar-weyne basin with subbasins created by GIS extension in HEC HMS

Table 5 Characteristics of the Darar-weyne subbasins

Characteristics	**Subbasin-1**	**Subbasin-2**	**Subbasin-4**	**Subbasin-5**	**Subbasin-6**
Area (km²)	19.7	5.1	0.5	43.9	40.0
Longest Flowpath length (km)	9.4	5.2	1.8	12.6	13.5
Longest Flowpath Slope (m/m)	0.01	0.01	0.02	0.01	0.01
Basin slope (m/m)	0.03	0.03	0.03	0.04	0.02
Basin relief (m)	135.8	93.6	38.2	263.	144.0

Time of concentration (T_c) discussed in section 2.7.5.1 can be estimated with different available formulas. The Giandotti equation, commonly used worldwide, is applied to estimate the time of concentration for most of the subbasins taking into consideration the longest flow path, the slope of the basin and the area of the basin (the parameters are provided in Table 5). Table 6 provides the time of concentration formulas used for each subbasin [44].

Table 6 Time of Concentration values

Subbasin	T_c **(hours)**	**Comments**	
Subbasin-1, Subbasin-2	Pezzoli; $\tau_c = 0{,}055 \cdot \frac{L}{\sqrt{i_m}}$	Mountain basins with a surface area < 20 km^2	L= Flowpath length i_m = Flowpath slope
Subbasin-4	Kirpich; $\tau_c = 0{,}0663 L^{0.77} S^{-0.385}$	Rural basins that present area between 0.0040 and 0.8094 km^2	L= Flowpath length S = Flowpath slope
Subbasin-5, Subbasin-6	Giandotti; $t_c = \frac{4\sqrt{A_b} + 1.5 L_a}{0.8\sqrt{z_m - z_0}}$	Basins in central and northern Italy	A_b= basin area L_a= longest flow path z_m = sub-basin average elevation z_o = sub-basin outlet elevation

2.8 NATURE-BASED SOLUTIONS

Nature-based solutions (NBS) refer to measures that contribute mitigating a problem using processes that naturally occur in nature. The current literature refers to NBS as an alternative to tackle many societal challenges: climate mitigation, water management, maintenance of biodiversity, reduction of energy consumption, economic, and social aspects [46].

As NBSs are assumed to deliver multiple environmental benefits, three different NBSs were considered here to contribute to improving water availability in the study area; sand dams,

semi-circular bunds, and increased vegetation cover in the selected sub-basins. According to the theoretical concept of SMA, the current infiltration rate is a function of the maximum infiltration rate, surface storage, and soil storage. Therefore, only these three parameters were adjusted to represent the effects of different MARs and to quantify their potential impact on aquifer recharge. Initially, each parameter was modified individually while keeping the remaining one's constant in the model to determine the independent effect of each parameter on aquifer recharge. Additionally, all three parameters were adjusted simultaneously to compare the scenarios before and after NBS implementation.

2.8.1 SAND DAMS

To address water scarcity in semi-arid regions, runoff should be captured and stored locally before they are lost to the sea. One approach to achieving this is to increase local storage capacity. Sand dams (also called sand-storage dams) have been successfully implemented in several semi-arid countries and are an example of such a system. A sand dam consists of a reinforced wall constructed on the bedrock during the dry season across a seasonal riverbed. During the rainy season, the sand carried by the river is deposited behind the wall; this accumulates until it is level with the top of the dam. The pore space in the sand is filled with water from the seasonal river which can then be abstracted by the local community during the dry season. Their utility is, however, twofold: storing water in the sand that is also trapped behind them, and facilitating aquifer recharge. Evaporation of water from the sand deposits is significantly reduced as the water table falls within the newly deposited soil, below the ground surface. Sand dams vary considerably in size; they can be 200 m wide but most sand dams are no more than 20 m wide. Research on sand dams shows that only 1–3% of the river discharge is retained behind any individual sand dam, the remainder continues its natural course towards the ocean. For the larger sand dams, infiltration galleries located on the river bed are preferred for abstracting water; for the smaller sand dams, hand dug wells and scoop holes are used [47].

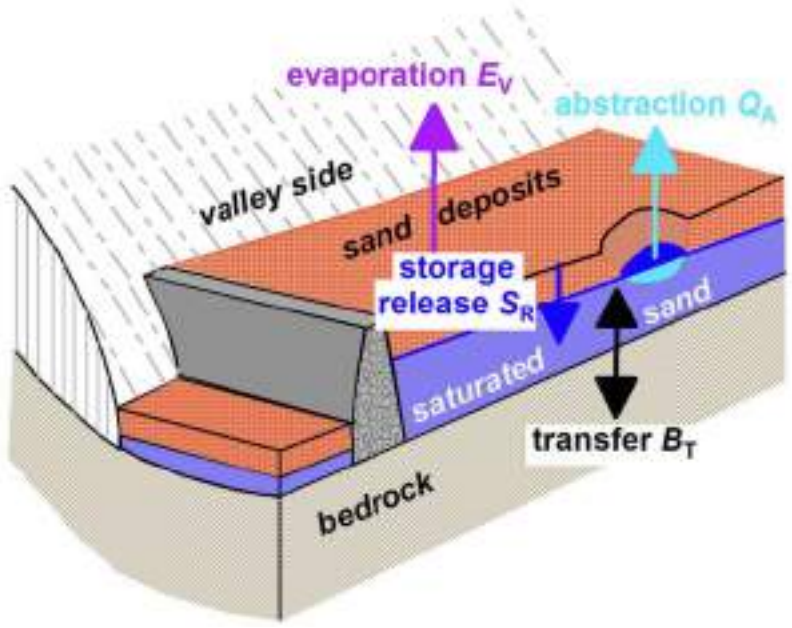

Figure 23 Schematic diagram of a sand dam showing important flow components (Source: Bouzouidja ,2021 [47])

To examine the impact of a sand dam on aquifer recharge, a sand dam application was considered using the Soil Moisture Accounting (SMA) method at the outlet of sub-basin-4.

Figure 24 Sand Dam considered in Subbasin-4

2.8.1.1 Sensitivity Analysis for Maximum Infiltration Rate

The primary effort was to identify suitable parameter values concerning soil conditions from literature or previous studies, due to the scarcity of field observations. For the ***max infiltration rate*** (MIR), sensitivity analysis was performed by increasing the baseline scenario's maximum infiltration rate by 30%, 60%, and 90%, respectively, due to the unavailability of specific values in the literature.

2.8.1.2 Experimental Design

An experimental sand dam design is used to estimate parameters, such as surface and soil storage, that can be derived from the design:

- Height: 3 meters (typical height of a sand dam)
- Width: 65 meters (horizontal distance between riverbanks, measured using the measure tool of QGIS)
- Length: 120 meters (measured using the elevation tool of QGIS)

For simplification it was assumed that the sediment accumulation behind the sand dam would form a triangular wedge. Thus, the volume of water capable of being stored, also known as ***surface storage*** (SS) was calculated using the volume formula for a triangle, resulting in 11,700 cubic meters of water storage:

$$V = \frac{1}{2} B \times H \times L \quad (8)$$

Where B= base, H= height and L= length.

The texture and arrangement of solid soil particles determine soil porosity, which for sandy surface soils may range from 35% to 50% [48]. The volume storage capacity was converted into surface storage depth by dividing the volume by the surface area of 7,800 square meters and multiplying the depth by the porosity of the sandy soil, taken as 0.35. This parameter was also adjusted by ±10% of the calculated value.

Soil storage, SoilS, was calculated using the following equation:

$$SoilS = n \times d \quad (9)$$

where n is the porosity of the soil, taken as 0.35 as mentioned above [48] and d is the depth of the soil, taken as 1.2 meters (1200 mm), based on the geological report of Darar-weyne, which indicated that sandy deposits were constant up to 1.2 meters across all hand-dug pits near the outlet of the basin. This parameter was also adjusted by ±10% of the calculated value. The parameters, based on the calculations and sensitivity analysis, are mentioned in Table 7.

Table 7 Parameters for the Sand dam NBS

	Surface Storage (mm)	Max Infiltration Rate (mm/hr)	Soil Storage (mm)
1.	-10% - 472.5	30%- 14.3	-10% -378
2.	Calculated -525	60% - 17.6	Calculated- 420
3.	+10% - 577.5	90% - 20.9	+10%- 462

2.8.2 SEMI-CIRCULAR SOIL BUNDS

Semi-circular soil bunds are the most common physical soil and water conservation (SWC) structure constructed across cultivated lands [49]. They are earth embankments in the shape of a semi-circle with the tips of the bunds on the contour [50]. They enhance both the retention of soil water and groundwater recharge. They also reduce effective steepness and length of natural slopes, reduce soil erosion and water loss, alleviate the severity of droughts, and ultimately benefit ecosystem restoration [49]. However, studies are rare on the effects of soil bunds on soil properties under different topographic set up [51].

Figure 25 Semi-circular soil bund

2.8.2.1 Experimental Design

Semi-circular soil bunds were considered in subbasin-2 with an area of 5.12 km^2 to analyze their contribution to aquifer recharge with the SMA method in HEC-HMS. Food and

agricultural organization of the United States provides designs for semi-circular soil bunds for areas of slope 1% or less, up to 2% and 4% [50]. However, the slope of the study basin is about 3%. Thus, interpolation calculation was performed to find out the bund design parameters at 3% slope. Table 8 indicates the bund design parameters at different slopes.

Figure 26 Semi-circular soil bunds considered in Subbasin-2

Table 8 Semi-circular soil bund design parameters at different % slopes

	FAO Design	Interpolated Values	FAO Design
Slope (%)	**2**	**3**	**4**
Radius (m)	20	15	10
Length (m)	63	47	31
Bunds per Hectare	4	10	16
Distance between two adjacent rows (m)	30	22.5	15
Tips of two adjacent structures (m)	10	7.5	5

The cross-section of the bund changes over its length. At the wing tip, the bund is only 10 cm high, but the height increases towards the middle of the base to 50 cm with side slopes of 3:1 (horizontal: vertical), and a top width of 10 cm. Corresponding base widths are 70 cm and 3.10 meters, respectively. Design has a C:CA (Catchment: cultivated area) ratio of 3:1. A larger C:CA ratio for bund design is possible but it should not exceed 5:1 [50].

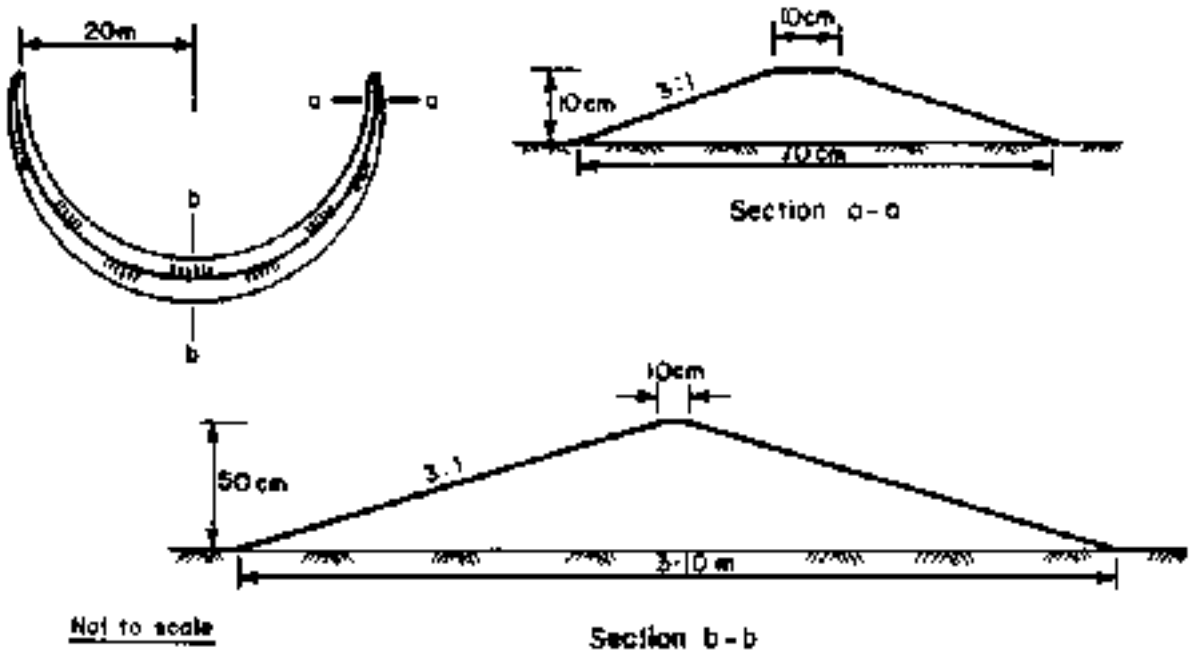

Figure 27 Semi-circular soil bund dimensions by FAO for 2% slope

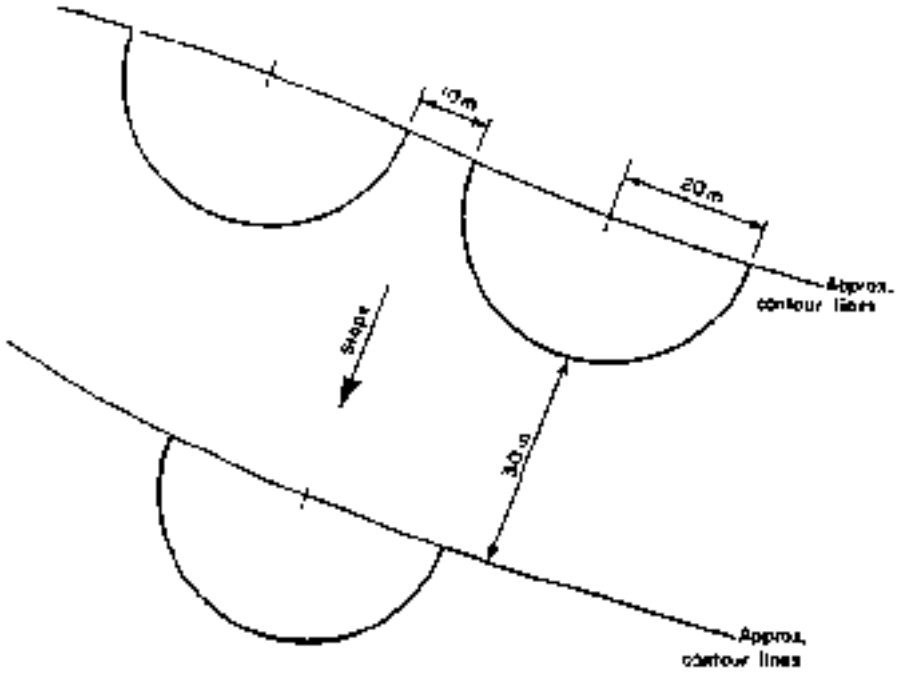

Figure 28 Semi-circular bunds field layout by FAO for slope 2%

Three classes of semi-circular soil bunds were defined based on their height for the modeling purpose. (i) 50cm bund height (ii) 70cm bund height (40% of 50cm, sensitivity analysis) and (iii) 80cm bund height (60% of 50cm, sensitivity analysis). Radius and bunds per hectare are unchanged and the bund length along the semi-circular arc depends on the radius and does not change with the height adjustment. Therefore, the length will remain approximately 47 meters. The three bund designs with their dimensions are described in Table 9.

Table 9 Semi-circular soil bund classes based on bund heights

	Based on FAO Design	40% of height	60% of height
Bund height (m)	**0.5**	**0.7**	**0.8**
Radius (m)	15	15	15
Length (m)	47	47	47
Bunds per Hectare	10	10	10
Base width (m)	3.1	4.3	4.9

The analyzed model parameters were max infiltration rate (mm/hr), surface storage (mm) and soil storage (mm).

Max infiltration rate, MIR values were acquired from the literature study of bund dimension impacts on soil physical properties and hydrology conducted on the highlands of Ethiopia. The soil types in the highlands of Ethiopia were classified as Leptosols, Nitisols, Vertisols, Cambisols, Alisols, Gleysols and Fluvisols [52]. Among these soil types, Fluvisol is one of the 30 soil groups in the classification system of the Food and Agriculture Organization (FAO). Fluvisols are found typically on level topography that is flooded periodically by surface waters or rising groundwater, as in river floodplains and deltas and in coastal lowlands [53]. Their texture can vary from coarse sand in levee soils to heavy clays in basin areas [54]. Therefore, the infiltration values deemed suitable to considered in relation to sandy deposits of Darar-weyne basin. The infiltration rates with respect to bund height are indicated in Table 10.

Table 10 Max Infiltration Rate (mm/hr) values for bunds from literature

Bund Height Range (cm) (from literature)	Semi-circular bund height (cm) (for modeling)	Infiltration rate (mm/hr)
30-55	50	**23.2**
55-75	70	**25.1**
75-110	80	**26.6**

Surface storage, SS for each bund class were calculated, as shown in Table 11.

Table 11 Surface Storage (mm) parameter for semi-circular soil bunds

Semi-circular soil bund classes (height based)	Vol. of a single bund (m^3)	No. of Bunds in Sub-basin 2	Total Volume of the bunds (m^3)	Surface Storage (mm)
50 cm	176.7	5,112	903,471.0	**176.7**
70 cm	247.4	5,112	1,264,859.4	**247.4**
80 cm	282.7	5,112	1,445,553.6	**282.7**

The volume of a single bund is estimated as:

$$V = \frac{1}{2} \times \pi^2 \times h \quad (10)$$

Where, V is the volume of the bund, r is the radius of the bund and h is the height of the half bund.

Soil storage, SoilS values were calculated using Equation 9 as described in the sand dam section.

For semi-circular bunds, the effective depth for soil storage estimation can be based on the height of the bund and the soil's infiltration capacity. Given that the study basin's soil were sandy deposits, the effective depths for each bund class were assumed for simplicity due to absence of literature and observations and are shown in Table 12.

Table 12 Soil Storage (mm) parameter for semi-circular soil bunds

Semi-circular soil bund classes (height based)	Porosity of soil	Effective depth (mm)	Soil storage (mm)
50 cm	0.35	600	**210**
70 cm	0.35	700	**245**
80 cm	0.35	800	**285**

2.8.3 INCREASED VEGETATION COVER

The efficiency of the rainfall transformation into soil water highly depends on the infiltration capacity, and this process is very important for soil water replenishment in water shortage regions. Many engineering measures have been developed to increase infiltration and

decrease runoff for preventing soil erosion. Vegetation restoration is one of the most important and effective measures to control soil and water loss [55]. Resistance of vegetation to low rainfalls or prolonged extreme drought is mainly driven by (1) the level of progressively increasing water limitation in the system, and (2) the resource use strategies of existing plants in the system. Multi-year drought causes prolonged water stress, which may result in the accumulation of drought effects. Yet, various species of plants have adapted strategies to deal with water limitation [56].

The present work refers to the global land cover raster data "MODIS/Terra+Aqua Land Cover Type Yearly L3 Global 500m SIN Grid V061" from NASA Earth Data for the study area to understand the existing landcovers. The MODIS/Terra + Aqua Land Cover Type Yearly L3 Global 500m SIN Grid dataset provides valuable data for understanding global land cover changes at yearly intervals (2001-2022). The MCD12Q1 Version 6.1 data product is derived using supervised classifications of MODIS Terra and Aqua reflectance data [57]. An NDVI map using Sentinel-2 data was also created. The NDVI map and land cover map for the basin are shown in Figure 29. The legends for the land cover map, retrieved from MODIS data, are shown in Figure 30.

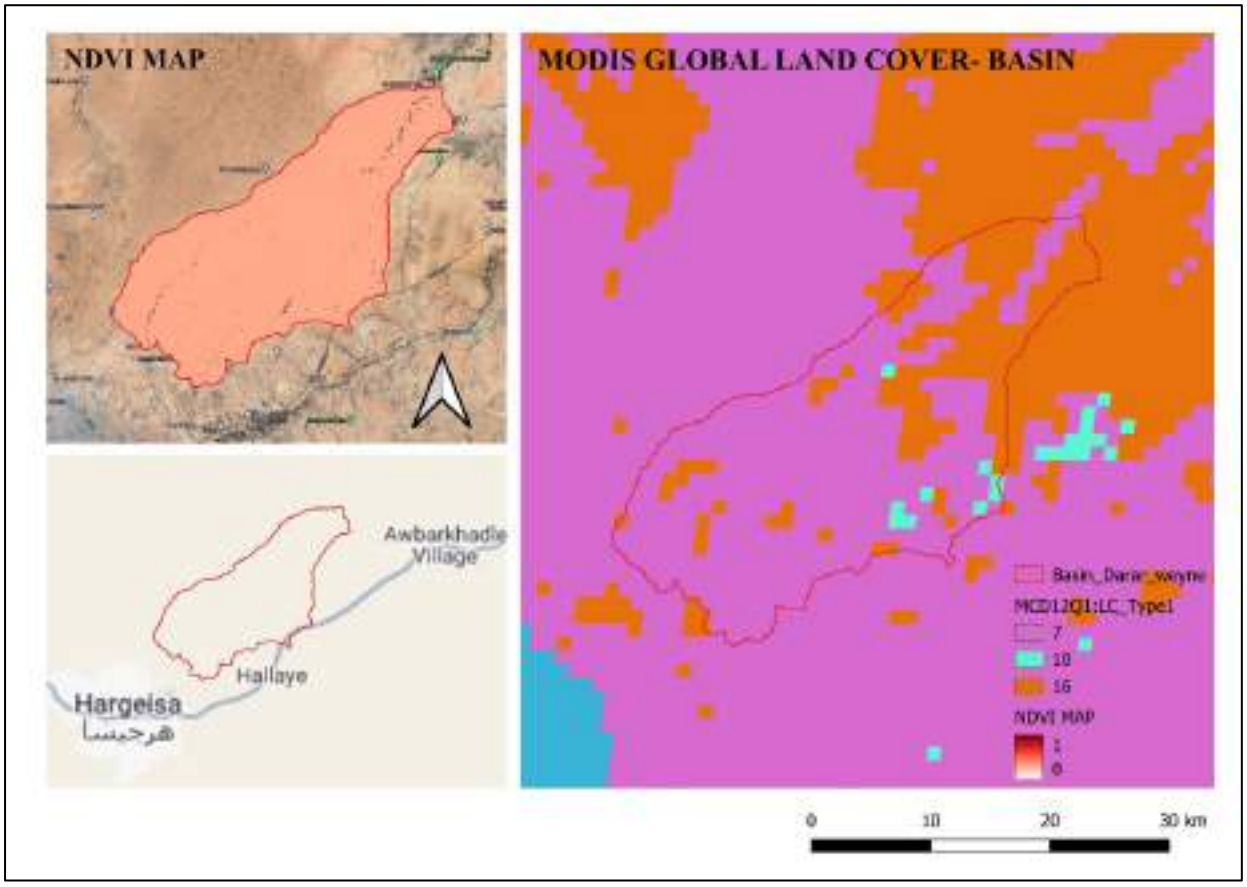

Figure 29 Land Cover and NDVI Map of the Darar-weyne basin

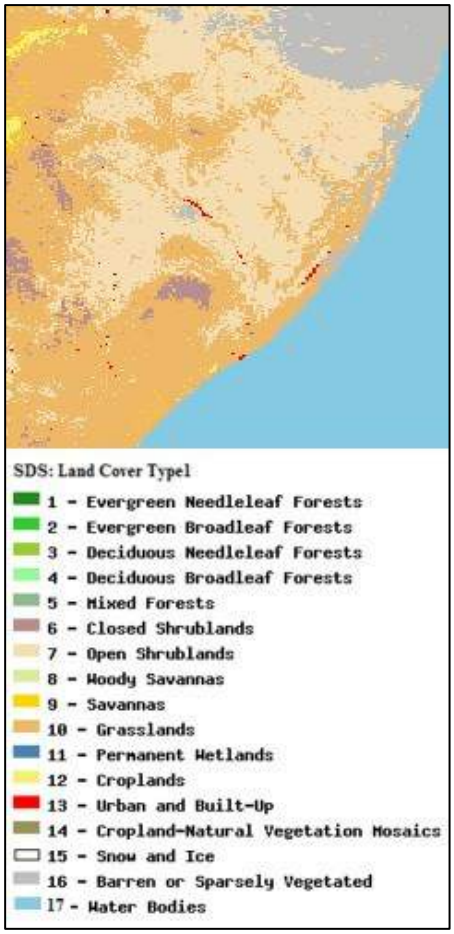

Figure 30 MODIS Land Cover Type- Legend

The collected information shows that the study basin hosts three main types of land cover:

(i) Open Shrublands

(ii) Grasslands

(iii) Sparse Vegetation

Among these land cover type, grassland was considered to employ as a nature-based solution to enhance the recharge in the aquifer. Although grasslands often exhibit low drought resistance, emerging studies suggests that these systems can have high resilience (capacity for recovery of function) to drought and that plant biomass can rapidly recover in a single year in humid grassland ecosystems and more arid grasslands may recover more slowly due to greater resource limitation and more severe impacts [56].

Subbasin-1, with an area of 19.73 km^2, was used to analyze the contribution of increased grassland to aquifer recharge with SMA method in HEC-HMS. The analyzed model parameters were max infiltration rate (mm/hr), surface storage (mm) and soil storage (mm).

Figure 31 Increased vegetation cover considered in Subbasin-1

Max Infiltration rate (MIR) values were taken from the literature for the grassland. ***Surface storage***, SS values are decided based on sensitivity analysis due to absence of literature and ***soil storage***, SoilS values are calculated from equation 9 where the depth parameter is acquired from literature. The max infiltration rate and soil storage parameters were also adjusted by ± 10% of the calculated value. Table 13 summarizes the values.

Table 13 Parameters for the increased vegetation cover NBS

	Surface Storage (mm)	**Max Infiltration Rate (mm/hr)**	**Soil Storage (mm)**
1.	6	-10%- 18.9	-10%- 126
2.	11	21 (from literature) [55]	140 (from literature) [58]
3.	14	+10%- 23.1	+10%- 154

3 RESULTS

This section presents the modeling results for the three nature-based solutions: sand dams, semi-circular bunds, and increased vegetation cover, which were analyzed to assess their impact on aquifer recharge. The key output layers considered in this study resulting from the SMA model include the average annual cumulative values (mm/year) for aquifer recharge, infiltration, direct runoff, and base flow.

Figure 32 presents the hydrological fluxes from the simulation run of the baseline scenario model, excluding the application of nature-based solutions; sand-dams, semi-circular bunds and increased vegetation cover.

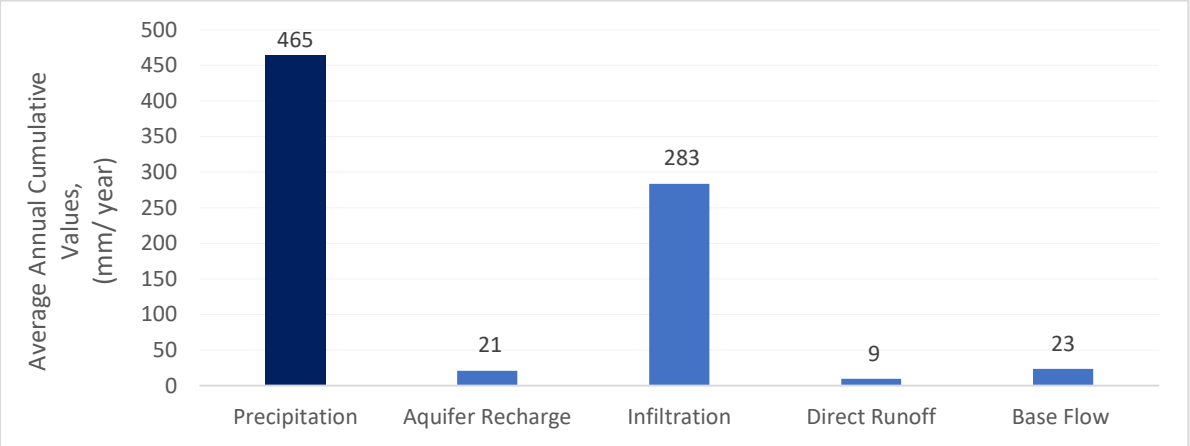

Figure 32 Hydrological fluxes, baseline scenario without NBS interventions

3.1 SAND DAM IMPLEMENTATION

3.1.1 ANALYSIS OF MAXIMUM INFILTRATION RATE (MIR) PARAMETER

Figure 33 shows the average annual cumulative values (mm/year) of different hydrological fluxes for different maximum infiltration rate scenarios in a sand dam NBS. The simulation was run using the Soil Moisture Accounting (SMA) loss method in HEC-HMS where only the maximum infiltration rate was varied.

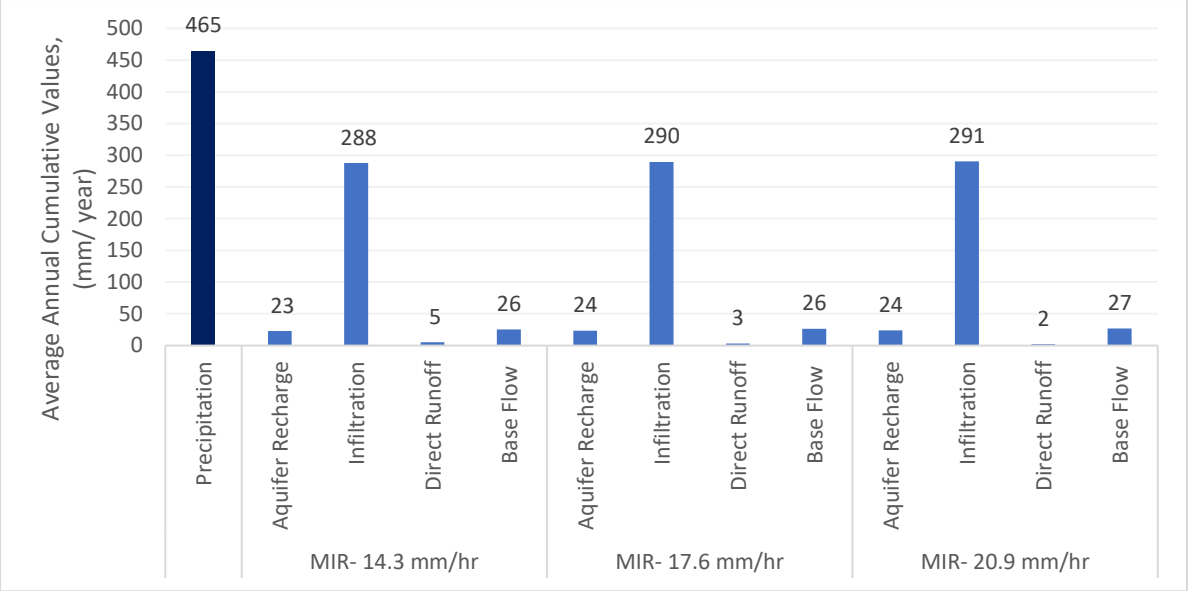

Figure 33 Hydrological fluxes resulting from Maximum Infiltration Rate (MIR) Analysis, Sand Dam

Comparing the results with the baseline scenario of 11 mm/hr maximum infiltration rate before the implementation of the sand dam technique, the following trends have been observed.

- *Aquifer Recharge:* Aquifer recharge increases from the baseline of 21 mm/year to 23 mm/year at an MIR of 14.3 mm/hr and further to 24 mm/year at higher MIRs of 17.6 mm/hr and 20.9 mm/hr. This gradual increase of up to 3 mm/year highlights that improved infiltration rate due to sand dam, enhances the groundwater recharge.

- *Infiltration:* Infiltration increases from 283 mm/year in the baseline to 288 mm/year at an MIR of 14.3 mm/hr, and further to 291 mm/year at an MIR of 20.9 mm/hr. The increase of up to 8 mm/year illustrates that the sand dam, along with a higher infiltration rate, significantly enhances the system's ability to absorb water.

- *Direct Runoff:* Direct runoff decreases from the baseline of 9 mm/year to 5 mm/year at an MIR of 14.3 mm/hr, and further to 2 mm/year at an MIR of 20.9 mm/hr. This reduction of up to 7 mm/year shows that the sand dam, promotes higher infiltration rate which significantly reduces surface runoff.

- *Base Flow*: Base flow improves from 23 mm/year in the baseline to 26 mm/year at an MIR of 14.3 mm/hr and remains stable at this level up to an MIR of 17.6 mm/hr, with a slight increase to 27 mm/year at an MIR of 20.9 mm/hr. The increase of up to 4 mm/year indicates that the sand dam, together with an improved infiltration rate, enhances the long-term sustainability of base flow.

These results imply that with an increased MIR, the infiltration of water and aquifer recharge are more efficient also resulting in improved base flow availability.

3.1.2 ANALYSIS OF SURFACE STORAGE (SS) PARAMETER

Figure 34 illustrates the average annual cumulative values (mm/year) of various hydrological fluxes for different surface storage scenarios in a sand dam NBS. The simulation was run using the Soil Moisture Accounting (SMA) loss method in HEC-HMS where the only parameter varied was the surface storage parameter.

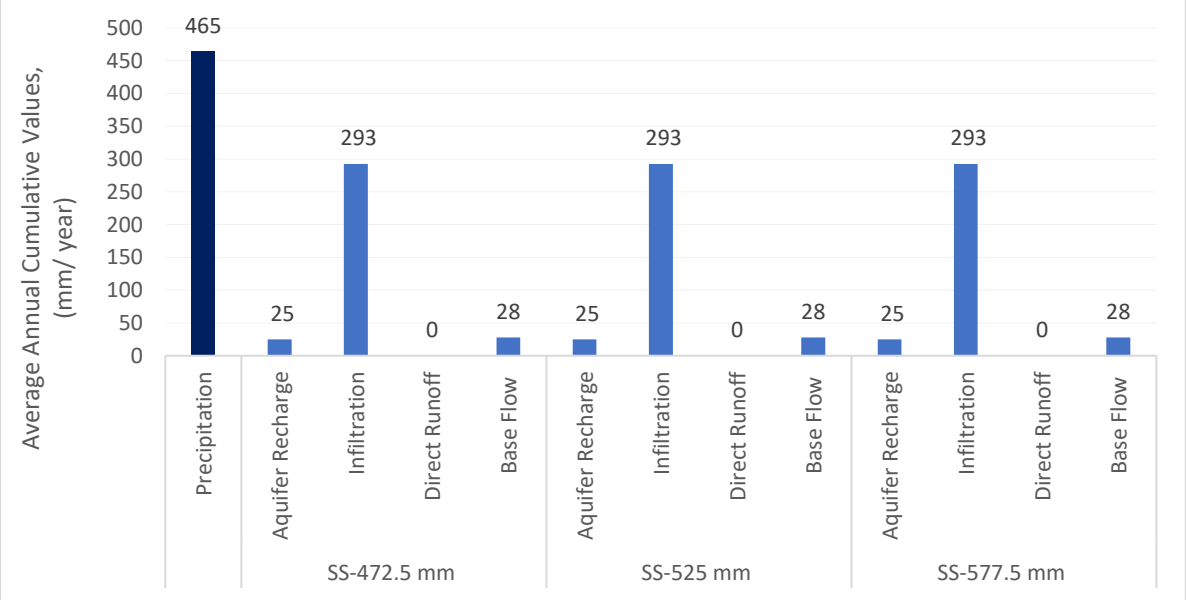

Figure 34 Hydrological fluxes resulting from Surface Storage (SS) Analysis, Sand Dam

The results from the comparison against the baseline scenario with 2 mm surface storage before the initiation of the sand dam technique application are as follows.

- *Aquifer Recharge:* The aquifer recharge increases from 21 mm/year in the baseline scenario to 25 mm/year across all levels of Surface Storage (SS). This represents an increase of 4 mm/year, demonstrating that the introduction of a sand dam enhances groundwater recharge, likely by retaining more surface water and promoting infiltration into the aquifer.

- *Infiltration:* Infiltration increases by 10 mm/year, from 283 mm/year in the baseline scenario to 293 mm/year across all SS levels. This increase highlights the sand dam's role in enhancing the overall infiltration capacity of the system, allowing more water to penetrate the ground compared to the baseline scenario without a sand dam.

- *Direct Runoff:* Direct runoff is completely eliminated (0 mm/year) across all SS levels, compared to 9 mm/year in the baseline scenario. This demonstrates that the sand dam is highly effective in capturing and storing surface water, preventing it from being lost as immediate runoff.

- *Base Flow:* Base flow increases from 23 mm/year in the baseline to 28 mm/year across all SS levels. This increase of 5 mm/year suggests that the sand dam contributes to maintaining a higher and more consistent base flow into the aquifer, compared to the baseline scenario without a sand dam.

However, despite varying the surface storage parameter in each simulation, the output values for all hydrological parameters after the implementation of sand dam remains consistent. This constancy indicates that within the specified used range of surface storage values (472.5-577.5 mm), the overall system's hydrological response is relatively insensitive to changes in surface storage. To explore this further, the surface storage parameter was adjusted repeatedly to identify any threshold that might influence the results. Through this process, it was determined that a threshold value of 52 mm exists. Below this threshold, changes in surface storage could potentially affect the hydrological outputs. However, once the surface storage parameter exceeds 52 mm, the results remain unchanged. This indicates that the system has reached a saturation point or a state where additional increases in surface storage no longer impact aquifer recharge, infiltration, base flow or other related hydrological processes as the soil could not hold more water for infiltration.

3.1.3 ANALYSIS OF SOIL STORAGE (SoilS) PARAMETER

Figure 35 illustrates the average annual cumulative values (mm/year) of various hydrological fluxes for different soil storage scenarios in a sand dam NBS hai. The simulation was run using the Soil Moisture Accounting (SMA) loss method in HEC-HMS where the only parameter varied was the soil storage parameter.

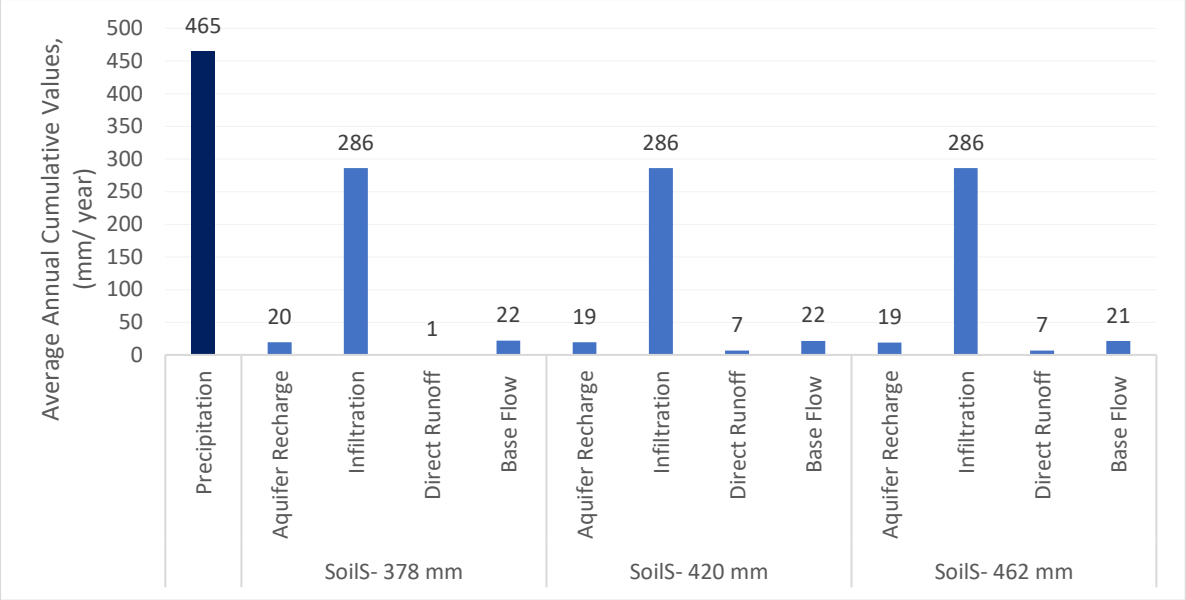

Figure 35 Hydrological fluxes resulting from Soil Storage (SoilS) parameter, Sand Dam

When comparing the results to the baseline scenario with 100 mm soil storage before implementing the sand dam technique, the following increasing and decreasing trends are observed.

- *Aquifer Recharge:* Aquifer recharge slightly decreases from the baseline of 21 mm/year to 20 mm/year at a SoilS of 378 mm, and further to 19 mm/year at higher SoilS values of 420 mm and 462 mm. These results suggest that higher soil storage may retain more water in the soil, reducing the amount available for aquifer recharge.

- *Infiltration:* Infiltration remains stable at 286 mm/year across all SoilS levels, showing only a slight increase of 3 mm/year from the baseline. This suggests that soil storage has a relatively minor impact on overall infiltration, but the presence of the sand dam still contributes to slightly higher infiltration as compared to no sand dam.

- *Direct Runoff:* Direct Runoff decreases to 1 mm/year at a SoilS of 378 mm, a significant reduction from the 9 mm/year in the baseline. However, it increases to 7 mm/year at higher SoilS values of 420 mm and 462 mm. Despite these fluctuations, the sand dam still effectively reduces runoff compared to the baseline, particularly at lower SoilS values. At higher SoilS, the dam's effect on reducing runoff might be less pronounced because the soil itself is already absorbing and holding a large amount of water, potentially leading to greater runoff once the soil is saturated.

- *Base Flow:* Base flow decreases slightly from the baseline of 23 mm/year to 22 mm/year at SoilS values of 378 mm and 420 mm, and further to 21 mm/year at 462 mm. The decrease of up to 2 mm/year suggests that higher soil storage may reduce the amount of water contributing to base flow, possibly due to greater water retention in the soil itself.

These results indicate that increasing soil storage values after the implementation of a sand dam reduces the amount of water available for aquifer recharge, and base flow. The higher retention within the soil may be beneficial for soil moisture but could lead to reduced water availability for other hydrological processes.

3.1.4 ANALYSIS OF COMBINED PARAMETER CHANGES ON HYDROLOGICAL OUTPUTS

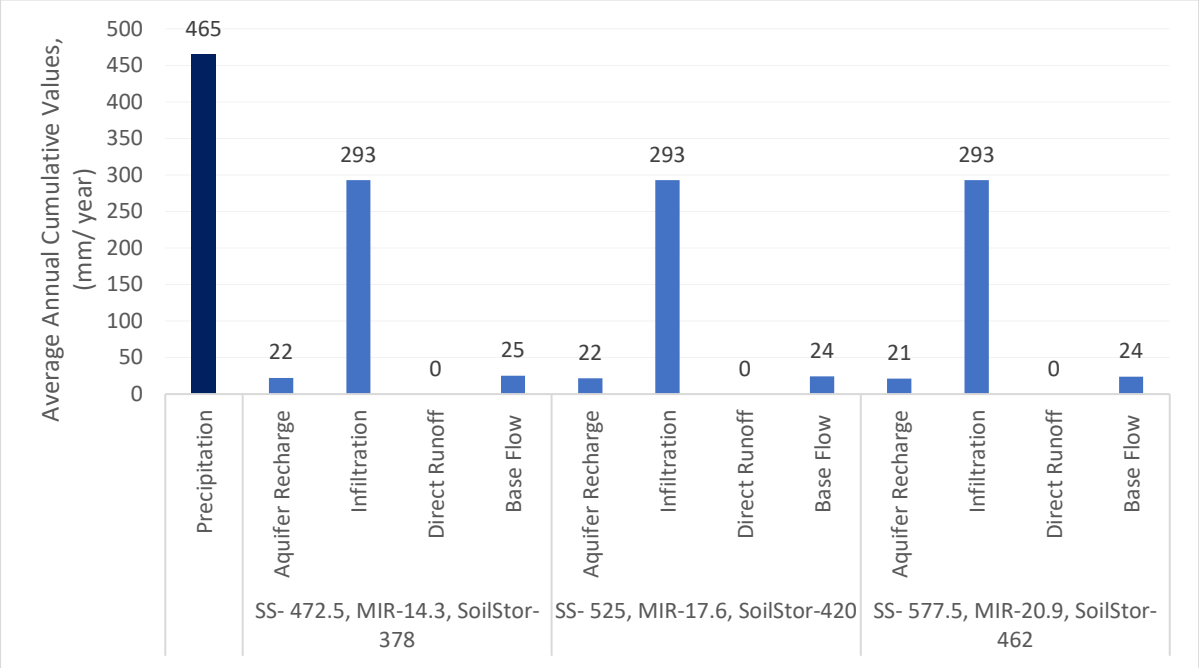

Figure 36 Hydrological fluxes resulting from combined parameter Maximum Infiltration Rate (MIR), Surface Storage (SS), Soil Storage (SoilS) changes, Sand Dam

Figure 36 in brief summarizes the analysis of combined changes of all the key parameters compared to baseline scenario.

Aquifer Recharge: When all parameters are varied together, aquifer recharge shows slight improvements over the baseline scenario, ranging from 21 mm/year to 22 mm/year. This indicates a modest increase of up to 1 mm/year, suggesting that while the combined effects of

SS, MIR, and SoilS do improve recharge slightly, the overall impact on recharge is smaller or less distinct than the impact seen when focusing on each individual parameter.

Infiltration: The combined scenario results in the highest infiltration rate of 293 mm/year, a 10 mm/year increase over the baseline. This confirms that optimal configurations of SS, MIR, and SoilS can maximize infiltration, significantly improving upon the baseline scenario.

Direct Runoff: is completely eliminated (0 mm/year) in all combined scenarios, which is a significant improvement over the baseline of 9 mm/year. This underscores the effectiveness of the sand dam in conjunction with optimized parameters in entirely preventing surface runoff.

Base Flow: is slightly reduced to 25 mm/year in the scenario with SS 472.5, MIR 14.3, and SoilS 378, and further down to 24 mm/year in other combined scenarios. These values still represent an increase of up to 2 mm/year over the baseline scenario, indicating that the combined effects of the sand dam and optimized parameters can sustain a higher base flow compared to the scenario without a sand dam.

The implementation of sand dams shows clear benefits across all hydrological parameters when compared to the baseline scenario without a sand dam. Aquifer recharge, infiltration, and base flow generally see notable increases, while direct runoff is significantly reduced or eliminated altogether. These improvements underscore the effectiveness of sand dams in enhancing water retention, promoting groundwater recharge, and reducing surface water loss.

3.2 SEMI-CIRCULAR SOIL BUND IMPLEMENTATION

3.2.1 ANALYSIS OF MAXIMUM INFILTRATION RATE (MIR) PARAMETER

Figure 37 illustrates the average annual cumulative values (mm/year) of various hydrological fluxes for different maximum infiltration rate scenarios in a semi-circular soil bunds technique. The simulation was run using the Soil Moisture Accounting (SMA) loss method in HEC-HMS where the only parameter varied was the maximum infiltration rate parameter.

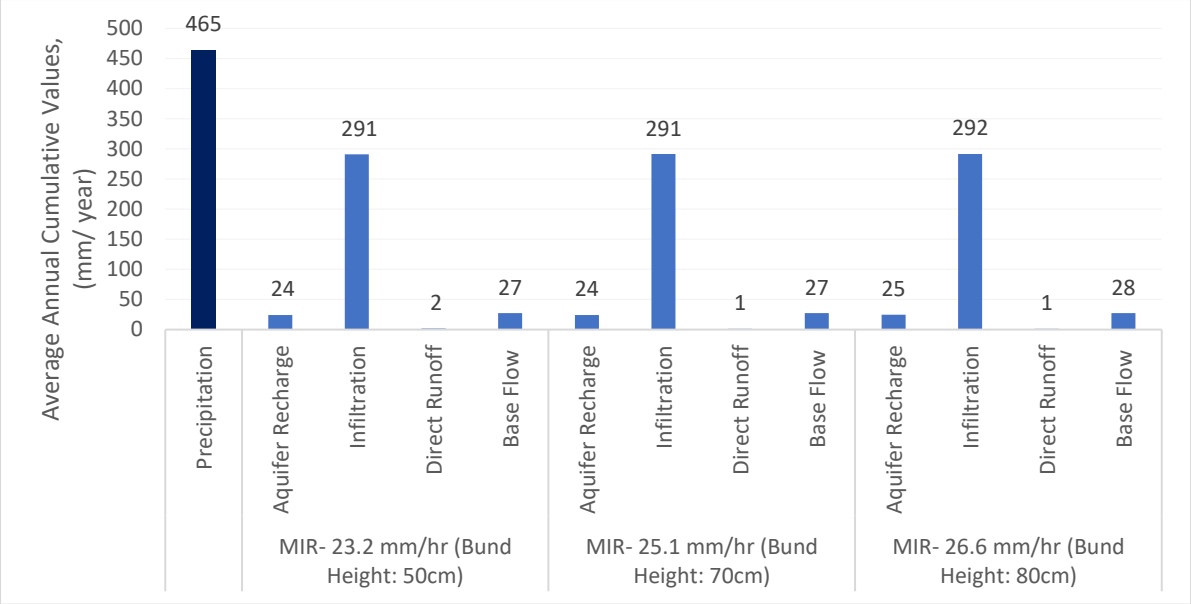

Figure 37 Hydrological fluxes resulting from Maximum Infiltration Rate (MIR) Analysis, Semi-circular soil bunds

The implementation of semi-circular soil bunds significantly altered the hydrological parameters in the study area. When comparing the results to the baseline scenario with an 11 mm/hr max infiltration rate before implementing the semi-circular soil bund technique, the following increasing and decreasing trends are observed:

- *Aquifer Recharge:* Aquifer recharge increases from the baseline of 21 mm/year to 24 mm/year at a Maximum Infiltration Rate (MIR) of 23.2 mm/hr (50 cm bund height) and remains stable at 24 mm/year for the MIR of 25.1 mm/hr (70 cm bund height), eventually increasing to 25 mm/year at an MIR of 26.6 mm/hr (80 cm bund height). This gradual increase of up to 4 mm/year illustrates that the bunds, by enhancing infiltration rates, help to boost aquifer recharge.

- *Infiltration:* Infiltration rises from 283 mm/year in the baseline to 291 mm/year at an MIR of 23.2 mm/hr (50 cm bund height) and increases slightly to 292 mm/year at an MIR of 26.6 mm/hr (80 cm bund height). The increase of up to 9 mm/year demonstrates that bunds, along with higher infiltration rates, significantly enhance water absorption into the soil.

- *Direct Runoff:* Direct runoff decreases from the baseline of 9 mm/year to 2 mm/year at an MIR of 23.2 mm/hr (50 cm bund height), and further to 1 mm/year at MIRs of 25.1 mm/hr and 26.6 mm/hr (70 cm and 80 cm bund heights). This reduction of up to

8 mm/year illustrates the effectiveness of bunds in reducing surface runoff, particularly as the infiltration rate increases.

- *Base Flow:* Base flow improves from 23 mm/year in the baseline to 27 mm/year at MIRs of 23.2 mm/hr and 25.1 mm/hr, and further to 28 mm/year at an MIR of 26.6 mm/hr (80 cm bund height). The increase of up to 5 mm/year illustrates that bunds, particularly when paired with higher infiltration rates, contribute to sustaining higher base flow compared to the baseline scenario.

These results demonstrate that as the MIR increases with the implementation of semi-circular soil bunds, the efficiency of water infiltration and aquifer recharge slightly improves. This shift directly enhances groundwater availability and base flow.

3.2.2 ANALYSIS OF SURFACE STORAGE (SS) PARAMETER

Figure 38 illustrates the average annual cumulative values (mm/year) of various hydrological fluxes for different surface storage scenarios in semi-circular soil bunds technique. The simulation was run using the Soil Moisture Accounting (SMA) loss method in HEC-HMS where the only parameter varied was the surface storage parameter.

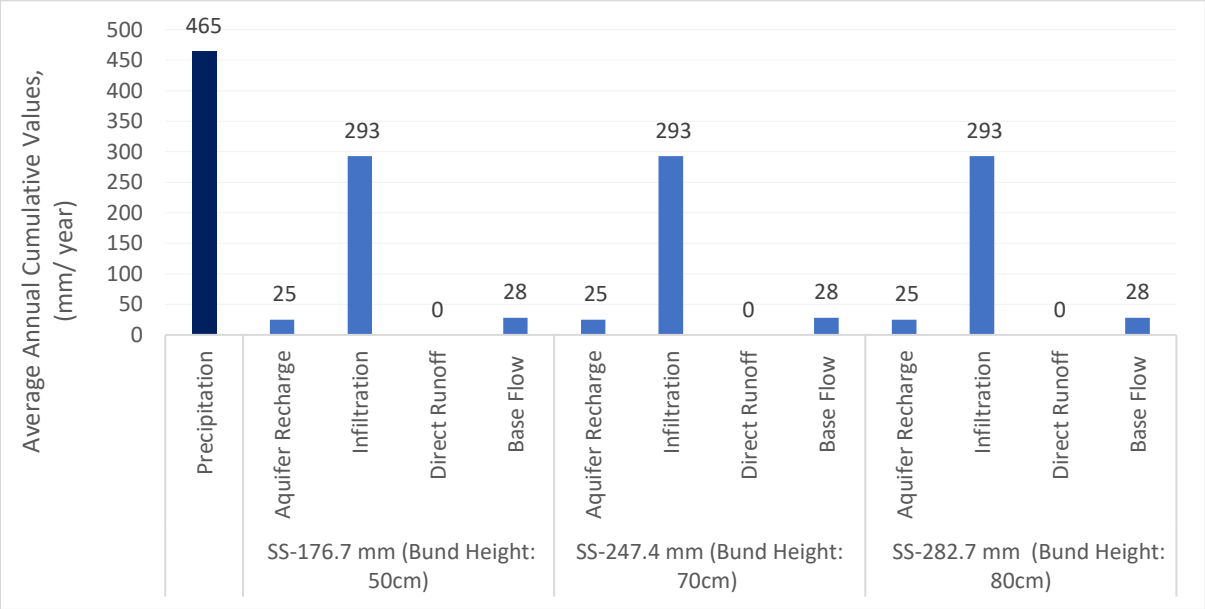

Figure 38 Hydrological fluxes resulting from Surface Storage (SS) Analysis, Semi-circular soil bunds

The results from the comparison against the baseline scenario with 2 mm surface storage before the initiation of the sand dam technique application are as follows.

- *Aquifer Recharge:* Aquifer recharge increases from 21 mm/year in the baseline to 25 mm/year across all Surface Storage (SS) levels (bund heights of 50 cm, 70 cm, and 80 cm). This increase of 4 mm/year shows that the semi-circular bunds significantly enhance groundwater recharge by promoting greater water retention and infiltration compared to the scenario without bunds.

- *Infiltration:* Infiltration increases from 283 mm/year in the baseline to 293 mm/year across all SS levels (bund heights). This consistent increase of 10 mm/year highlights the role of semi-circular bunds in enhancing the system's overall infiltration capacity compared to the scenario without bunds.

- *Direct Runoff:* Direct runoff is completely eliminated (0 mm/year) across all SS levels, compared to 9 mm/year in the baseline scenario. This indicates that the semi-circular bunds are highly effective in capturing and holding surface water, thereby preventing it from becoming runoff, a significant improvement over the baseline scenario without bunds.
- *Base Flow:* Base flow increases from 23 mm/year in the baseline to 28 mm/year across all SS levels. This increase of 5 mm/year suggests that the bunds help to maintain a higher base flow by increasing water retention and promoting infiltration, leading to more consistent water availability in the aquifer compared to the baseline scenario without bunds.

When analyzing the results for different scenarios of surface storage in both the sand dam and semi-circular soil bund techniques, a notable pattern emerges. The observation that the hydrological parameter values remain constant despite varying surface storage across different bund heights for semi-circular soil bund and sand dam techniques, even though they are distinct methods, raises important considerations about the modeling approach and the underlying system characteristics in HEC-HMS. Also, this uniformity in the results indicates that within the specific range of SS values used, the overall hydrological response of the system is insensitive to changes in surface storage for both techniques. There could be following possible reasons for the noticeable constant pattern:

I. **THRESHOLD VALUE:** In the case of sand dams, through adjusting the surface storage parameter with different values it was determined that there exists a threshold value of 52 mm surface storage, below which variations in SS can influence the

hydrological outputs but it was appeared that once this threshold is surpassed, additional increases in SS do not affect the hydrological processes such as aquifer recharge or groundwater storage. The same threshold effect seems to apply to the semi-circular soil bund technique. This suggests that, regardless of the technique, the soil and overall catchment system reach a saturation point where further increments in surface storage do not lead to significant changes in infiltration or groundwater recharge. This is likely because the soil reaches its maximum capacity to hold water, beyond which additional surface storage is either lost as runoff or remains unused on the surface without contributing to infiltration.

II. **HEC-HMS AND SMA LOSS METHOD IMPLICATIONS:** The consistent results across both sand dam and semi-circular soil bund techniques, despite their differences in design and purpose, suggest that the SMA loss method in HEC-HMS may no longer influences the infiltration process or takes into account the additional water from surface storage once the soil reaches a certain moisture threshold.

III. **FIELD APPLICATONS OF THE TECHNIQUES:** While the model results indicate insensitivity to SS changes beyond a certain threshold, this does not diminish the practical importance of these techniques. In the field, both sand dams and semi-circular soil bunds play critical roles in managing surface runoff, increasing water retention, and supporting local water needs. The model results suggest that once a certain level of water retention is achieved, the benefits of further increasing surface storage diminish, highlighting the importance of optimizing, rather than maximizing, surface storage in these interventions**.**

3.2.3 ANALYSIS OF SOIL STORAGE (SoilS) PARAMETER

Figure 39 illustrates the average annual cumulative values (mm/year) of various hydrological fluxes for different soil storage scenarios in semi-circular soil bunds technique. The simulation was run using the Soil Moisture Accounting (SMA) loss method in HEC-HMS where the only parameter varied was the soil storage parameter.

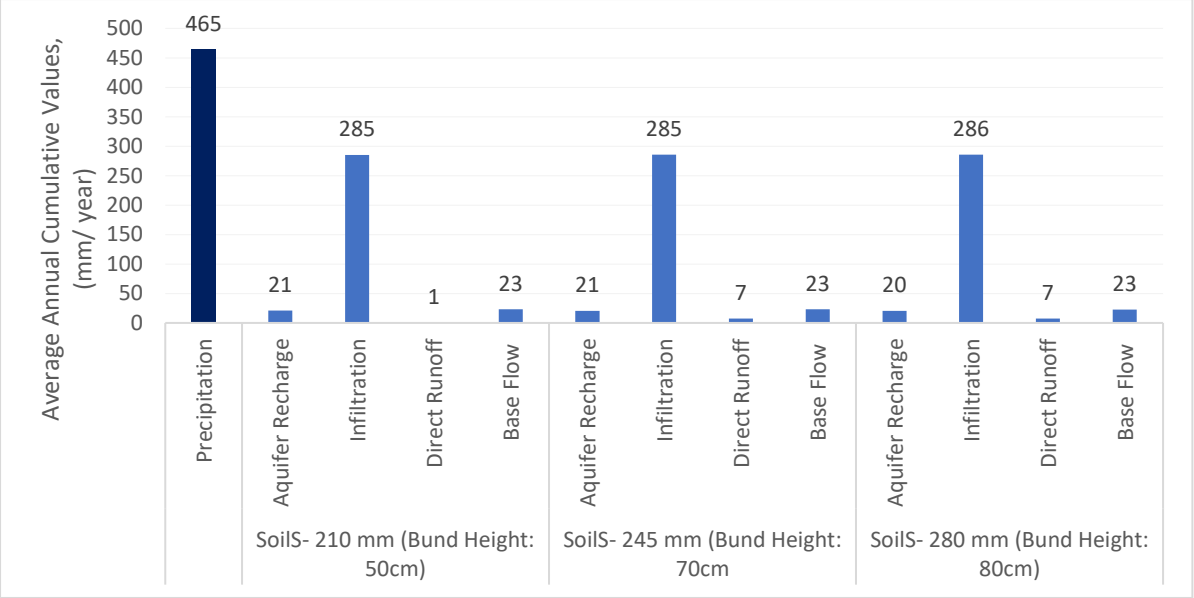

Figure 39 Hydrological fluxes resulting from Soil Storage (SoilS) Analysis, Semi-circular soil bunds

When comparing the results to the baseline scenario with a soil storage value of 100 mm before implementing the semi-circular soil bund technique, the following trends have been observed:

- *Aquifer Recharge:* Aquifer recharge remains the same as the baseline at 21 mm/year for Soil Storage (SoilS) values of 210 mm (50 cm bund height) and 245 mm (70 cm bund height), but decreases slightly to 20 mm/year at a SoilS of 280 mm (80 cm bund height). This suggests that, at higher SoilS levels, the bunds may cause more water to be retained in the soil, reducing the amount that infiltrates deeper into the aquifer, slightly decreasing recharge compared to the baseline.

- *Infiltration:* Infiltration sees a minor increase, reaching 285 mm/year at SoilS values of 210 mm and 245 mm, and 286 mm/year at 280 mm. The increase of up to 3 mm/year suggests that while bunds do enhance infiltration slightly, the effect is less pronounced when SoilS is the only varying factor, compared to the baseline scenario.

- *Direct Runoff:* Runoff drops significantly to 1 mm/year at a SoilS of 210 mm (50 cm bund height), compared to 9 mm/year in the baseline scenario. However, it increases to 7 mm/year at higher SoilS values of 245 mm and 280 mm (70 cm and 80 cm bund heights). This pattern suggests that while bunds are effective at reducing runoff at

lower SoilS values, higher soil storage might lead to increased runoff as the soil reaches saturation, similar to what was observed in the sand dam scenario.

- *Base Flow*: Base flow remains the same as the baseline at 23 mm/year across all SoilS levels (50 cm, 70 cm, and 80 cm bund heights). This indicates that varying soil storage alone has minimal impact on base flow, suggesting that other factors, such as infiltration rate and surface storage, play a more significant role in enhancing base flow compared to the baseline.

The results demonstrate that as soil storage capacity increases with the implementation of semi-circular soil bunds, aquifer recharge, and base flow tend to decrease slightly. This is because more water is retained within the soil, reducing the amount available for other hydrological processes. While infiltration rates increase slightly, the overall effect of increased soil storage have a focus on enhancing soil moisture retention.

3.2.4 ANALYSIS OF COMBINED PARAMETER CHANGES ON HYDROLOGICAL OUTPUTS

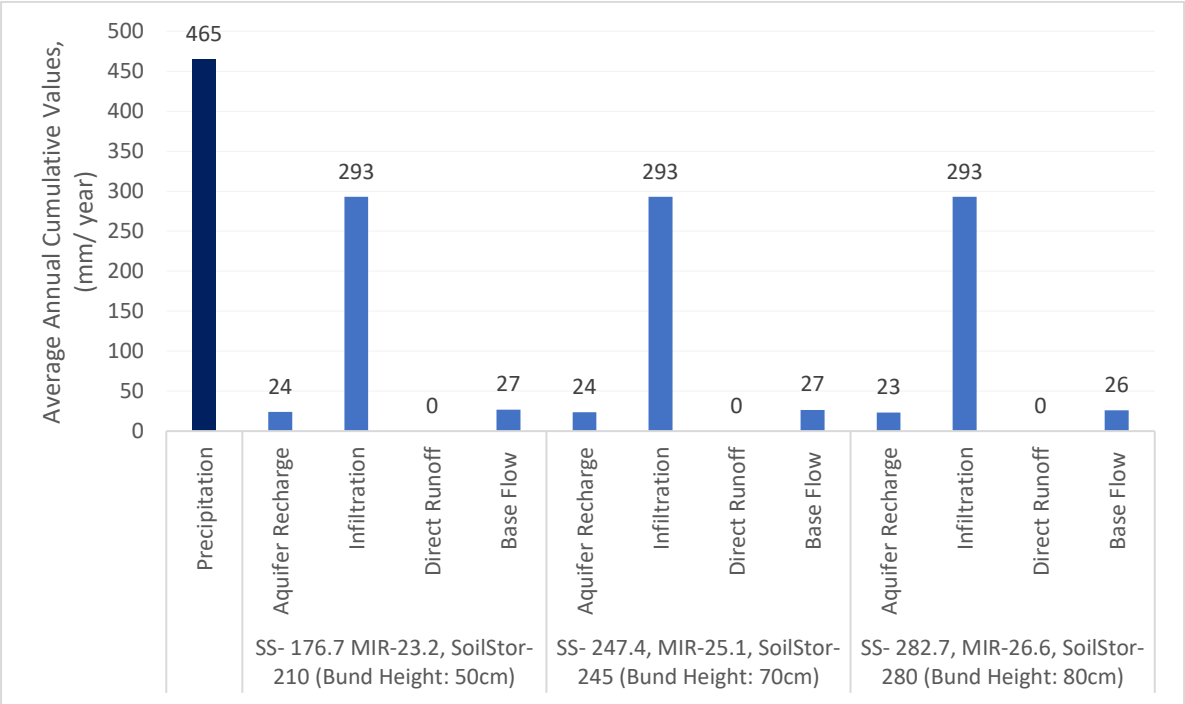

Figure 40 Hydrological fluxes resulting from combined parameter Maximum Infiltration Rate (MIR), Surface Storage (SS), Soil Storage (SoilS) changes, Semi-circular soil bunds

Figure 40 in brief summarizes the analysis of combined changes of all the key parameters compared to baseline scenario.

Aquifer recharge: when all parameters are varied together, aquifer recharge improves to 24 mm/year for the lower and middle bund heights (50 cm and 70 cm) and slightly decreases to 23 mm/year at the highest bund height (80 cm). This still represents an increase of up to 3 mm/year over the baseline, indicating that while semi-circular bunds do improve recharge, the benefits are most significant at lower and moderate bund heights.

Infiltration: The infiltration remains at 293 mm/year across all combined scenarios, representing a 10 mm/year increase over the baseline. This confirms that semi-circular bunds, when optimized with other factors, can significantly boost the infiltration process compared to the scenario without bunds.

Direct Runoff: Direct runoff is eliminated (0 mm/year) across all combined scenarios, a significant improvement from the baseline of 9 mm/year. This highlights the effectiveness of semi-circular bunds, especially when combined with optimal SS, MIR, and SoilS values, in completely preventing surface runoff compared to the scenario without bunds.

Base flow: Base flow shows a slight improvement, reaching 27 mm/year at the 50 cm and 70 cm bund and slightly reduces to 26 mm/year at the 80 cm bund. Despite the slight variation, this still represents an increase of up to 4 mm/year over the baseline, indicating that semi-circular bunds, especially at lower bund heights, contribute to maintaining a higher and more consistent base flow compared to the baseline scenario without bunds.

The implementation of semi-circular soil bunds shows clear benefits across all hydrological parameters when compared to the baseline scenario without bunds. Aquifer recharge, infiltration, and base flow generally see notable increases, while direct runoff is significantly reduced or eliminated altogether. The results indicate that semi-circular bunds are effective in enhancing water retention, promoting groundwater recharge, and reducing surface water loss. The comparison also highlights that intermediate bund heights of 50 and 70 cm seems to provide the best overall balance between enhancing aquifer recharge, and base flow. As the bund height increases beyond 70 cm to 80 cm, the benefits for aquifer recharge and base flow diminish slightly, indicating that further increases in height may not be necessary or effective for these specific goals. Higher bund heights might be more suitable for areas where increasing soil moisture is the primary goal.

3.3 AN INCREASED VEGETATION

3.3.1 ANALYSIS OF MAXIMUM INFILTRATION RATE (MIR) PARAMETER

Figure 41 illustrates the average annual cumulative values (mm/year) of various hydrological fluxes of different maximum infiltration rate scenarios in an increased vegetation cover scenario. The simulation was run using the Soil Moisture Accounting (SMA) loss method in HEC-HMS where the only parameter varied was the maximum infiltration rate parameter. The increase in the vegetation cover, particularly grassland has produced notable changes in the hydrological parameters of the study area.

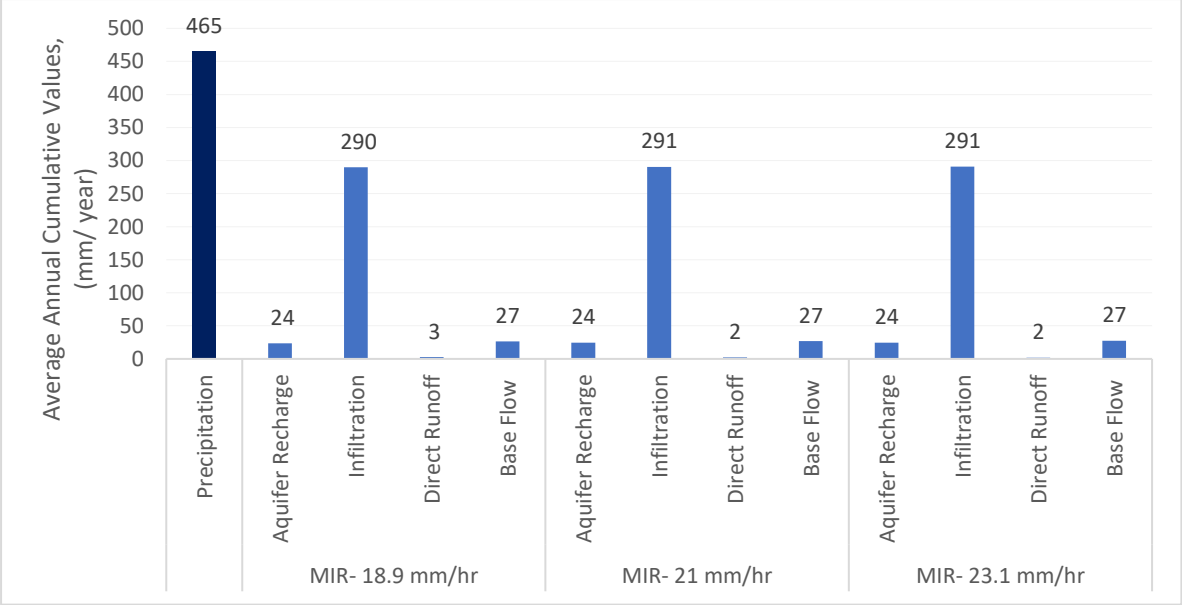

Figure 41 Hydrological fluxes resulting from Maximum Infiltration Rate (MIR) Analysis, Increased Vegetation Cover

Compared to the baseline scenario, where the maximum infiltration rate was 11 mm/hr before enhancing vegetation cover, the following trends are observed.

- *Aquifer Recharge:* Aquifer recharge increases to 24 mm/year across all levels of Maximum Infiltration Rate (MIR) (18.9 mm/hr, 21 mm/hr, and 23.1 mm/hr), compared to the baseline of 21 mm/year. This consistent increase of 3 mm/year suggests that the improved infiltration rates due to increased vegetation help in better groundwater recharge, providing a more sustainable water supply compared to the scenario without increased vegetation.

- *Infiltration:* Infiltration increases steadily from 283 mm/year in the baseline scenario to 290 mm/year at an MIR of 18.9 mm/hr and further to 291 mm/year at an MIR of

23.1 mm/hr. This increase of up to 8 mm/year shows that increased vegetation, by enhancing the infiltration rate, significantly improves the soil's water absorption ability compared to the baseline.

- *Direct Runoff:* Direct runoff decreases to 3 mm/year at an MIR of 18.9 mm/hr and further to 2 mm/year at an MIR of 21 mm/hr and 23.1 mm/hr, compared to the baseline of 9 mm/year. This significant reduction of up to 7 mm/year highlights that increased vegetation, by enhancing the soil's infiltration capacity, effectively reduces surface runoff compared to the baseline.

- *Base Flow:* Base flow improves to 27 mm/year across all MIR levels (18.9 mm/hr, 21 mm/hr, and 23.1 mm/hr), compared to the baseline of 23 mm/year. This consistent increase of 4 mm/year indicates that increased vegetation, by enhancing infiltration rates, contributes to sustaining higher base flow compared to the scenario without increased vegetation.

These results demonstrate that the increase in vegetation cover, particularly grassland, positively influences the hydrological cycle by improving water infiltration, and base flow while reducing direct runoff. These changes collectively enhance water availability and sustainability in the study area.

3.3.2 ANALYSIS OF SURFACE STORAGE (SS) PARAMETER

Figure 42 illustrates the average annual cumulative values (mm/year) of various hydrological fluxes for different surface storage scenarios in an increased vegetation cover scenario. The simulation was run using the Soil Moisture Accounting (SMA) loss method in HEC-HMS where the only parameter varied was the surface storage parameter.

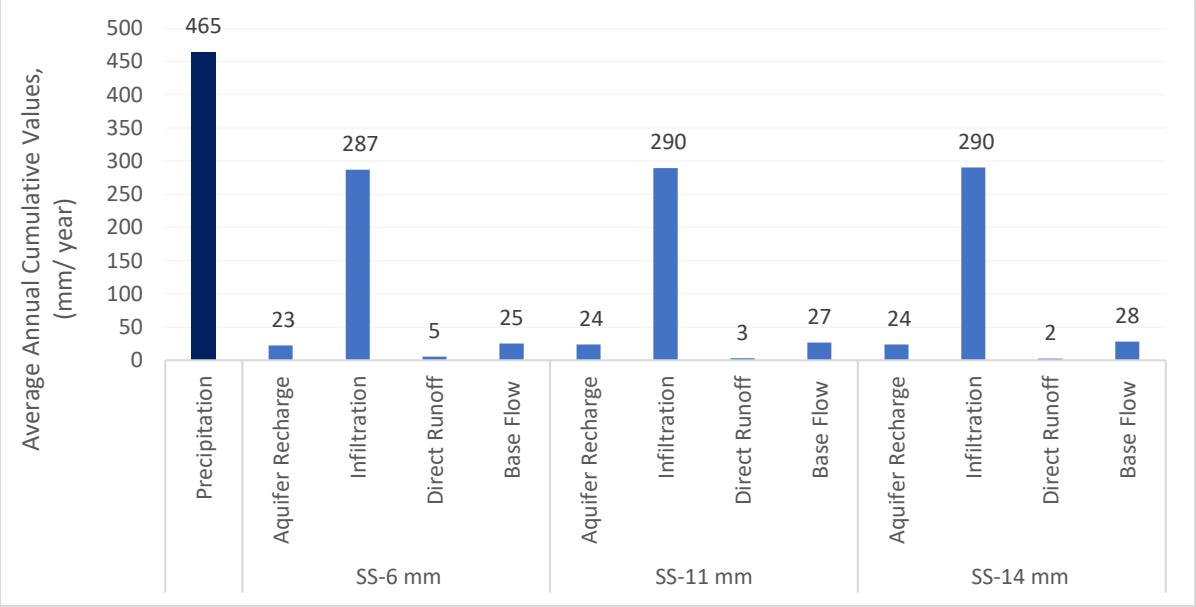

Figure 42 Hydrological fluxes resulting from Surface Storage (SS) Analysis, Increased Vegetation Cover

When compared to the baseline scenario, where the surface storage was 2 mm, the following trends are observed:

- *Aquifer Recharge:* Aquifer recharge increases from 21 mm/year in the baseline to 23 mm/year at a Surface Storage (SS) of 6 mm and further to 24 mm/year at SS levels of 11 mm and 14 mm. This improvement of up to 3 mm/year indicates that increased vegetation cover enhances the soil's ability to absorb and retain water, leading to greater groundwater recharge compared to the baseline scenario without increased vegetation.

- *Infiltration:* Infiltration increases from 283 mm/year in the baseline to 287 mm/year at an SS of 6 mm, and further to 290 mm/year at SS levels of 11 mm and 14 mm. The increase of up to 7 mm/year highlights that increased vegetation improves the soil's capacity to absorb water, resulting in better infiltration compared to the baseline scenario.

- *Direct Runoff:* Direct runoff decreases from 9 mm/year in the baseline to 5 mm/year at an SS of 6 mm, and further to 2 mm/year at an SS of 14 mm. This reduction of up to 7 mm/year demonstrates the effectiveness of increased vegetation in reducing surface runoff, as vegetation cover slows down water movement, allowing more water to infiltrate into the soil compared to the baseline scenario.

- *Base Flow:* Base flow increases from 23 mm/year in the baseline to 25 mm/year at an SS of 6 mm, and further to 28 mm/year at an SS of 14 mm. This increase of up to 5 mm/year shows that increased vegetation, by promoting better infiltration and reducing runoff, helps maintain a higher and more consistent base flow compared to the baseline scenario.

The results clearly demonstrate the positive impacts of increased vegetation on the hydrological cycle, particularly in terms of water storage in the study area.

3.3.3 ANALYSIS OF SOIL STORAGE (SoilS) PARAMETER

Figure 43 illustrates the average annual cumulative values (mm/year) of various hydrological fluxes for different soil storage scenarios in an increased vegetation cover scenario. The simulation was run using the Soil Moisture Accounting (SMA) loss method in HEC-HMS where the only parameter varied was the soil storage parameter.

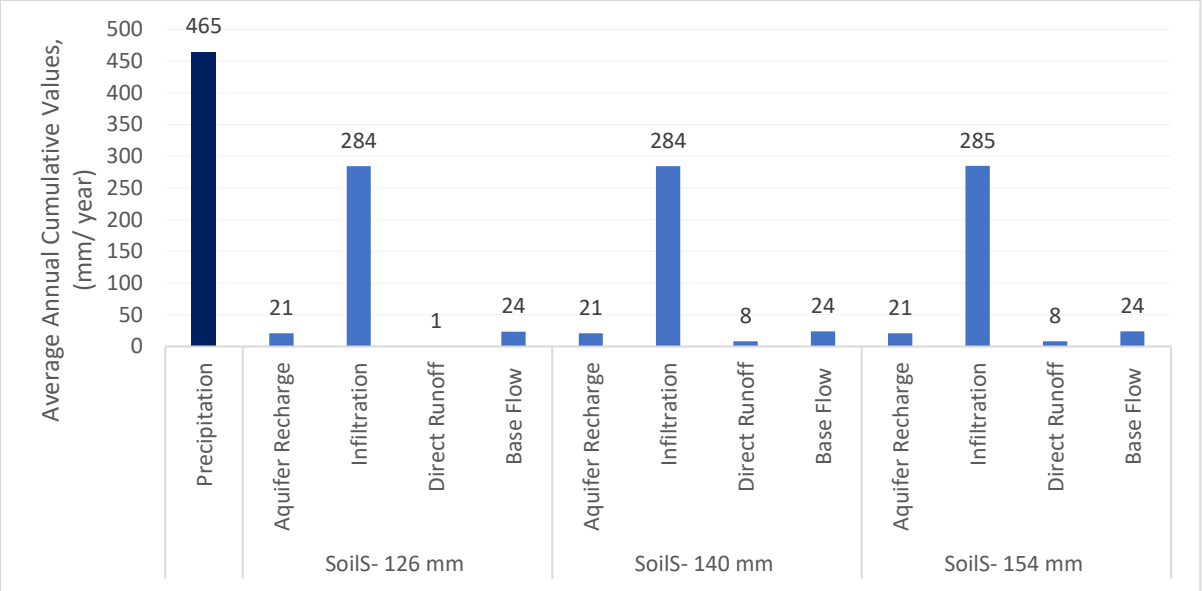

Figure 43 Hydrological fluxes resulting from Soil Storage (SoilS) Analysis, Increased Vegetation Cover

The analysis of the increased soil storage values reveals its effects on the hydrological parameters of the study area, compared to the baseline scenario where the soil storage was 100 mm. The observed trends are as follows:

- *Aquifer Recharge:* Aquifer recharge remains the same as the baseline at 21 mm/year across all Soil Storage (SoilS) levels (126 mm, 140 mm, and 154 mm). This suggests

that while increased vegetation improves other hydrological aspects, the direct impact on aquifer recharge is minimal when SoilS is the only varying factor.

- *Infiltration*: Infiltration increases slightly to 284 mm/year at a SoilS of 126 mm and further to 285 mm/year at 154 mm, compared to the baseline of 283 mm/year. This modest increase of up to 2 mm/year indicates that increased vegetation slightly enhances infiltration, but the impact is less pronounced when SoilS is the only varying factor.

- *Direct Runoff:* Direct runoff decreases significantly to 1 mm/year at a SoilS of 126 mm, but then increases to 8 mm/year at SoilS levels of 140 mm and 154 mm, compared to 9 mm/year in the baseline scenario. This pattern suggests that while increased vegetation reduces runoff at lower SoilS levels, higher soil storage may lead to increased runoff as the soil becomes saturated, similar to other scenarios involving soil storage changes.

- *Base Flow*: Base flow remains almost the same as the baseline at 24 mm/year across all SoilS levels (126 mm, 140 mm, and 154 mm). This suggests that while increased vegetation improves base flow slightly, the direct impact is minimal when SoilS is the only varying factor.

In summary, the increase in soil storage has led to improved soil moisture retention and a slight enhancement in infiltration rates, while its impact on aquifer recharge, and base flow remains relatively modest. The findings suggest that while increased soil storage is beneficial for surface and near-surface water processes, it has limited influence on deeper groundwater dynamics and overall water availability in the catchment area.

3.3.4 ANALYSIS OF COMBINED PARAMETER CHANGES ON HYDROLOGICAL OUTPUTS

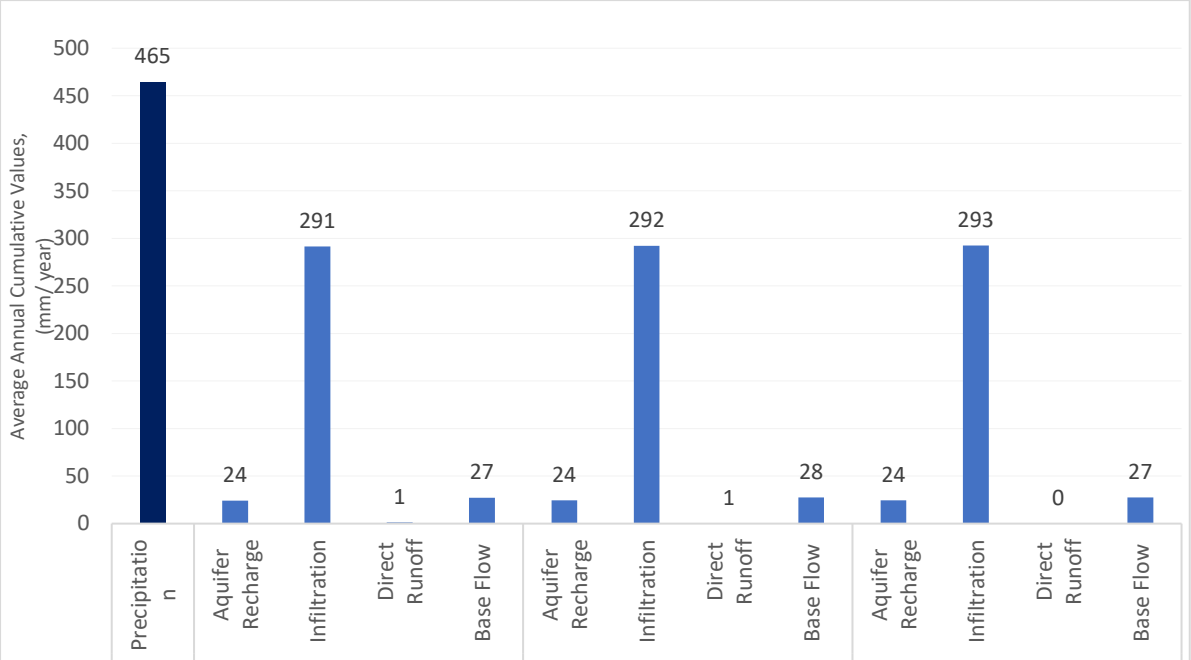

Figure 44 Hydrological fluxes resulting from combined parameter Maximum Infiltration Rate (MIR), Surface Storage (SS), Soil Storage (SoilS) changes, Increased Vegetation Cover

Figure 44 in brief summarizes the analysis of combined changes of all the key parameters compared to baseline scenario.

Aquifer Recharge: when all parameters are varied together, aquifer recharge improves to 24 mm/year across all scenarios, representing an increase of 3 mm/year over the baseline. This consistent improvement underscores that increased vegetation cover, when combined with optimal SS, MIR, and SoilS values, significantly enhances aquifer recharge compared to the baseline scenario.

Infiltration: when all parameters are varied together, infiltration improves significantly to 291 mm/year at the lowest bund height and further to 293 mm/year at the highest bund height, representing an increase of up to 10 mm/year over the baseline. This significant improvement shows that increased vegetation cover, when combined with optimal SS, MIR, and SoilS values, greatly enhances the system's overall infiltration capacity compared to the baseline scenario**.**

Direct Runoff: decreases significantly to 1 mm/year at the lower bund heights and is completely eliminated (0 mm/year) at the highest bund height, compared to 9 mm/year in the

baseline scenario. This substantial reduction of up to 9 mm/year demonstrates the effectiveness of increased vegetation cover in minimizing surface runoff.

Base Flow: improves to 27 mm/year at the lowest bund height and slightly increases to 28 mm/year at the middle bund height, compared to the baseline of 23 mm/year. This increase of up to 5 mm/year shows that increased vegetation cover, contributes to maintaining a higher base flow compared to the baseline scenario without increased vegetation.

The analysis of increased grassland cover on hydrological parameters reveals that grassland has a generally positive impact on aquifer recharge, infiltration rates, and base flow while direct runoff is significantly reduced when compared to the baseline scenario without increased vegetation. The results indicate that increased vegetation cover is effective in enhancing water retention, promoting groundwater recharge, and reducing surface water loss.

4 DISCUSSION ON ANALYSIS

4.1 PERCENTAGE CHANGE IN HYDROLOGICAL PARAMETERS DUE TO SAND DAM

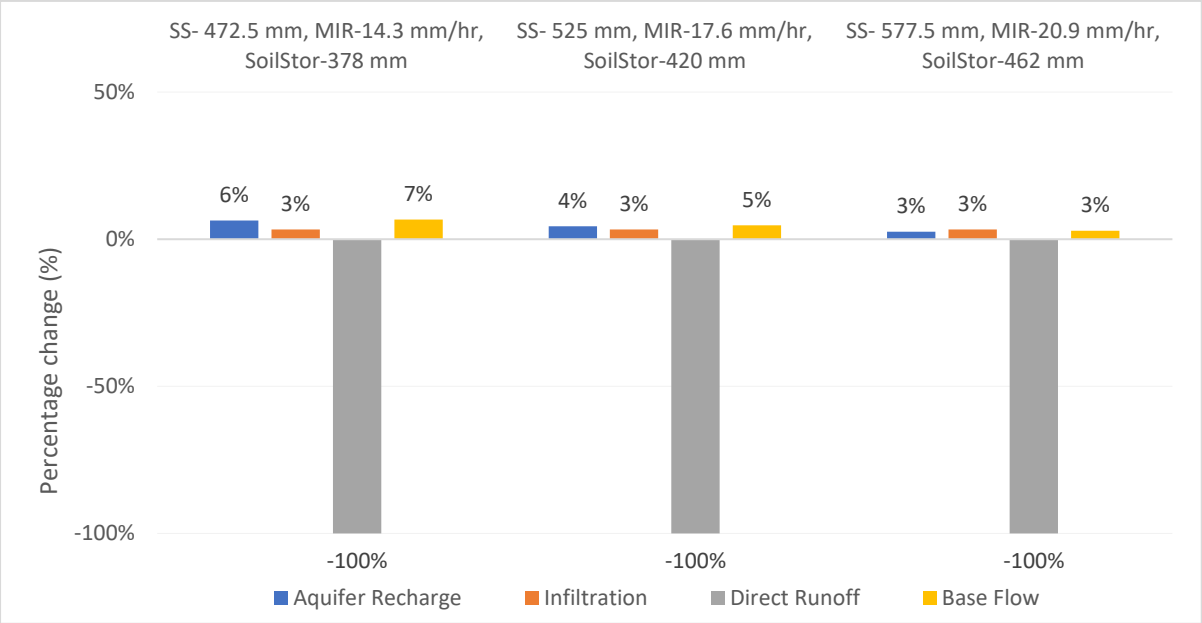

Figure 45 Percentage Change in Hydrological Fluxes Across Scenarios with Sand Dams (SS: Surface Storage, MIR: Maximum Infiltration Rate, SoilS: Soil storage)

Figure 45 shows the implementation of sand dams leads to a moderate increase in aquifer recharge, ranging from 3% to 6%. This indicates that sand dams enhance groundwater recharge by increasing water retention and infiltration, though the effect diminishes slightly with increasing storage and infiltration rates. Infiltration consistently increases by 3% across all scenarios, demonstrating that sand dams effectively improve the soil's ability to absorb water, contributing to overall hydrological balance. The most significant impact of sand dams is the complete elimination of direct runoff, with a 100% reduction across all scenarios. This underscores the effectiveness of sand dams in retaining surface water, preventing runoff, and promoting infiltration. Base flow increases between 3% and 7%, indicating that sand dams contribute to a sustained release of groundwater into streams, supporting base flow even during dry periods. This positive impact, though decreasing slightly with larger storage and infiltration rates, highlights the role of sand dams in maintaining streamflow.

4.2 PERCENTAGE CHANGE IN HYDROLOGICAL PARAMETERS DUE TO SEMI-CIRCULAR SOIL BUNDS

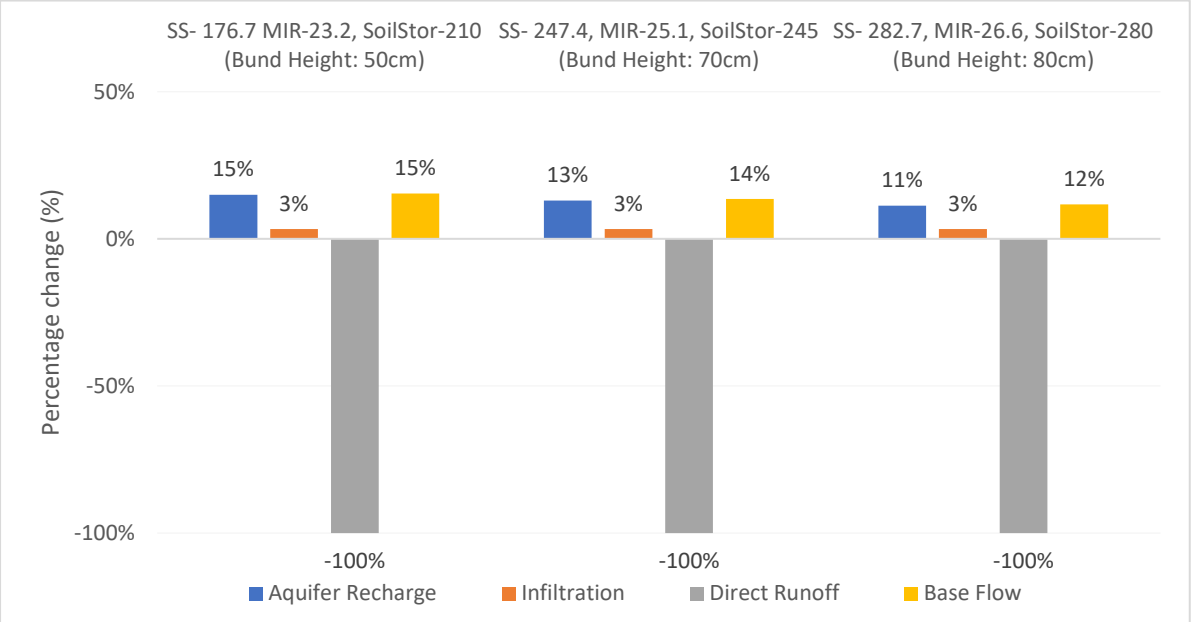

Figure 46 Percentage Change in Hydrological Fluxes Across Scenarios with Semi-circular (SS: Surface Storage, MIR: Maximum Infiltration Rate, SoilS: Soil storage)

Figure 46 indicates that semi-circular soil bunds lead to a significant increase in aquifer recharge, ranging from 11% to 15%. This higher recharge rate compared to sand dams suggests that bunds are particularly effective in promoting groundwater replenishment, especially in areas with intermediate bund heights. Infiltration increases by 3% across all scenarios, indicating that bunds also enhance the soil's ability to absorb water, contributing to overall water conservation. Soil bunds result in a 100% reduction in direct runoff, demonstrating their efficiency in capturing and retaining surface water, thereby minimizing water loss through runoff. Base flow increases significantly, between 12% and 15%. This suggests that semi-circular soil bunds are effective in sustaining groundwater contributions to streamflow.

4.3 PERCENTAGE CHANGE IN HYDROLOGICAL PARAMETERS DUE TO AN INCREASED VEGETATION COVER

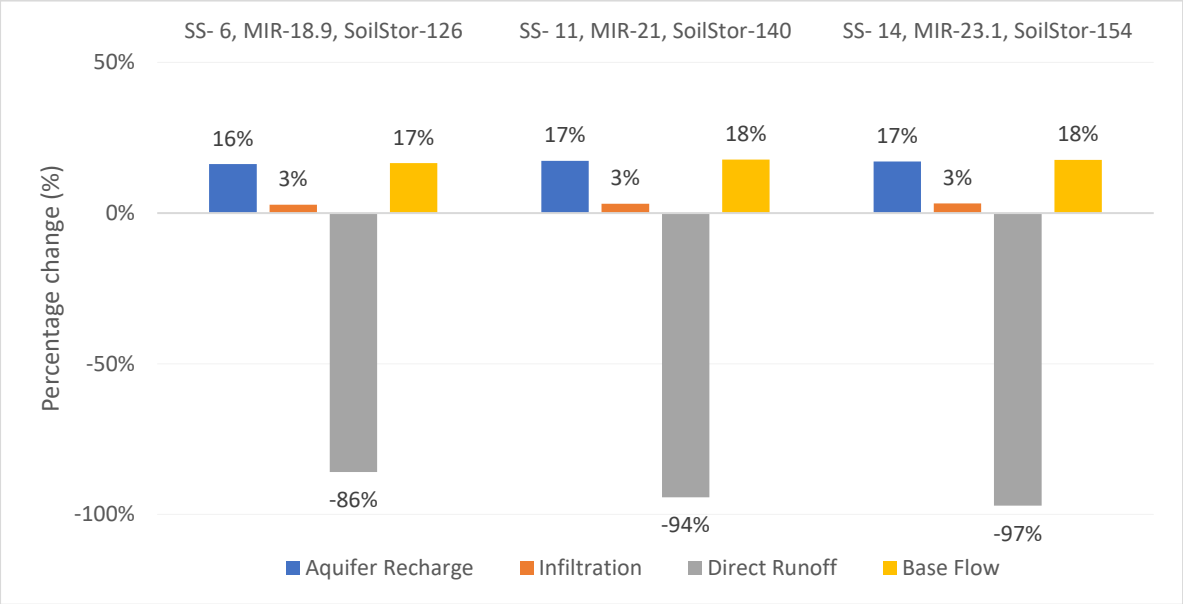

Figure 47 Percentage Change in Hydrological Fluxes Across Scenarios with Increased Vegetation Cover (SS: Surface Storage, MIR: Maximum Infiltration Rate, SoilS: Soil storage)

Figure 47 shows that increased vegetation cover leads to the highest increase in aquifer recharge, ranging from 16% to 17%. This suggests that vegetation plays a crucial role in enhancing groundwater recharge by promoting deeper infiltration of water into the soil. Infiltration improves by 3% across all scenarios, consistent with the other NBS strategies. This indicates that vegetation cover effectively increases the soil's permeability and its ability to retain water. There is a substantial reduction in direct runoff, ranging from 86% to 97%, with the most significant decrease occurring in scenarios with higher surface storage and infiltration rates. This highlights that increased vegetation cover is effective in reducing surface runoff, thereby preventing soil erosion and water loss. Base flow increases by 17% to 18%, the highest among the three NBS strategies. This demonstrates that increased vegetation cover not only enhances groundwater recharge but also supports the sustained release of groundwater into streams, maintaining base flow throughout the year.

Table 14 summarizes the percentage changes in hydrological fluxes compared to the baseline scenario for the scenarios of sand dams, semi-circular soil bunds, and increased vegetation cover.

Table 14 Summary of percentage changes in hydrological fluxes compared to the baseline scenario for the scenarios of sand dams, semi-circular soil bunds, and increased vegetation cover

	Sand Dam	Semi-circular soil bunds	Increased Vegetation Cover
Aquifer Recharge	3-6%	11-15%	16-17%
Infiltration	3%	3%	3%
Direct Runoff	reduced 100%	reduced 100%	reduced 86-97%
Base Flow	3-7%	12-15%	17-18%

Each NBS - sand dams, semi-circular soil bunds, and increased vegetation cover shows distinct impacts on the hydrological cycle. While all strategies significantly reduce direct runoff and improve infiltration, their effects on aquifer recharge and base flow vary. Sand dams and semi-circular soil bunds offer substantial benefits, particularly in eliminating direct runoff and sustaining base flow, with bunds showing slightly higher efficiency in recharging aquifers than sand dam. Increased vegetation cover, however, stands out for its superior performance in aquifer recharge and base flow enhancement, making it an effective strategy for long-term water resource sustainability.

5 CONCLUSION

This thesis study investigated the possibilities of sustainable MAR strategies to address water scarcity in Darar-weyne basin in Somaliland where hydrological data is limited and environmental conditions are harsh. By using global hydrological datasets and SMA method within HMS hydrological model, the study assessed the effectiveness of NBSs such as sand dams, semi-circular soil bunds and increased vegetation cover to recharge aquifer and meet local water demand. The comparison of satellite-derived datasets showed that data selection is crucial in hydrological modeling in data-scarce areas. GPM rainfall estimates were found to be more representative of rainfall in Darar-weyne basin than other satellite-based rainfall datasets and a better basis for modeling and analysis. The outcomes of the evaluated MAR strategies provide insightful information about the benefits of each NBSs and their effects on the water fluxes defining the hydrologic balance of the area.

Beyond the specifics of the model, the results offer important insights that bridge a gap in the technical literature, which often lacks quantitative evaluations of the effectiveness of MAR techniques. The steady increase in aquifer recharge, ranging from 3–17% across all techniques, highlights how MAR strategies can improve groundwater supplies over time. The estimated changes in baseflow, which often increased between 3-18% with the application of the NBSs techniques, indicates the potential for improved stream flows in the future, implying more consistent water availability in the drier periods of the year. The efficiency of these NBSs techniques in increasing water percolation into the soil, supporting groundwater recharge, and in capturing surface runoff is also supported by the consistent estimated 3% rise in infiltration rate across all evaluated scenarios and from 86-100% reduction in the direct runoff.

However, it is critical to appropriately manage NBS techniques, such as regular maintenance of structures like sand dams and bunds to prevent sediment buildup, and to monitor vegetation cover to ensure it can survive in semi-arid areas. The literature emphasizes that simply planting vegetation is not enough, it requires careful selection of drought-resistant species and ongoing maintenance to ensure survival. Grasslands are generally more resilient to drought compared to other vegetation types, but they still require proper species selection and initial irrigation to establish. In semi-arid regions, the survival of grasslands hinges on their ability to withstand extended dry periods and competition for limited water resources. Without proper management, the vegetation may not survive the harsh conditions, leading to reduced

effectiveness over time. Therefore, continuous monitoring and adaptive management for NBS are essential to prevent diminishing returns in terms of water infiltration and to maximize the efficiency of these techniques in enhancing aquifer recharge.

It is evident that MAR strategies are useful in improving water resources availability in arid lands. The quantitative estimates produced here support the widely held qualitative notion that nature-based solutions can help enhance aquifer recharge. This study is also providing useful practical indications on how to apply MAR strategies in real-world situations. In conclusion, this work shows that hydrological modelling and remote sensing estimates of rainfall can be combined to provide a quantitative evaluation of different NBSs. Further, the combined use of the NBSs explored here may increase the benefits of these interventions in mitigating water scarcity in arid areas like Somaliland. While each option has its own advantages, when applied collectively, they can offer a more robust and sustainable method of managing water resources, hence contributing to the long-term availability of clean water for rural communities.

6 REFERENCES

[1] Ismail, A. A., & Duale, H. A. (2023). Assessment of Awareness on Health Impact of Drinking Unsafe Water in Hargeisa, Somaliland. J Emerg Med OA, 1(1), 29-34.

[2] Jirde, M. I., Koech, O. K., & Karuma, A. N. (2021). An Analysis of Perceptions, Knowledge, And Management of Rainwater Harvesting (RWH) Technologies Among Agropastoralists in Odwayne District, Somaliland. Tropical and Subtropical Agroecosystems, 24(3).

[3] Aydrous, A. E., Elamin, A. M., Abuzied, M. H., Salih, S. A. R., & Mahmoud Elsheik, M. A. (2015). Effect of some micro catchment water harvesting techniques on some soil physical properties. Agric. For. Fish, 4(2), 55-58.

[4] Omer, A. B., & Tekile, A. K. (2023, March). Potential Hafir Dam Site Selection Using GIS and Remote Sensing Techniques in Gabiley District, Somaliland. In International Conference on Civil Engineering Innovative Development in Engineering Advances (pp. 137-149). Singapore: Springer Nature Singapore.

[5] Eklöw, K., & Krampe, F. (2019). Climate-related security risks and peacebuilding in Somalia. Stockholm International Peace Research Institute (SIPRI).

[6] Alam, S., Borthakur, A., Ravi, S., Gebremichael, M., & Mohanty, S. K. (2021). Managed aquifer recharge implementation criteria to achieve water sustainability. Science of the Total Environment, 768, 144992.

[7] NASA Jet Propulsion Laboratory. (2015, June 16). Map of groundwater storage trends for Earth's 37 largest aquifers. GraceFO. Retrieved August 20, 2024 from https://gracefo.jpl.nasa.gov/resources/48/map-of-groundwater-storage-trends-for-earths-37-largest-aquifers/.

[8] NASA Jet Propulsion Laboratory. (n.d.). GRACE mission overview. Grace. Retrieved August 20, 2024 from https://grace.jpl.nasa.gov/mission/grace/.

[9] Mawer, C., Parsekian, A., Pidlisecky, A., & Knight, R. (2016). Characterizing heterogeneity in infiltration rates during managed aquifer recharge. Groundwater, 54(6), 818-829.

[10] Dillon, P. (2005). Future management of aquifer recharge. Hydrogeology journal, 13(1), 313-316.

[11] Omer, M. A. (2024). Climate variability and livelihood in Somaliland: a review of the impacts, gaps, and ways forward. Cogent Social Sciences, 10(1), 2299108.

[12] Gaur, M. K., & Squires, V. R. (2018). Geographic extent and characteristics of the world's arid zones and their peoples. Climate variability impacts on land use and livelihoods in drylands, 3-20.

[13] Naorem, A., Jayaraman, S., Dang, Y. P., Dalal, R. C., Sinha, N. K., Rao, C. S., & Patra, A. K. (2023). Soil constraints in an arid environment—challenges, prospects, and implications. Agronomy, 13(1), 220.

[14] Jain, S., Tiwari, V., Thapa, A., Mangla, R., Jaiswal, R. K., Kumar, V., ... & Pandey, K. (2022). Performance evaluation of Google Earth Engine based precipitation datasets under different climatic zones over India. Remote Sensing in Earth Systems Sciences, 5(4), 263-276.

[15] Xiang, Y., Chen, J., Li, L., Peng, T., & Yin, Z. (2021). Evaluation of eight global precipitation datasets in hydrological modeling. Remote Sensing, 13(14), 2831.

[16] Somaliland Central Statistics Department. (2003). Somaliland in figures 2003. Retrieved August 21, 2024 from https://www.somalilandcsd.org/wp-content/uploads/2021/08/somaliland_in_figures_2003.pdf

[17] Ullah, S. (2016). Territorial diagnostic report of the land resources of Somaliland. FAO-SWALIM, Nairobi, Kenya. Retrieved August 21, 2024 from https://faoswalim.org/resources/site_files/L%20-21%20Land%20diagnostic%20report%20.pdf

[18] Ali, N. M., & Jemal, K. (2017). Mitigating Natural Disasters in Somaliland Policy Options and Strategies.

[19] Republic of Somaliland, Ministry of Planning & National Development, Water For Rural Resilience Project 'Barwaaqo', Construction Investment Report - Darar-weyne Site, Maroodi Jeeh Region, Somaliland State, Hydro Nova. (2024).

[20] Somaliland Ministry of Foreign Affairs and International Cooperation. (n.d.). History. Retrieved July 31st, 2024 from https://mfa.govsomaliland.org/article/history-4.

[21] GURE, A. Assessment of Drought Recurrence in Somaliland: Causes, Impacts and Mitigations.

[22] Miigane, A. M., Farah, A. I., Allardyce, E., Zdunnek, G., Wirth, G., Hartmann, I., ... & Golznig, P. Somaliland Baseline Study.

[23] Bile, M. S., & Limbu, P. (2022). Spatiotemporal Variability of Drought and its Relationships to ENSO and IOD Indices in Somaliland. *Tanzania Journal of Science*, *48*(4), 816-831.

[24] Banks, D. (2008). Potable water strategies in southern Mudug, Somalia, with special reference to the local economics of motorised borehole systems for watering nomadic livestock. Hydrogeology Journal, 16, 765-777.

[25] Hasan, A. A., Mohamed, Z. A., & Alam, P. Factors Affecting Project Performance: A Case of Ministry of Water Resources Development, Somaliland.

[26] FAO SWALIM. (2023). Somalia Climate Time Series Data. Retrieved May 21, 2024, from https://climseries.faoswalim.org/station/

[27] Aksu, H., Cavus, Y., Aksoy, H., Akgul, M. A., Turker, S., & Eris, E. (2022). Spatiotemporal analysis of drought by CHIRPS precipitation estimates. Theoretical and Applied Climatology, 148(1), 517-529.

[28] Climate Hazards Center. (n.d.). CHIRPS precipitation data. University of California, Santa Barbara. Retrieved August 1, 2024, from https://www.chc.ucsb.edu/data/chirps.

[29] Rivera, J. A., Hinrichs, S., & Marianetti, G. (2019). Using CHIRPS Dataset to Assess Wet and Dry Conditions along the Semiarid Central-Western Argentina. Advances in Meteorology, 2019(1), 8413964.

[30] Nawaz, M., Iqbal, M. F., & Mahmood, I. (2021). Validation of CHIRPS satellite-based precipitation dataset over Pakistan. Atmospheric Research, 248, 105289.

[31] Tan, J., Huffman, G. J., Bolvin, D. T., & Nelkin, E. J. (2019). IMERG V06: Changes to the morphing algorithm. Journal of Atmospheric and Oceanic Technology, 36(12), 2471-2482.

[32] Pradhan, R. K., Markonis, Y., Godoy, M. R. V., Villalba-Pradas, A., Andreadis, K. M., Nikolopoulos, E. I., ... & Hanel, M. (2022). Review of GPM IMERG performance: A global perspective. Remote Sensing of Environment, 268, 112754.

[33] European Centre for Medium-Range Weather Forecasts. (n.d.). ERA5-Land: Data documentation. ECMWF Confluence Wiki. Retrieved August 23rd, 2024, from https://confluence.ecmwf.int/display/CKB/ERA5-Land%3A+data+documentation.

[34] Copernicus Climate Change Service (C3S). (2017). ERA5: Fifth generation of ECMWF atmospheric reanalyses of the global climate. Copernicus Climate Change Service (C3S) Climate Data Store (CDS). Retrieved August 23rd, 2024, from https://doi.org/10.24381/cds.68d2bb30.

[35] FAO SWALIM. (2007, October). *Climate in Somalia*. Food and Agriculture Organization. Retrieved June 13, 2024, from https://www.faoswalim.org/content/w-01-climate-somalia.

[36] Roy, D., Begam, S., Ghosh, S., & Jana, S. (2013). Calibration and validation of HEC-HMS model for a river basin in Eastern India. ARPN journal of Engineering and Applied Sciences, 8(1), 40-56.

[37] Halwatura, D., & Najim, M. M. M. (2013). Application of the HEC-HMS model for runoff simulation in a tropical catchment. Environmental modelling & software, 46, 155-162.

[38] Bennett, T. H., & Peters, J. C. (2000). Continuous soil moisture accounting in the hydrologic Engineering Center Hydrologic Modeling System (HEC-HMS). In Building partnerships (pp. 1-10).

[39] U.S. Army Corps of Engineers. (n.d.). Selecting a loss method. HEC-HMS Hydrologic Modeling System User's Manual. Retrieved June 2, 2024, from https://www.hec.usace.army.mil/confluence/hmsdocs/hmsum/4.10/subbasin-elements/selecting-a-loss-method

[40] Hydrologic Engineering Center. (2000). HEC-HMS: Hydrologic modeling system technical reference manual (CPD-74B). U.S. Army Corps of Engineers. Retrieved August 28, 2024, from https://www.unife.it/ing/lm.civile/insegnamenti/idrologia/materiale-didattico/esercitazioni/hec-hms/tech_reference/at_download/file

[41] Chea, S., & Oeurng, C. (2017). Flow simulation in an ungauged catchment of Tonle Sap Lake Basin in Cambodia: Application of the HEC-HMS model. Water Utility Journal, 17, 3-17.

[42] U.S. Army Corps of Engineers. (n.d.) Selecting a transform method. HEC-HMS Hydrologic Modeling System User's Manual. Retrieved June 3, 2024, from https://www.hec.usace.army.mil/confluence/hmsdocs/hmsum/4.7/subbasin-elements/selecting-a-transform-method.

[43] Yannopoulos, S., Christidis, C., Loukas, A., & Giannopoulou, I. (2013, June). A sensitivity analysis on the parameters of Clark instantaneous unit hydrograph. In Proceedings of the 8th International Conference of EWRA (European Water Resources Association)—Water Resources Management in An Interdisciplinary and Changing Context, Porto, Portugal (pp. 26-29).

[44] De Almeida, I. K., ALMEIDA, A. K., ANACHE, J. A. A., STEFFEN, J. L., & SOBRINHO, T. A. (2014). Estimation on time of concentration of overland flow in watersheds: a review. Geosciences= Geociências, 33(4), 661-671.

[45] Wardhana, P. N., & Kusumawijaya, L. P. (2021, December). Gajahwong river continuous flow simulation by using Soil Moisture Accounting (SMA) of HEC HMS. In IOP

Conference Series: Earth and Environmental Science (Vol. 930, No. 1, p. 012032). IOP Publishing.

[46] Bouzouidja, R., Béchet, B., Hanzlikova, J., Sněhota, M., Le Guern, C., Capiaux, H., ... & Lebeau, T. (2021). Simplified performance assessment methodology for addressing soil quality of nature-based solutions. Journal of Soils and Sediments, 21, 1909-1927.

[47] Quinn, R., Rushton, K., & Parker, A. (2019). An examination of the hydrological system of a sand dam during the dry season leading to water balances. *Journal of Hydrology X*, *4*, 100035.

[48] Hao, X., Ball, B. C., Culley, J. L. B., Carter, M. R., & Parkin, G. W. (2008). Soil density and porosity. Soil sampling and methods of analysis, 2, 743-759.

[49] Demissie, S., Meshesha, D. T., Adgo, E., Haregeweyn, N., Tsunekawa, A., Ayana, M., ... & Wubet, A. (2022). Effects of soil bund spacing on runoff, soil loss, and soil water content in the Lake Tana Basin of Ethiopia. Agricultural Water Management, 274, 107926.

[50] Food and Agriculture Organization of the United Nations. (1991). Water harvesting: A manual for the design and construction of water harvesting schemes for plant production. https://www.fao.org/4/U3160E/u3160e07.htm#5.4%20semi%20circular%20bunds

[51] Goba, W. B., Muluneh, A., & Wolka, K. (2022). Soil Bunds Effect on Soil Properties under Different Topographies of Southwest Ethiopia. Journal of Environmental & Earth Sciences, 4(1), 54-63.

[52] Jemberu, W., Baartman, J. E., Fleskens, L., Selassie, Y. G., & Ritsema, C. J. (2017). Assessing the variation in bund structure dimensions and its impact on soil physical properties and hydrology in Koga catchment, Highlands of Ethiopia. Catena, 157, 195-204.

[53] Britannica, T. Editors of Encyclopaedia (2011, June 29). Fluvisol. Encyclopedia Britannica. Retrieved June 11, 2024 from https://www.britannica.com/science/Fluvisol.

[54] ISRIC - World Soil Information. (n.d.). Fluvisols. ISRIC - World Soil Information. Retrieved June 11, 2024 from https://www.isric.org/sites/default/files/major_soils_of_the_world/set4/fl/fluvisol.pdf

[55] Huang, Z., Tian, F. P., Wu, G. L., Liu, Y., & Dang, Z. Q. (2017). Legume grasslands promote precipitation infiltration better than gramineous grasslands in arid regions. Land Degradation & Development, 28(1), 309-316.

[56] Xu, C., Ke, Y., Zhou, W., Luo, W., Ma, W., Song, L., ... & Yu, Q. (2021). Resistance and resilience of a semi-arid grassland to multi-year extreme drought. *Ecological Indicators*, *131*, 108139.

[57] NASA Land Processes Distributed Active Archive Center (LP DAAC). (2024). MODIS/Terra + Aqua Land Cover Type Yearly L3 Global 500m SIN Grid. NASA Earth data. Retrieved June 27, 2024 from https://search.earthdata.nasa.gov/search.

[58] Eckert Jr, R. E., Bleak, A. T., Jos. H. Robertson, & Naphan, E. A. (1961). Responses of Agropyron cristatum, A. desertorum, and other range grasses to three different sites in eastern Nevada. Ecology, 775-783.

APPENDIX A: MEAN MONTHLY PET IN SOMALIA (1963-1990)

Name	Lon	Lat	Alt	JAN	FEB	MAR	APR	MAY	JUN	JUL	AUG	SEP	OCT	NOV	DEC
Afgoi	45.13	2.13	83	172.3	161.4	184.3	151.6	134.9	118.5	137.4	143.2	154.2	150.5	135	153
Afmadu	42.06	0.51	29	168.8	153.7	170.5	133.2	124.5	120.5	120.3	131.9	144	137.4	127.5	134.5
Alessandra	42.70	0.50	25	153.6	148	170.7	129.7	121.1	101.9	104.4	116.3	126.6	129.9	117.1	131.6
Alula	50.75	11.96	6	119.4	122.4	153.1	151.7	180.3	244.8	289.7	265.7	224.4	142.9	92.7	107.3
Balad	45.38	2.36	95	139.8	134.9	158.8	144.1	138.5	121.6	125.7	129.8	129.5	140.2	130.6	134.9
Bardera	42.30	2.35	116	199.9	173.6	190.7	141.9	154.1	157.4	158.5	169.1	177.2	151.2	144.7	158
Barro-uen	45.50	2.86	104	148.4	151.8	169.9	137.8	128.9	110.7	112.2	123.6	133.7	137.4	131.5	143.9
Belet-uen	45.21	4.70	173	158.9	157.3	161.4	138.7	138.1	146.3	142.9	154.8	165.1	138.5	130.3	145.5
Berbera	45.03	10.43	89	156.3	142.1	165.4	172.5	224	408.4	437.8	439.8	310	204.2	166.8	149.9
Borama	43.18	9.93	1454	102.1	94.6	116.2	115	120.8	111.2	105.4	109.3	108.5	108	104.7	105.7
Bosaso	49.18	11.28	6	119.4	122.4	153.1	151.7	180.3	244.8	289.7	265.7	224.4	142.9	92.7	107.3
Brava	44.03	1.10	6	128.9	113.2	134.9	128.6	123.6	109.6	113	119.7	119.2	121.7	118.7	125.8
Bulo-burti	45.56	3.25	158	179.1	180.5	208.2	170.1	152.9	152.3	150.7	160.1	171.5	157.2	152.2	160.7
Bur-acaba	44.06	2.78	194	163.6	156.1	172	137	125.2	118.8	108.9	123.2	130.9	118.5	119.6	136.3
Burao	45.56	9.51	1032	156.3	142.1	165.4	172.5	224	408.4	437.8	439.8	310	204.2	166.8	149.9
Burdhuxul	43.30	4.10	400	166.3	167	182.1	169.3	148.4	165	167.4	176.2	175.8	141.1	134.2	148.4
Capo-guard	51.25	11.81	244	151.5	131.3	174.5	180.3	240.2	279.5	273.1	276.9	255.5	183	144.4	149.3
Dinsor	42.98	2.41	280	199.9	173.6	190.7	141.9	154.1	157.4	158.5	169.1	177.2	151.2	144.7	158
Eil	49.78	7.95	36	155.7	136.1	166.9	166.5	188	228.9	195.4	214.8	211.8	167.3	130.5	131
El-bur	46.61	4.68	175	159.7	156.3	183.1	145.2	144.6	132.7	145.6	161.3	175.7	144.4	130.3	142.3
El-mugne	44.76	1.71	12	132.9	115.3	136.8	123.8	119.2	107.2	111.3	114.7	121.2	128.4	117.1	125.8
Erigavo	47.36	10.61	1744	119.4	122.4	153.1	151.7	180.3	244.8	289.7	265.7	224.4	142.9	92.7	107.3
Galcayo	47.43	6.85	302	151.3	143.2	181.5	163.4	173.3	204.6	195.3	197.3	181.8	137.7	129.6	155.3
Gebiley	43.28	9.61	1563	102.1	94.6	116.2	115	120.8	111.2	105.4	109.3	108.5	108	104.7	105.7
Genale	44.75	1.83	69	134.8	132.2	141.4	129.1	121.5	103.5	103	117.8	127.3	125	111.5	121.4
Jowhar	45.50	2.76	108	148.4	151.8	169.9	137.8	128.9	110.7	112.2	123.6	133.7	137.4	131.5	143.9
Giumbo	42.60	-0.21	30	125.5	116	138.7	124	117	96.8	99.5	105.7	114.9	125.3	111.1	123.4
Hargeisa	44.08	9.50	1326	153.6	148.7	197.7	201.5	210.1	248.6	257.6	256.9	225.9	239.8	162	147.7
Huddur	43.90	4.16	500	166.3	167	182.1	169.3	148.4	165	167.4	176.2	175.8	141.1	134.2	148.4
Baidoa	43.66	3.13	487	163.6	156.1	172	137	125.2	118.8	108.9	123.2	130.9	118.5	119.6	136.3
Mubarak	44.66	3.68	135	166.3	167	182.1	169.3	148.4	165	167.4	176.2	175.8	141.1	134.2	148.4
Jilib	42.80	0.43	23	153.6	148	170.7	129.7	121.1	101.9	104.4	116.3	126.6	129.9	117.1	131.6
Jonte	42.46	-0.33	8	125.5	116	138.7	124	117	96.8	99.5	105.7	114.9	125.3	111.1	123.4
Mareere	42.71	0.43	12	153.6	148	170.7	129.7	121.1	101.9	104.4	116.3	126.6	129.9	117.1	131.6
Kismayo	42.43	-0.36	8	152.1	142.8	150.9	148.8	123.7	115.8	120	126.9	137	148.8	140.5	147.6
Lafoole	45.15	2.10	100	172.3	161.4	184.3	151.6	134.9	118.5	137.4	143.2	154.2	150.5	135	153
Las-anod	47.36	8.46	705	151.3	143.2	181.5	163.4	173.3	204.6	195.3	197.3	181.8	137.7	129.6	155.3
luuq	42.45	3.58	165	205.6	177.2	198.2	160.6	172	181.9	173.1	168.1	181.7	167	158.2	169.2
Mahaddey	45.51	2.95	125	148.4	151.8	169.9	137.8	128.9	110.7	112.2	123.6	133.7	137.4	131.5	143.9
Jamame	42.73	0.05	10	153.6	148	170.7	129.7	121.1	101.9	104.4	116.3	126.6	129.9	117.1	131.6
Modun	44.00	1.15	50	128.9	113.2	134.9	128.6	123.6	109.6	113	119.7	119.2	121.7	118.7	125.8
Mogadiscio	45.35	2.03	9	139.8	134.9	158.8	144.1	138.5	121.6	125.7	129.8	129.5	140.2	130.6	134.9
Mogambo	42.75	0.06	10	153.6	148	170.7	129.7	121.1	101.9	104.4	116.3	126.6	129.9	117.1	131.6
Obbia	48.56	5.33	10	115.9	120	152.8	153.1	130.2	133.4	128.3	128.1	120.4	128.4	125	119.5
Qardo	49.08	9.50	810	155.7	136.1	166.9	166.5	188	228.9	195.4	214.8	211.8	167.3	130.5	131
Sablaale	43.80	1.30	50	128.9	113.2	134.9	128.6	123.6	109.6	113	119.7	119.2	121.7	118.7	125.8
Scusciuban	50.23	10.30	344	151.5	131.3	174.5	180.3	240.2	279.5	273.1	276.9	255.5	183	144.4	149.3
Shiekh	45.18	9.91	1441	156.3	142.1	165.4	172.5	224	408.4	437.8	439.8	310	204.2	166.8	149.9
Villabruzzi	45.48	2.75	108	148.4	151.8	169.9	137.8	128.9	110.7	112.2	123.6	133.7	137.4	131.5	143.9